

#785

SPARTAN
X-RAY DATA FROM SPARTAN-A

85-048E-01A

Table of Contents

1. Introduction
2. Errata/Change Log
3. LINKS TO RELEVANT INFORMATION IN THE ONLINE NSSDC INFORMATION SYSTEM
4. Catalog Materials
 - a. Associated Documents
 - b. Core Catalog Materials

1. INTRODUCTION:

The documentation for this data set was originally on paper, kept in NSSDC's Data Set Catalogs (DSCs). The paper documentation in the Data Set Catalogs have been made into digital images, and then collected into a single PDF file for each Data Set Catalog. The inventory information in these DSCs is current as of July 1, 2004. This inventory information is now no longer maintained in the DSCs, but is now managed in the inventory part of the NSSDC information system. The information existing in the DSCs is now not needed for locating the data files, but we did not remove that inventory information.

The offline tape datasets have now been migrated from the original magnetic tape to Archival Information Packages (AIP's).

A prior restoration may have been done on data sets, if a requestor of this data set has questions; they should send an inquiry to the request office to see if additional information exists.

2. ERRATA/CHANGE LOG:

NOTE: Changes are made in a text box, and will show up that way when displayed on screen with a PDF reader.

When printing, special settings may be required to make the text box appear on the printed output.

Version	Date	Person	Page	Description of Change
01				
02				

3 LINKS TO RELEVANT INFORMATION IN THE ONLINE NSSDC
INFORMATION SYSTEM:

<http://nssdc.gsfc.nasa.gov/nmc/>

[NOTE: This link will take you to the main page of the NSSDC Master Catalog. There you will be able to perform searches to find additional information]

4. CATALOG MATERIALS:

- a. Associated Documents To find associated documents you will need to know the document ID number and then click here.
<http://nssdcftp.gsfc.nasa.gov/miscellaneous/documents/>

- b. Core Catalog Materials

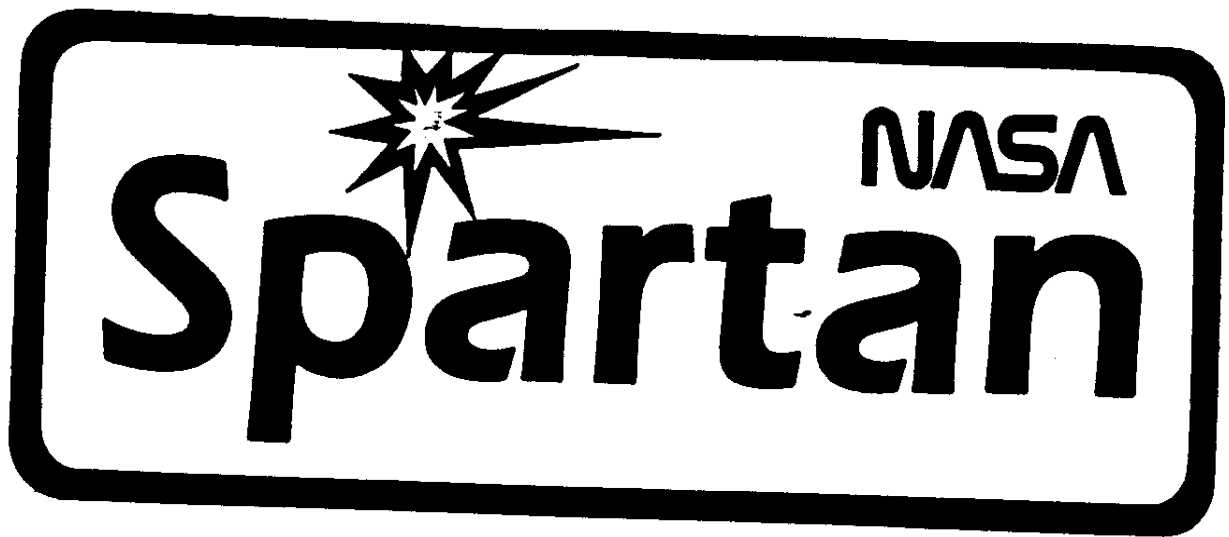
SPARTAN

X-RAY DATA TAKEN FROM SPARTAN

85-048E-01A SOXR-00048

This dataset catalog consists of two binary tapes. The D tapes are 9-track 6250 BPI, and the C tapes are 3480 cartridges. They were created on the VAX. The D and C numbers along with their time spans are as follows

D#	C#	FILES	START TIME SPAN					
			MONTH	DAY	YEAR	HR.	MIN.	SEC.
D-83166	C-32488	1	06	20	85	00	00	33
			END TIME SPAN					
			06	21	85	09	07	25
			START TIME SPAN					
			MONTH	DAY	YEAR	HR.	MIN.	SEC.
D-83167	C-32489	1	06	21	85	09	07	25
			END TIME SPAN					
			06	21	85	17	32	10



S P A R T A N
P R O C E S S I N G
P R O D U C T I O N
O N T H E V A X

Kevin Carmody
William A. Snyder

Last revision 13 March 1987
Second version 25 October 1985
Original version 15 May 1985

Table of Contents

I.	Introduction	5
A.	Format of this document	5
B.	Overview of program flow	6
II.	Vax Production Programs	8
A.	ET programs	8
1.	PETMOUNT	8
2.	VETMOUNT	8
3.	PETHALT	8
4.	VETHALT	8
5.	ETDISPLAY	8
6.	ETSHOW	9
7.	ETREAD	9
B.	CSD Programs	11
1.	CSDGEN	11
2.	CSDSHOW	12
3.	CSDPLOT	12
4.	CSDCORRELATE	12
5.	CSDREAD	12
6.	CSDACCESS	12
7.	CSDCORRECT	13
8.	CSDPARAMS	13
9.	CTSGEN	13
10.	CRSGEN	13
11.	CRSGENALT	14
12.	CRSBKGDGEN	14
13.	CSSADD	14
14.	CSSSHOW	15
C.	SPD Programs	16
1.	SPDGEN	16
2.	SPDSHOW	16
3.	STSGEN	17
4.	SRSGEN	17
5.	SRSGENALT	17
6.	SPSADD	17
7.	SPSSHOW	17
8.	SPSPLOT	18
9.	SPSSUBTRACT	18
10.	SPSSUM	19

D. ACS Programs	20
1. ACSGEN	20
2. ACSMERGE	20
3. ACSSHOW	20
4. ACSPLOT	21
E. Scan Programs (SCANS)	22
1. SFGEN	22
2. SCANPLOT	22
3. SFMAXENT	22
4. SFPLOT	22
F. Plot Programs (PLOTS)	23
1. CONSLICE	23
2. CRTSHOW, CRTSTOR	23
3. PLOTSAV	23
4. PLOTREAD	23
5. PLOTCONTOUR	23
6. CONSCALE	23
7. ANALYZE	24
8. SUBTR	24
9. RADIAL	24
10. PAREA	24
11. SCANLOAD	24
12. WARP	24
13. PLOT4	24
G. Utility Programs (UTIL)	25
1. CENTER	25
2. CONTENTS	25
3. SFITSMOUNT	25
4. SFITSHALT	25
5. SBMSMAP	25
6. SMAPSBM	26
7. SMAPFITS	26
8. FITSHEAD	26

H. Miscellaneous Spartan Programs (SPAR)	27
1. TIMECONV	27
2. TIMEEVAL	27
3. SEXCONV	27
4. SEXEVAL	28
5. EULER	28
6. CORRELATION	28
7. PROB	28
8. DGAUSPRB	28
9. TARGETS	28
10. TARGEVAL	29
11. MAPCEN	29
12. ROTVAL	29
13. MAPEVAL	29
14. FELINE	29
15. FELEVAL	29
16. SPIND	29
17. POLYMOD	30
18. CIRCLE	30
III. Data Structures	32
A. Integration Unit	32
B. IU Paragraph	36
C. Differences between IU format and SPD and CSD record formats ..	39
D. Condensed Scan Sum (CSS) record and file structure	42
E. Spectral Sum (SPS) record and file structure	44
F. Attitude Control System (ACS) record structure	46
IV. Algorithms	48
A. Radial summing algorithm (CRSGENALT, SRSGENALT)	49
B. Revised radial summing algorithm (CRSGEN, SRSGEN)	52
C. SPS iron line rebinning (SPSADD)	55
V. Miscellaneous	57
A. Description of target-event codes	58
B. Target maneuver times	60

I. Introduction

A. Format of this document

This document is intended to help individuals become familiar with current Vax Spartan I data processing programs. The Vax production programs presented here allow the user to readily access the Spartan I database that initially resides on a tape medium (an experimenters tape or ET), and then to either display that information immediately, or create secondary Vax disk databases that will later be used to provide specific types of information.

In section II, are brief descriptions of what the various Vax production programs do. Section II is divided into eight subsections: ET, SPD, CSD, ACS, SCANS, PLOTS, UTIL, and SPAR programs.

The primary function of the experimenter tape (ET) programs are to easily access and display information that resides on an experimenters tape. The primary functions of the SPD, CSD, and ACS programs are to either create or access Vax disk databases for the analysis of spectral, condensed, or ACS information, respectively. The SCANS programs are for creating and displaying files for individual scans, and the PLOTS programs are for displaying images of the targets. The UTIL programs are a set of independent utilities written especially for Spartan, and the SPAR library is a set of miscellaneous programs, mostly subroutines. The MAXENT library is for servicing the maximum entropy programs that run on the Cray.

Programs that read an experimenters tape and generate a particular Vax database all contain GEN in their program name (CSDGEN, SPDGEN, ACSGEN, etc.); programs that contain SHOW or DISPLAY or their names allow the user to view individual records within the database; programs that contain PLOT in their names use IGL routines to plot the contents of database files.

In section III, we present a brief summary of the various SPARTAN I data structures. We have found it instructive to compare the schematic record structure found within this section to the output of various SHOW programs. Although we have attempted to provide as much information as needed when discussing various data structures, this document assumes that the user already has some familiarity with the PCM paragraph format as supplied by NASA.

Detailed descriptions of various algorithms used in Spartan programs are given in section IV. Section V contains miscellaneous tables.

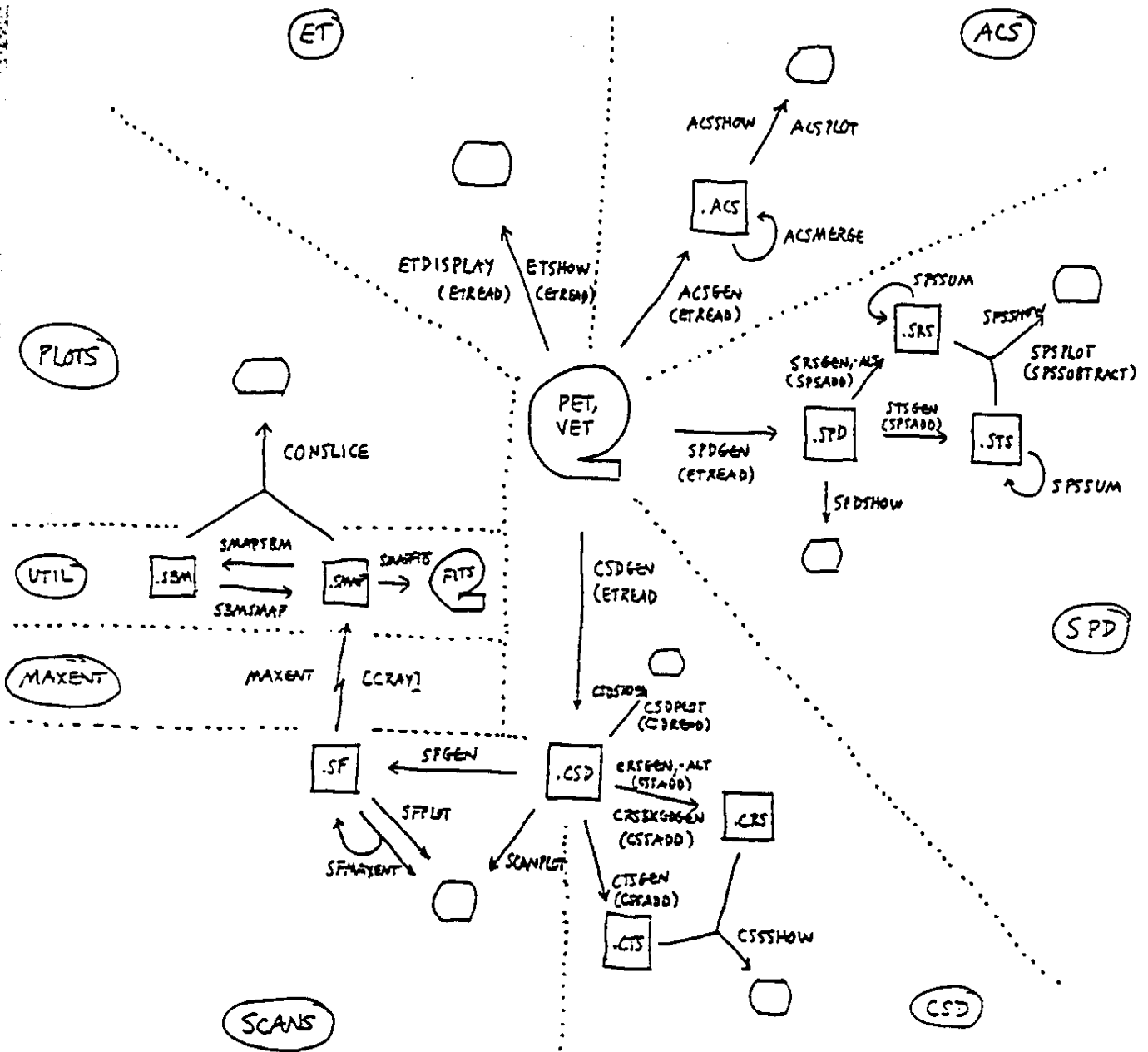
B. Overview of program flow

On the next page is an illustration of Spartan Vax program flow. As the legend indicates, the Q-shaped figure in the center is a mag tape, the PET/VET. A PET (Preliminary Experimenters' Tape) is an experimenters' tape without aspect solution (the corresponding IU elements are zero); a VET is an experimenters' tape with aspect solution. All the Vax software starts with a PET/VET and all the programs that work directly on a VET will also work on a PET; however, other programs that work on the files produced from a VET, since they require aspect, will not work on files produced from a PET.




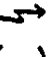




The round-edged empty box indicates the screen; e.g., ETSHOW displays a PET/VET directly on the screen. The rectangular boxes indicate files; e.g., SPDGEN generates an SPD file from a PET/VET. The dotted lines separate program library areas.

Besides the programs and files shown on this diagram, NRL also maintains four libraries (Cameras, Aspect, AMF, and Onestar) which generate aspect solution and insert it into a PET to create a VET. These programs are not shown in this diagram. Also not shown are calibration libraries, the libraries which are maintained on a Data General Eclipse microcomputer for creating PET's from NASA tapes, and image analysis libraries for and on the Cray.

Spartan Vax program flow (except aspect and calibration programs)



Legend

-  mag tape
-  file
-  screen
-  program direction
-  program outside of Vax
-  subroutine
-  program library
-  program library boundary

II. VAX PRODUCTION PROGRAMS

A. Experimenter Tape (ET) Programs

Command procedure PETMOUNT

Before running programs that require an Experimenter Tape (ET) input, and after physically mounting the ET on a tape drive, the PETMOUNT.COM file should be executed in order to ALLOCATE the tape drive and logically MOUNT the PET tape.

Command procedure VETMOUNT

VETMOUNT is identical to PETMOUNT except that the tape unit is given the logical name VET. The distinction between PET and VET is necessary when two tapes are being run by the same program. Currently VET is used only by ETMERGE.

Command procedure PETHALT

The PETHALT.COM file DISMOUNTS the PET tape and DEALLOCATES the tape drive.

Command procedure VETHALT

VETHALT dismounts the VET tape and deallocates the tape drive.

Program ETDISPLAY

This program allows the user to access individual Integration Units (IU's) on an Experimenters Tape (ET), and display to CRT screen parameters of interest in the IU. The output format closely matches the Nova/Macintosh SPARTAN groundstation format; however, only the contents of one IU (two paragraphs) are displayed page sequentially. An additional page not present in the groundstation format, page 0, displays summary and aspect information present in the IU, but not present in the paragraphs. One option allows the user to select display pages, and another option allows one to display a range of integration units.

Items displayed include PHA channels and coincident count rates, detector temperatures, pressures, and voltages, and aspect information, if available. All telemetry values are converted to useful engineering units. To display the contents of an IU, one simply enters the IU number. IU's are numbered on the tape starting with 1.

Program ETSHOW

Reads an integration unit from an experimenters' tape (ET) and displays it in integer (coded) format. The user supplies the IU number. IU's are numbered on the tape starting with 1.

The IU is displayed by lines, along with the line number, in a 53 line by 32 column format reflecting the data structure of an IU (see Integration Unit Structure write-up in section III). The following data types are used for display: area 1 (the IU header) is displayed in integer*2 decimal (except that the target name is displayed in ASCII), the integer*4 elements on lines 1 and 3 are displayed in integer*4 decimal, and the bitmaps on lines 3 and 4 are displayed in hexadecimal; areas 2-5 (PHA data) are displayed in integer*2 decimal; and areas 6 and 7 (the paragraphs) are displayed as follows: column 0 and the status array are output as a signed integer in the normal range of -32768 and + 32767, except that the two words of the paragraph counter are output in the range 0 to 65535; column 1 is output as a value in the range 0 to 255 for the upper byte, and two nibble values (range 0 to 15) for the lower byte; and the line data (columns 2 to 15) are output as the positive value of bits 0 to 15 (range 0 to 32767), preceded by a 'P' if bit 16 is set (the parity error flag or PEF).

Subroutine ETREAD

Reads a record from an experimenters' tape (ET) and returns pointers to an integration unit from the record. The user passes an IU number (IU's start on the tape numbered 1), and returns IREC, IUREC, and BUFFER in the common block /IUBUFFER/. IREC is the number of the record on the tape which contains the IU. IUREC is the IU number within the record (there are 4 IU's per record), and BUFFER is the 53 line x 32 column x 4 IU record read from the tape. The first two dimensions correspond to the IU record structure (see Integration Unit Structure write-up in section III), while the third dimension (returned by the subroutine) flags one of the 4 IU's per input tape record as the IU of current interest. [Examples: a request for IU number 3 returns IREC=1 and IUREC=3; IU=6 returns IREC=2 and IUREC=2.] ETREAD automatically keeps track of all tape and IU positioning. [Note that while it is possible to back up the tape in order to view an IU placed on the tape prior to the current tape position, in practice this is usually an extremely slow procedure, and should be avoided.]

The entire record is passed in the common block /IUBUFFER/ as an integer*2 array BUFFER dimensioned (0:31,0:52,4). BUFFER consists of four contiguous IU's; the last dimension is the pointer to the IU's. Thus if you wish to access the element in column 3, line 1 in the IU you have asked to read, the reference should be to BUFFER(3,1,IUREC). The normal way to use this routine is to call it with the IU number you wish to read and always reference BUFFER with IUREC in the last dimension.

IREC must not be changed in the calling program, otherwise ETREAD will not know where it truly is on the tape. Set IREC=0 before the first call to ETREAD and do not change it thereafter. The first call to ETREAD must be with IU=0 to open the tape unit 'ET'. Thereafter, call ETREAD with the IU number you wish to read. IU's are numbered starting with 1.

To rewind the tape, call ETREAD with IU=-1. Normally this should be the last call to ETREAD.

ETREAD has two possible RETURN conditions. The first return label is used when the end of the tape is detected. The second return condition is used when a value of IU less than -1 is passed.

B. Condensed Scan Data (CSD) programs

Program CSDGEN

Generates a file of CSD records from an experimenters' tape (ET). A CSD record is a Condensed Scan Data record and consists of two lines of 32 words each. The first line of the CSD record (except for word 4), is the same as the first line of the SPD record [which except for words 5 and 6 is the same as the first line of the integration unit (IU)]. (See section III for a schematic of the first line differences between SPD and CSD records.) Word 4 in the CSD first line consists of XCRAS flags, the upper byte for detector 1, the lower byte for detector 2, with the following bit assignments in each byte:

- bit 0: H. V. off
- bit 1: auto shutdown
- bit 2: calibration on
- bit 3: purge valve open

The second line is assigned as follows:

- words 0- 1: XCTR 1- 2
- words 2- 4: XCTR 5- 7
- words 5- 6: XCTR 8- 9
- words 7- 9: XCTR 12-14
- words 10-11: sync/PEF for D1-D2 resp. (high byte: L1; low byte: L2)

Within each byte of words 10 and 11, bits 7-3 are assigned to broadband PHA channels 0-4 respectively, where each bit indicates whether a sync error OR PEF was set in any single PHA channel which is included in the broadband sum.

A broadband PHA channel is a sum of individual PHA channels within the detector and layer. The telemetric 128 channel PHA spectrum is divided into 5 intervals, corresponding to fixed energy bands [i.e., channel 0 : 0.1-2 keV; channel 1 : 2-5 keV; channel 2 : 5-7 keV; channel 3 : 7-14 keV; and channel 4 : > 14 keV]. The actual PHA channels summed into various wide bins is based on the PHA channel containing the Fe-line calibration peak.

The broadband channels are assigned to the following CSD words of the second line :

- words 12-16: D1L1 broadband channels 0-4 resp.
- words 17-21: D1L2 broadband channels 0-4 resp.
- words 22-26: D2L1 broadband channels 0-4 resp.
- words 27-31: D2L2 broadband channels 0-4 resp.

The iron line channel is coded for each detector and layer in line 0, words 6 and 7. Detector 1 is coded in word 6 and detector 2 in word 7; layer 1 is coded in the upper byte, and layer 2 in the lower byte. In each byte, the channel code = $NINT(10*(channel-50))$, where NINT means nearest integer. See section III for a diagram of the CSD record.

This program generates a file of any rootname and gives it the extension '.CSD'. A start and stop time is specified by the user, and CSD records are written to the file for those IU's that fall within this range. The CSD file is indexed with the same key as the SPD file, mission elapsed time. Users should expect to allocate 26 blocks of disk space per flight minute when creating CSD files.

Program CSDSHOW

Reads an integration unit from a condensed scan data file and displays it in integer (coded) format, in a 2 line by 32 column arrangement reflecting the CSD record structure. The user supplies the MET (mission elapse time). The program finds the IU at that MET or the next one after. Before running this program, the VAX SET TERM/WIDTH=132 command should first be executed in order to properly set the terminal screen for display.

The CSD record is displayed by lines, along with the line number, in the following format: in line 0, the target name is displayed in ASCII, the integer*2 elements are displayed in integer*2 decimal, the integer*4 elements in integer*4 decimal, the XRAS flags in hexadecimal, and the iron line channels are displayed in decimal by bytes; line 1 is displayed in integer*2 decimal except for the PEF bitmaps, which are displayed in hexadecimal.

Program CSDPLOT

Allows the user to access any CSD data file and display PHA and Coincident counts as a function of time between specified START and STOP times. When running the program, one specifies the CSD root filename to be accessed (an '.CSD' extension is assumed), a START and STOP time, and coincident (XCTR) and/or broadband (i.e., wide) PHA channels that are to be displayed. Counts as a function of time are then plotted to CRT screen. It is possible to plot up to 4 channels simultaneously, with scaling dependent upon the number of plots selected.

Program CSDCORRELATE

Reads two channels from either PHA or coincident (XCTR) data from CSD files and searches for correlations in count rate between them. A series of time intervals is specified by the user. The program calls the subroutine CORRELATION to calculate the linear correlation coefficient and probability of no correlation, and it calls SUPERFIT to compute a linear best fit. The results can be plotted to the screen.

Subroutine CSDREAD

This subroutine accesses any CSD data file and returns up to 4 broad-band (i.e., wide) PHA and/or coincident Counters as a function of time for data between START and STOP times specified by the user.

Subroutine CSDACCESS

Extracts up to 4 combinations of PHA or coincident (XCTR) data from Condensed Scan Data (CSD) files that lie between START and STOP times specified by the user. Based on CSDREAD.

Subroutine CSDCORRECT

Extracts up to 4 combinations of PHA or coincident (XCTR) data from Condensed Scan Data (CSD) files that lie between START and STOP times specified by the user.

This subroutine is identical to CSDACCESS, except that it attempts to correct XCTR rollover problems.

Subroutine CSDPARAMS

Used to extract information for accessing up to 4 combinations of PHA or coincident (XCTR) data from Condensed Scan Data (CSD) files. This subroutine can be used in conjunction with CSDACCESS for easy access of CSD data files.

Program CTSGEN

Generates a file of summed records from a CSD file. The user specifies start and stop times, and all the CSD records in that interval are summed into a single record. The record is placed in a sum file, which is always given the extension '.CTS' (Condensed Time Sum). This can be repeated many times for a single sum file, each interval generating one summed record.

The CTS record and the CRS (Condensed Radial Sum) record have a common structure which is called CSS (Condensed Scan Sum). Ctsgen calls the subroutine Ccssadd to add the CSD record to the CTS/CSS record. See section III.D for a schematic of the CSS record.

Program CRSGEN

Generates or adds to a file of radially summed records, using data from a CSD file. This program uses the center line algorithm for the radial test. Each sum file consists of a series of sums for the rings around a single central point. The sum file is given the extension '.CRS' (Condensed Radial Sum).

If the CRS file does not exist, the user specifies the start and stop times, the RA and dec of the center of the rings, and the boundary radii of the rings. All the CSD records which have aspect solution between the two times are binned into the rings. If a CSD record overlaps a ring boundary, it is split proportionately, fractional counts being added to the ring totals and sums. When the binning is done, the records are written to the CRS file.

If the CRS file already exists, the counts from the CSD records are added to the rings which are present in the CRS file.

The CRS record and the CTS (Condensed Time Sum) record have a common structure which is called CSS (Condensed Scan Sum). Crsgen calls the subroutine Cssadd to add the CSD record to the CRS/CSS record. See section III.D for a schematic of the CSS record.

See section IV.B for a description of the revised radial summing algorithm used in this program.

Program CRSGENALT

This program differs from CRSGEN only in that the old scan line algorithm is used. See section IV.A for a description of the original radial summing algorithm used in this program.

Program CRSBKGDGEN

Adds to a file of radially summed records, using data from a CSD file. Each sum file consists of a series of sums for the rings around a single central point. The sum file has the extension '.CRS' (Condensed Radial Sum).

This program differs from CRSGEN in that no aspect solution is required to sum data into a background ring. All that is required is that the background region be defined by start and stop MET's. The data within these time intervals is added into a single output record and appended to the CRS file.

Subroutine CSSADD

Sums a CSD record to a sum record called CSS (Condensed Scan Sum). The total number of CSD detector-layer areas added to each CSS detector-layer area is in the CSS field 'total'.

The actual value added to the CSS record can be modified with the parameter 'factor': all the counts in the CSD record are multiplied by 'factor' and then added to CSS, and 'factor' is added to the 'total' fields. For this reason, the CSS counts and totals are floating.

The detector counts of CSD that are added to CSS are controlled with the parameter 'idets': if idets=1, detector 1 (only) is added; likewise for detector 2; and if idets=3 (or any other value but 1 or 2), both detectors are added.

The total number of records attempted to be added to CSS is kept in irecs.

Program CSSSHOW

Reads a condensed scan summed (CSS) file, which may be either a CTS file or a CRS file, and displays any record. For a time-sequential sum (CTS file), the user supplies the MET of the first IU in the sum; for a radial sum (CRS file), the user supplies the inner radius of the ring.

C. Spectral Data (SPD) Programs

Program SPDGEN

Generates a file of SPD records from an experimenters' tape (ET). An SPD record has the same structure as an Integration Unit (IU) except that areas 6 and 7 (the original paragraphs that make up the IU) are not duplicated. The SPD record is so named because it preserves the detailed Spectral Data present in an IU.

The program generates an SPD file of any rootname and gives an '.SPD' extension to the file. It asks for a range of times to be written to the file and looks for all the IU's on the tape whose MET (mission elapse time) falls within the range. For each IU that matches, it writes an SPD record. The SPD file is indexed with MET as the key. Many temporal ranges can be written to the same file.

SPDGEN makes the following changes to words 5, 6, and 7 of line 0 of the IU: Word 5 is now the experimenter flag word which is intended to be used as a field of bit flags in other programs. It is presently set to 0 in this program. Words 6 and 7 are the iron line channel codes: the upper byte of word 6 is the channel code for the iron line peaks in this IU for detector 1, layer 1 (D1L1); the lower byte of word 6 is the iron line channel code for D1L2; the upper byte of word 7 is for D2L1; and the lower byte of word 7 is for D2L2. The channel code is derived from the iron line channel by the following formula: channel code = NINT(10*(channel-50)), where NINT means nearest integer. See section III for a schematic of the differences between an SPD record and the IU header.

Users should expect to allocate 226 blocks of disk space per flight minute when creating SPD files.

Program SPDSHOW

Reads an SPD record from a spectral data file and displays it to a CRT in integer (coded) format. The user supplies the MET (mission elapse time). The program finds the SPD record at that MET or the next one after. The SET TERM/WIDTH=132 command should first be executed in order to properly display the 21 line x 32 column format that reflects the SPD data structure.

The SPD record is displayed by lines, along with the line number, in the following format: area 1 (see IU header description in section III) is displayed in integer*2 decimal, except that the target name is displayed in ASCII, the integer*4 elements in line 1 are displayed in integer*4 decimal, and the bitmaps on lines 3 and 4 are displayed in hexadecimal; and areas 2-5 (PHA data) are displayed in integer*2 decimal.

Program STSGEN

Generates a file of summed records from an SPD file. The user specifies start and stop times, and all the SPD records in that interval are summed into a single record. The record is placed in a sum file, which is always given the extension '.STS' (Spectral Time Sum). This can be repeated many times for a single sum file, each interval generating one summed record.

The STS record and the SRS (Spectral Radial Sum) record have a common structure which is called SPS (Spectral Sum). Stsgen calls the subroutine Spsadd to add the SPD record to the STS/SPS record. See section III.E for a schematic of the SPS record.

Program SRSGEN

Generates or adds to a file of radially summed records, using data from an SPD file. This program uses the center line algorithm for the radial test. Each sum file consists of a series of sums for the rings around a single central point. The sum file is given the extension '.SRS' (Spectral Radial Sum).

If the SRS file does not exist, the user specifies the start and stop times, the RA and dec of the center of the rings, and the boundary radii of the rings. All the SPD records which have aspect solution between the two times are binned into the rings. If an SPD record overlaps a ring boundary, it is split proportionately, fractional counts being added to the ring totals and sums. When the binning is done, the records are written to the SRS file.

If the SRS file already exists, the counts from the SPD records are added to the rings which are present in the SRS file.

The SRS record and the STS (Spectral Time Sum) record have a common structure which is called SPS (Spectral Sum). Srsgen calls the subroutine Spsadd to add the SPD record to the SRS/SPS record. See section III.E for a schematic of the SPS record.

See section IV.B for a description of the revised radial summing algorithm used in this program.

Program SRSGENALT

This program differs from SRSGEN only in that the old scan line algorithm is used. See section IV.A for a description of the original radial summing algorithm used in this program.

Subroutine SPSADD

Sums an SPD record to a sum record called SPS (Spectral Sum). The total number of SPD detector-layer areas added to each SPS detector-layer area is in the SPS field 'total'.

The actual value added to the SPS record can be modified with the parameter 'factor': all the counts in the SPD record are multiplied by 'factor' and then added to SPS, and 'factor' is added to the 'total' fields. For this reason, the SPS counts and totals are floating.

The detector counts of SPD that are added to SPS are controlled with the parameter 'idets': if idets=1, detector 1 (only) is added; likewise for detector 2; and if idets=3 (or any other value but 1 or 2), both detectors are added.

Spsadd incorporates the fact that the detector gain varies significantly throughout the mission, changing the channel frequencies. Spsadd calls Feline on every add to find out where the iron line is and then rebins the SPD data accordingly when it add it to SPS.

Since the gain decreases relative to the channel number throughout the mission, the channels of SPS by default are assigned the frequencies which the detectors had at turnon (MET = 02:54:20). These frequencies may be changed the first time Spsadd is called.

See section IV.C for a full description of the SPS iron line rebinning algorithm used in this program.

The parameter irecs is the number of SPD records added to an SPS record. The parameter itot is the number of calls to Spsadd by the calling program.

Program SPSSHOW

Reads a spectral sum (SPS) file, which may be either an STS file or an SRS file, and displays any record. For a time-sequential sum (STS file) the user supplied the MET of the first IU in the sum; for a radial sum (SRS file), the user supplies the inner radius of the ring.

Program SPSPLOT

Used to plot summed spectral (STS or SRS) files. The overflow PHA channel (127) is not plotted.

Subroutine SPSSUBTRACT

Used to extract one or two records of 128 channel PHA data from summed SPD files (STS or SRS). If a second record is specified, it is assumed to be a background record and is subtracted from the first.

Program SPSSUM

With this program the user can add STS or SRS records together one at a time and put the summed record into a new file. The output file is the same type as the input file. You specify an input file which already exists, an output file name which does not already exist, and then key values (MET for STS or inner radius for SRS) one by one to be added to a record which will be written to the output file.

You can do multiple summing operations in one session so that the output file contains multiple records. Do this by responding 'R' instead of a key value. The program will write the current output record and start a new one.

D. Attitude Control System (ACS) programs

Program ACSGEN

Generates a file of ACS records from an experimenters' tape (ET) or a preliminary experimenters' tape (PET). An ACS record is generated for every PARAGRAPH between start and stop times specified by the user. This means that two ACS records are generated for every valid input Integration Unit (IU).

This program generates a file of any rootname and gives it the extension '.ACS'. One file can include many time ranges. The ACS file is INDEXED with mission elapse time (in integer-milliseconds) the primary key. The Index counter of the paragraph functions as a secondary key. Users should expect to allocate 52 blocks of disk space per flight minute when generating an ACS data file.

An ACS record consists of two lines of 31 words each, assigned as follows:

```
Line 0: words 0- 1: MET
        words 2- 3: paragraph counter
        word  4  : index counter
        word  5  : sync error total
        word  6  : PCM column 12, line 0
        word  7  : PCM column 13, line 0
        words 8-10: PCM column 15, lines 15-17
        words 11-31: PCM column 10, lines 11-31
Line 1: words 0- 9: unassigned
        words 10-31: paragraph column 11, lines 10-31
```

See section III for a schematic of the ACS record structure.

Program ACSMERGE

Adds one or more .ACS files to a base .ACS file. In the case of two records with the same MET, the conflicting MET is reported and the old record is left unaltered.

Program ACSSHOW

Reads any record within an ACS data file and displays it in integer (coded) format. The record is displayed by lines, along with the line number. The integer*2 elements are displayed in integer*2 decimal, and the integer*4 elements are displayed in integer*4 decimal. To chose a record, the user supplies the mission elapse time (MET). The program then finds the record with that MET or the next one after. Before running this program, the VAX command SET TERM/WIDTH=132 command should be executed in order to properly set the terminal for display.

Program ACSPLOT

Reads a single word from any ACS data file that was created by ACSGEN, and plots the content of that location between start and stop times specified by the user. The plotting routine used is INTGRAPH. Output units can be either COUNTS or VOLTS (assuming a standard 0-5 Volt conversion). Multiplexed data can be selected by specifying the appropriate paragraph Index counter.

E. Scan programs (SCANS)

Program SFGEN

Creates scan files, optionally background subtracted, that are compatible with image reconstruction programs. The program constructs these files from CSD data files. One has the option of subtracting a background term based on using background polynomial coefficients for fit of XCTR6 determined in the program CSDCORRELATE.

The program writes an Ascii scan file in the following format: on the first six lines are one parameter each: the sweep rate in degrees per second (followed by a comment field); the time each data bin sums over; the total time duration of the scan; the RA of the start point of the scan; the dec of the start point of the scan; and the scan angle. Each line thereafter corresponds to one data bin. On each line are: the time since the beginning of the scan of the center of the bin; the total counts summed in the bin minus background if desired; and the error in that value.

Program SCANPLOT

Plots either PHA or coincident (XCTR) data from CSD files, between start and stop times specified by the user. The read segment is similar to CSDREAD, but only extracts one data quantity. Multiple IU's can be grouped into one output bin. Modified to use CSDPARAMS and CSDCORRECT (which attempts to correct coincident counts). The plot routine used is INTGRAPE.

Program SFMAXENT

This program deconvolves an SF file using the collimator response function in the scan (5 arc minute) direction only. Based on routine MXNTSWP written by R. Cruddace. Expanded and extensively modified by W.A.Snyder 1/5/87 to handle new scan data format and to include plotting of deconvolved and convolved scans. Modified by W.A.Snyder 1/6/87 to allow scaling of deconvolved to convolved data counts on each iteration.

Program SFPLOT

Used to plot SF (scan) files.

F. Plot programs (PLOTS)

Program CONSLICE, Version 2, by Joseph L. Hora

The purpose of this program is to display and analyze two dimensional maps by contour plotting and selection of cuts. A description of the program and the commands is in CONSLICE.DOC. This program uses the graphics utility functions in the GRO - OSSE graphics Library.

Following modifications were made 29 May 1986:

- Local loading of include files
- Option for loading of data from binary file
- Option for reversal of RA axis

Subroutines CRTSHOW and CRTSTOR in Arrdis.for

The routine CRTSHOW displays the specified matrix to the screen. The entry CRTSTOR writes the matrix to the specified file. These routines are called by CONSLICE.

Subroutine PLOTSAV in Arrdis.for

The following subroutine stores the map in one of two standard plot format: ASCII (SMAP file) or binary (SBM file). These routines are called by Conslice.

Subroutine PLOTREAD in Arrdis.for

This routine reads data from a file written in one of two standard plot formats and places it in the array RMAP. The two formats are ASCII SMAP files and binary SBM files. These routines are called by Conslice.

Subroutine PLOTCONTOUR, by Joseph L. Hora

Scales and Plots part of 2-p array (XDM x YDM) defined by x-values from IXLO for NXP points, y-values from IYLO for NYP points. Note: This is W.N. Johnson's PLOT_CONTOUR routine with the scaling procedures altered to label the axis with real values.

Subroutine CONSCALE in Plotcontour.for

Select scaling parameters for display of channels CMIN thru CMAX maximum of MAXTICS labeled tics on axis returns NTICS - actual # of labeled tics, MINTICS - number of minor tics per tic, plot scaling variables PMIN, PMAX, PDELTA, and format of labels - FORM.

Subroutine ANALYZE in Plotcontour.for

The following subroutine will calculate the "slice" as used in matrix and other programs. The routine divides the slice into 150 segments and will either average or integrate the values across the width of the segment. This will be done in the direction from $[V(1,1),V(1,2)]$ to $[V(4,1),V(4,2)]$. These values will be in the matrix plot(150) when the routine has finished.

Subroutine SUBTR in Psubtr.for

This routine is designed to be used with the Conslice program. The purpose is to subtract a source from a reconstructed image interactively. The input parameters are the low and high pixel coordinates in each of the coordinate directions.

Subroutine RADIAL in Radialx.for, by W. R. Purcell, adapted by Joseph Hora

This subprogram will calculate the flux vs. radial distance. Also it will find the radii for the FWHM, 50% and 90% counts as well as the number of counts within these radii.

Subroutine PAREA in Radialx.for

This will be a subroutine to calculate the area of a pixel with (x,y) as the lower left-hand coordinate within a circle of radius r . Note: Coordinates are relative to the center of the desired circle. Program will only work for pixels part which must be in the first quadrant. Also program will not work for pixel in which the origin is located.

Subroutine SCANLOAD

This routine loads the scans into the matrices required for the BACKPRO, MAXENT4, and MENT programs. This routine can handle data files in the CLUSMOD format or the "galactic center" format used in the SCANSWP program.

Subroutine WARP in Warper.for, by Joseph L. Hora

The purpose of the following routines is to convert from a curved space of RA and DEC to a flat space centered on $(0,0)$, and to perform the reverse transformation. The routines actually merely rotate the coordinates to 0,0 in degrees, which is as close to flat as we want it! The routines are entirely self-contained.

Subroutine PLOT4

Written by Anne L. Kinney at Northwestern University for the plotting of SPD files of the Spartan project. Modified by Jim Pendleton.

G. Utility programs (UTIL)

Program CENTER

Computes best fit to a set of points in one of two ways: (1) the centroid of two or more points, or (2) the center of a circle from three or more points on the circle. Specify the coordinates in namelist format in a CEN data file. The program asks for the name of the data file, the accuracy to which the solution is to be taken, and then uses a random walk to find the center. The results of each iteration are reported, ending with the iteration in which the desired accuracy is achieved. If desired, the solution may be then be taken to greater accuracy.

The accuracy is defined as the size of the step in x and y beyond which the solution yields a poorer fit. In case 1, the fit is performed by minimizing the sum of squares of the distances from the current center point and the stepped-away center points to the input points. In case 2, the fit is performed by calculating the distances from the current center point and the stepped-away center points to the input points and then minimizing the standard deviations.

Program CONTENTS

Determines the record contents of indexed Spartan files. For those files whose records are spaced apart in IU-length intervals, Contents prints the key values of first and last records of each series of records it finds that are spaced in IU-length intervals. For other records, it prints the start and stop values of each record in the file.

Command procedure SFITSMOUNT

For mounting tape containing Fits-format SMAP files. Mount the tape physically and then type the command SFITSMOUNT. When prompted, type the name of the tape unit. SFITSMOUNT allocates and mounts the unit. After you are done with the tape drive, use the command SFITSHALT to release the unit.

Command procedure SFITSHALT

Used to dismount tape mounted by SFITSMOUNT.

Program SBMSMAP

Converts an SBM file to an SMAP file. An SMAP file is an ASCII map file produced by the Cray program MAXENT and converted to an image by the plotting program CONSLICE. An SBM file is a binary version of an SMAP file.

Program SMAPSBM

Converts an SMAP file to an SBM file. An SMAP file is an ASCII map file produced by the Cray program MAXENT and converted to an image by the plotting program CONSLICE. An SBM file is a binary version of an SMAP file.

Program SMAPFITS

Writes SMAP files to a FITS tape. Allows multiple files to one tape, overwriting any files that already exist on the tape. The program also allows the option of changing the scale factor, which is the number that the pixel values in the disk file are multiplied by in order to get suitable integer values for the tape. The FITS header contains the actual value of the scale factor, so you are free to choose any factor that works for the data.

Program FITSHEAD

Reads and prints FITS headers from a FITS tape. Since the tape may have more than one file, the user specifies the file number whose header he wishes to display. Files are numbered consecutively starting with 1. The program gives the user the option of writing the output to a .FHDR file.

H. Miscellaneous Spartan programs (SPAR)

TIMECONV subroutines

The following eight subroutines are used in translating between three time formats: sexagesimal character ('hh:mm:ss.sss'), target-event (explained below), array (hour, minute, second, and millisecond), and integer millisecond (the total time expressed in milliseconds). These routines reference a character variable, an integer*4 array, and an integer*4 variable. The character variable must be declared 12 characters long, and the array must consist of four 4-byte integers, which are hour, minute, second, and millisecond, in order.

There are eight routines:

TIMESTRARR	converts sexagesimal or target-event string to array
TIMEARRVAL	converts array to integer millisecond value
TIMESTRVAL	converts sexagesimal or target-event string to integer millisecond value
TIMEVALARR	converts integer millisecond value to array
TIMEARRSTR	converts array to sexagesimal string
TIMEVALSTR	converts integer millisecond value to sexagesimal string
CODETIME	converts target-event string to integer millisecond
TIMECODE	converts integer millisecond to target-event string

TIMESTRARR and TIMESTRVAL have an alternate return which is taken when there is a format error in the character variable.

The seventh routine, CODETIME, is called by TIMESTRARR and TIMESTRVAL to convert target-event format to integer millisecond. See section V for a detailed description and list of target-event codes.

Program TIMEEVAL

Evaluates times using the TIMECONV routines.

SEXCONV subroutines

These routines convert between decimal and sexagesimal (degree, minute, second) formats. There are four routines:

SEXDEC	converts from three integers (degree, minute, second) to floating degree.
DECSEX	converts from floating degree to three integers (degree, minute, second).
SEXVAL	converts from character variable in DDD.MM'SS' format to floating degree.
VALSEX	converts from floating degree to DDD.MM'SS' character variable.

Program SEXEVAL

Converts between decimal and sexagesimal notation (degree/hour, minute, second). At the prompt you may enter a value in either format and the value will be displayed in both. The format for sexagesimal notation is DDD.MM'SS". Fractional seconds are not allowed.

Subroutine EULER

Written by Daryl J. Yentis, Naval Research Laboratory, Space Science Division, 1977.

Transforms between astronomical coordinate systems. Input is (ai, bi) and output is (ao, bo).

Angles are input and output in radians.

ai,ao = azimuthal angle (longitude) = 0 to 360 degrees

bi,bo = copolar angle (latitude) = -90 to +90 degrees

The transformation is about the three orthogonal Euler angles phi, theta, and psi, performed as a single rotation about the line of nodes.

```
***          ***          ***          ***          ***
* C(BO)C(AO-PSI) *      * 1      0      0 * * C(BI)C(AI-PHI) *
*              *      *      *      *      * * * * C(BI)C(AI-PHI) *
* C(BO)S(AO-PSI) * = * 0      CTHETA  STHETA * * C(BI)S(AI-PHI) *
*              *      *      *      *      * * * * C(BI)S(AI-PHI) *
*      S(BO)      *      * 0 -STHETA  CTHETA * *      S(BI)      *
**              ***          ***          ***          ***
```

Subroutine CORRELATION

Using two data arrays, this subroutine calculates the linear correlation coefficient and the probability of no correlation (from "Random data" by Bendat and Piersol, p.128).

Subroutine PROB

Evaluates the Gaussian integral from - x to + x using DGAUSPRB.

Function DGAUSPRB, by John F. Meekins

This routine is designed to generate an approximate Gaussian probability function, i.e., the area under $\exp(x^2/2)$ from minus infinity to x.

Subroutine TARGETS

Used to define target position (RA,dec), sequence, and name at a given mission elapsed time (MET) in integer milliseconds. This program also returns circuit number.

Program TARGEVAL

Uses the subroutine TARGETS to display target information at a given MET.

Subroutine MAPCEN

Defines a coordinate system with (racen, deccen) at (0,0) for subsequent calls to Euler routines. Racen and deccen should be in degrees, although calls to Euler should be in radians.

Subroutine ROTVAL

Performs coordinate transformations between systems rotated at a given angle with respect to one another.

Program MAPEVAL

Converts between (x,y) and (ra,dec) coordinates. You may specify a rotation angle: if you are converting from (ra,dec) to (x,y), first a conversion to orthogonal (x,y) is made, and then the (x,y) coordinates are rotated counterclockwise to (xl,y1); if you are converting from (x,y) to (ra,dec), the input is taken to be oblique and is first rotated clockwise to orthogonal (x,y), and then the (x,y) is converted to (ra,dec). You may enter all the arguments in either decimal or degree-minute-second format. Output is both in decimal and degree-minute-second.

Subroutine FELINE

Calculates the channel in which the iron line peaks in each detector and layer for a given mission elapsed time (MET). The iron line channels are returned in FECHAN, which is a 2x2 matrix: the first dimension is detector, and the second is layer.

Program FELEVAL

Uses the subroutine FELINE to display the calculated position of the iron line at a given MET.

Subroutine SFIND

This routine searches the array lword for the word iword and returns its position in nword. If not found, nword = 0.

Subroutine POLYMOD

Polynomial evaluation routine.

Subroutine CIRCLE

Determines the values of x and y for n points on the circle centered at (x_{cen}, y_{cen}) with given radius.

III. DATA STRUCTURES

A. Integration Unit structure

Each ET tape record consists for four integration units, simply concatenated. An integration unit consists of 1696 words and hence a tape record consists of 6784 words or 13568 bytes.

An integration unit (IU) consists of 53 lines, numbered 0 to 52, of 32 words each, numbered 0 to 31. Lines 0 to 4 form area 1, the IU header; lines 5 to 8 form area 2, the area for the PHA data from detector 1, layer 1 (D1L1); lines 9-12 are area 3, for D1L2; lines 13-16, area 4, D2L1; lines 17-20, area 5, D2L2; lines 21-36 are area 6, where the paragraph for layer 1 is duplicated; and lines 37-52 are area 7, where the paragraph for layer 2 is duplicated. See schematic at end of write-up.

Following is a description of the contents of each word in IU area 1 (see IU schematic):

Data in header (area 1):

Line 0:	Word(s)	Name	Data type
	0- 1	Target name	ASCII
	2	Target sequence no.	integer*2
	3	Orbit no.	integer*2
	4	Memory ID/index counter	bits
		high byte: layer 1	
		bit 15: memory ID	
		bits 12-8: index counter	
		low byte: layer 2	
		bit 7: memory ID	
		bits 4-0: index counter	
	5	Day of year	integer*2
	6- 7	GMT	4
	8- 9	Mission elapsed time (MET)	4
	10-11	Paragraph counter, layer 1	4
	12-13	Paragraph counter, layer 2	4
	14	Data quality flag (0-okay)	2
	15	Aspect monitor flag	2
	16-17	Tracker start x-coord. in deg. x 10,000	4
	18-19	Tracker start y-coord. in deg. x 10,000	4
	20-21	Tracker stop x-coord. in deg. x 10,000	4
	22-23	Tracker stop y-coord. in deg. x 10,000	4
	24-25	Scan angle in degrees x 10,000	4
	26	Target angle in degrees x 100	2

27	Earth angle in degrees x 10	2
28	Sun angle in degrees x 10	2
29	Satellite longitude in degrees x 10	2
30	Satellite latitude in degrees x 10	2
31	Satellite altiutde in kilometers x 10	2

Line 1: Word(s) Name Data type

0-15	XRAS1 channels 0-15	integer*2
16-31	XRAS2 channels 0-15	2

Line 2: Word(s) Name Data type

0-31	XRAS3 channels 0-31	integer*2
------	---------------------	-----------

Line 3: Word(s) Name Data type

0- 6	XCTR1-XCTR7	integer*2
7-13	XCTR8-XCTR14	2
14-15	Target RA in degrees x 10,000	4
16-17	Target dec in degrees x 10,000	4
18-25	(unassigned)	
26	Sync error total	2
	(no. bits set in sync error bitmaps)	
27	PHA PEF total	2
	(no. bits set in PHA PEF bitmaps)	
28-29	Sync error bitmaps, layer 1	4
	bits 31-0 map lines 0-31 resp.	
30-31	Sync error bitmaps, layer 2	4
	bits 31-0 map lines 0-31 resp.	

Line 4: Word(s) Name Data type

0- 7	PHA PEF bitmaps, D1L1	integer*2
8-15	PHA PEF bitmaps, D1L2	2
16-23	PHA PEF bitmaps, D2L1	2
24-31	PHA PEF bitmaps, D2L2	2
	In all PHA PEF bitmap areas:	
	word 0, bits 31-0 map channels 0-31, resp.	
	word 1, bits 31-0 map channels 32-63, resp.	
	...	
	word 7, bits 31-0 map channels 96-127, resp.	

PHA data (areas 2-5):

The counts for each channel are recorded one channel to a word. In the paragraph the PHA data word includes a PEF and a memory bit; in the PHA data area these are stripped from the word and the word is right shifted one bit. In the first line are channels 0 to 31, in the second line 32-63, in the third, 64-95, and in the last, 96-127. Since these lines are sequential in the buffer, the channel number plus the address of the start of the area gives the address of the channel number in the buffer.

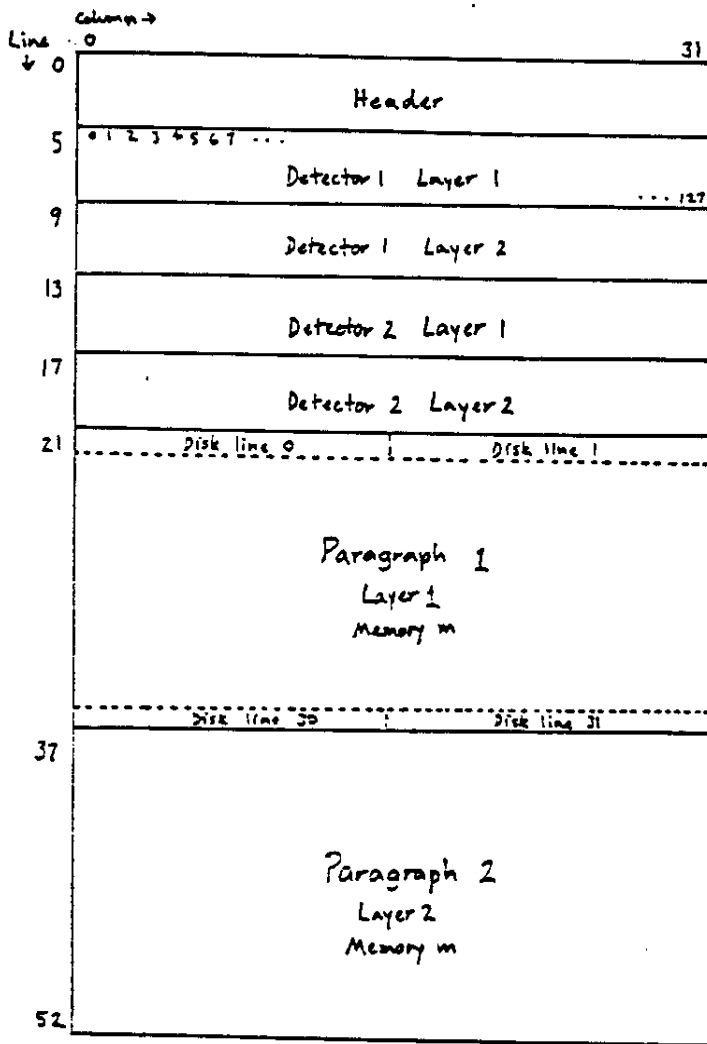
Paragraphs (areas 6 and 7):

The two paragraphs from which the IU is generated are reproduced in these two areas.

9/18/86

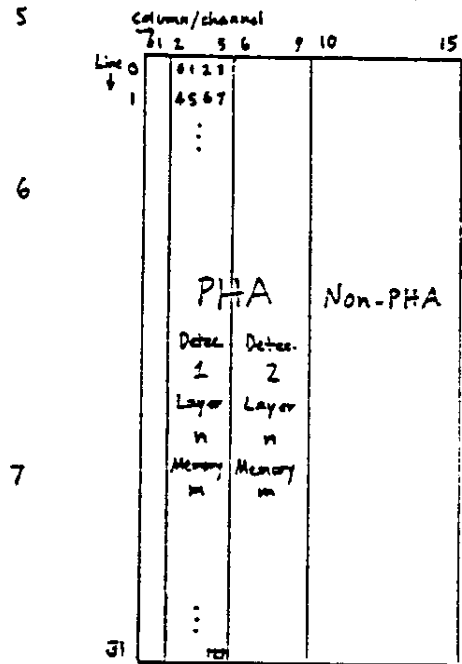
Integration unit format

Output from ETGEN (Experimenters' tape generator)

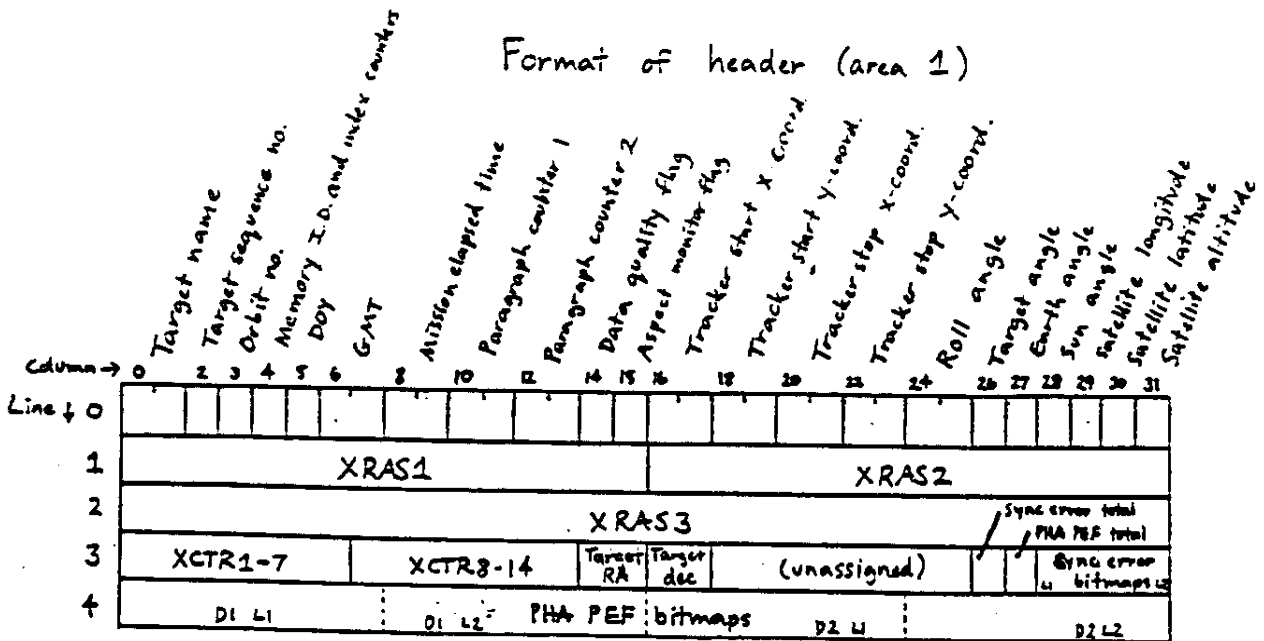


An integration unit (left and bottom) is constructed from two disk paragraphs (below). PHA channels run from 0 to 127 in each layer; this order is preserved in areas 2-5 of the integration unit. The paragraphs are preserved in their original format in areas 6 and 7. Two paragraph lines (16 words) equal one integration unit line (32 words).

Disk paragraph



Format of header (area 1)



B. IU Paragraph Structure

The paragraph is designed to be a self-sufficient package of information. Each paragraph is arranged as 32 lines by 16 columns of 16-bit words.

Column 1 of each line contains two distinct bytes of information:

Upper byte: The sync error for that line. This is either an exceptional condition reported on NASA tapes or the result of an error by an NRL program. The sync error is 0 unless one of two conditions holds: (1) the minutes byte of the corresponding line in the NASA paragraph is over 60, in which case the sync error is equal to this number; or (2) one of the ICNT values indicates that there was a read error on either STC or SGEN which affected this line, in which case the sync error is set to 110 (STC read error) or 121 (SGEN read error). STC and SGEN are part of NRL's software system for converting NASA tapes to experimenters' tapes.

Lower byte: In the two nibbles (a nibble is a data unit of 4 bits), two counts of parity error flags (PEF's) set on that line. PEF's are errors that are reported on NASA tapes.

Upper nibble: The total of PEF's set in channels 2 through 9 (the PHA channels) of the line.

Lower nibble: The total of PEF's set in channels through 15 (non-PHA channels) of the line.

Column 0 of the disk paragraph is assigned a variety of parameters, a different one to each line. These parameters pertain to the paragraph as a whole. By line number, these parameters are:

0- 3 Paragraph time. These four words are the hour, minute, second, and millisecond given by NASA in the line 0 of the tape paragraph. In the event the minute in line 0 has been overwritten by a sync code, the following line(s) are searched until a non-error minute code is located. In this process the seconds are also watched as the lines are searched, and if the seconds turn over, the minute when found is turned back one.

4- 5 Lines 4 and 5 contain the paragraph counter assigned by NASA to each paragraph, which should be a unique identifier for every paragraph of NASA data. They are stored in the tape paragraph in two data words on line 31 in channels 14 and 15 and are therefore transmitted to the same location in the disk paragraph. Since only 9 bits of each 16-bit word are used by NASA, the high part is only 2^{*9} times as significant as the low part rather than 2^{*16} . In order to provide a FORTRAN-format integer for the paragraph counter, then, the high part is multiplied by 2^{*9} and added to the low part and the result stored as a 4-byte integer in lines 4 and 5, high part first, and this is the version which is also stored in the status array in the key file.

- 6 Grand error total. This is simply the total of lines 7 to 10 and is intended as a quick indication of the reliability of the data in the paragraph. Zero in this word indicates that no errors of any kind were discovered in the course of generating this paragraph.
- 7 PHA PEF total. This is the sum of all 32 parity error flag counts in the upper nibble of the lower byte in column 1 and as such is the number of parity error flags set in the PHA channels in the paragraph.
- 8 Non-PHA PEF total. This is the sum of the parity error flag counts in the lower nibble of the lower byte in column 1 and as such is the number of parity error flags set in the non-PHA channels in the paragraph.
- 9 Sync error total. This is the total number of sync errors in the paragraph, that is, the number of nonzero entries in the upper bytes of column 1.
- 10 Read error total. This is the total number of read errors affecting this paragraph, that is, the number of positive entries in lines 12, 14, 25, and 27 of column 0.
- 11 Data quality flag. This is set as follows: it has the value 256 if the read error total is nonzero; otherwise it is the total of the PHA error total for all 32 lines. The PHA error total is defined as 8 if the sync error for the line is nonzero; otherwise it is the PHA PEF count for the line.
- 12-13 The IER and ICNT values written to the 6250 bpi tape by STC.
- 14-15 The IER and ICNT values returned by the reads in SGEN.
- 16-22 The mission start (release) time as recorded in record 0 of the NASA tape is given here for positive identification of the data in this paragraph. The format is year, month, day, hour, minute, second, and millisecond.
- 23 The tape number as recorded in record 0 of the NASA tape.
- 24 The tape number as recorded in record 0 of the 6250 bpi STC tape. This is the tape number specified in the STC.IN file by the user of STC.
- 25-26 The IER and ICNT values which are written to the 6250 bpi tape by STC for the read from record 0 of the NASA tape.
- 27-28 The IER and ICNT values which are returned in SGEN for the read of record 0 of the 6250 bpi tape.
- 29-31 Unused.

Columns 2-15 of the IU paragraph correspond to the original data format as supplied by NASA.

Paragraph format on disk Output from SGEN (Spartan database generator)

Column →

Line ↓

	0	1	2	...	14	15
0	par. time: hr.	sync err.	PHA PEF	NPA PEF		
1	min	"	"	"		
2	sec.	"	"	"		
3	msec.	"	"	"		
4	par. ctr: hi	"	"	"		
5	lo	"	"	"		
6	grand err. total	"	"	"		
7	PHA PEF total	"	"	"		
8	NPHA PEF total	"	"	"		
9	sync err. total	"	"	"		
10	read err. total	"	"	"		
11	data opt. flag	"	"	"		
12	STC ier	"	"	"	Spacecraft	
13	STC icnt	"	"	"		
14	SGEN ier	"	"	"	data	
15	SGEN icnt	"	"	"		
16	launch: yr.	"	"	"		
17	mo.	"	"	"		
18	day	"	"	"	channels 2-15	
19	hr.	"	"	"		
20	min.	"	"	"		
21	sec.	"	"	"		
22	msec.	"	"	"		
23	NASA tape no.	"	"	"		
24	STC tape no.	"	"	"		
25	STC rec. # ier	"	"	"		
26	STC rec. # icnt	"	"	"		
27	SGEN rec. # ier	"	"	"		
28	SGEN rec. # icnt	"	"	"		
29	(unassigned)	"	"	"		
30	(unassigned)	"	"	"		
31	(unassigned)	"	"	"	par. ctr. hi	par. ctr. lo

Notes

1. Data units are 16-bit words.
2. STC and SGEN status words are generated by tape reads during the respective programs. Ier if positive is the read error, if negative is -icnt. Icnt is the number of bytes successfully read in the record.
3. STC tape number is assigned by the user during STC to each NASA tape.
4. Format of channel 2: upper byte is the line minute byte if over 60, else 0; upper nibble of lower byte is the number of PEF's (parity error flags) in the PHA channels (2-9) on that line; lower nibble of lower byte is same for the non-PHA channels (10-15).
5. Words (0,0) to (0,6) form the status array. Word (0,6) is simply a total of (0,7) through (0,10).
6. Word (0,11) is the sum of PHA totals for each line. PHA total is 8 if sync error for that line is nonzero, else the PHA PEF count for that line.
7. Par. counter in (14,31) and (15,31) is 9-bit version; in (0,4) and (0,5) is 16-bit version.

C. Differences between IU format and SPD and CSD records formats

An SPD record has the same structure as and Integration Unit (IU) except that areas 6 and 7 (the original paragraphs that make up the IU) are not duplicated. The SPD records is so named because it preserves the detailed Spectral Data present in an IU.

SPDGEN makes the following changes to words 5, 6, and 7 of line 0 of the IU: Word 5 is now the experimenter flag word which is intended to be used as a field of bit flags in other programs. It is presently set to 0 in this program. Words 6 and 7 are the iron line channel codes: the upper byte of word 6 is the channel code for the iron line peaks in this IU for detector 1, layer 1 (D1L1); the lower byte of word 6 is the iron line channel code for D1L2; the upper byte of word 7 is for D2L1; and the lower byte of word 7 is for D2L2. The channel code is derived from the iron line channel by the following formula: channel code = NINT(10*(channel-50)), where NINT means nearest integer.

A CSD (Condensed Scan Data) record consists of two lines of 32 words each. The first line of the CSD record, except for word 4, is the same as the first line of the SPD record, which except for words 5 and 6 is the same as the first line of the integration unit (IU). Word 4 in the CSD first line consists of XCRAS flags, the upper byte for detector 1, the lower byte for detector 2, with the following bit assignments in each byte:

bit 0: H. V. off
bit 1: auto shutdown
bit 2: calibration on
bit 3: purge valve open

The second line is assigned as follows:

words 0- 1: XCTR 1- 2
words 2- 4: XCTR 5- 7
words 5- 6: XCTR 8- 9
words 7- 9: XCTR 12-14
words 10-11: sync/PEF for D1-D2 resp. (high byte: L1; low byte: L2)

Within each byte of words 10 and 11, bits 7-3 are assigned to broadband PHA channels 0-4 respectively, where each bit indicates whether a sync error OR PEF was set in any single PHA channel which is included in the broadband sum.

A broadband PHA channel is a sum of individual PHA channels within the detector and layer. The telemetric 128 channel PHA spectrum is divided into 5 intervals, corresponding to fixed energy bands [i.e., channel 0 : 0.1-2 keV; channel 1 : 2-5 keV; channel 2 : 5-7 keV; channel 3 : 7-14 keV; and channel 4 : > 14 keV]. The actual PHA channels summed into various wide bins is based on the PHA channel containing the Fe-line calibration peak.

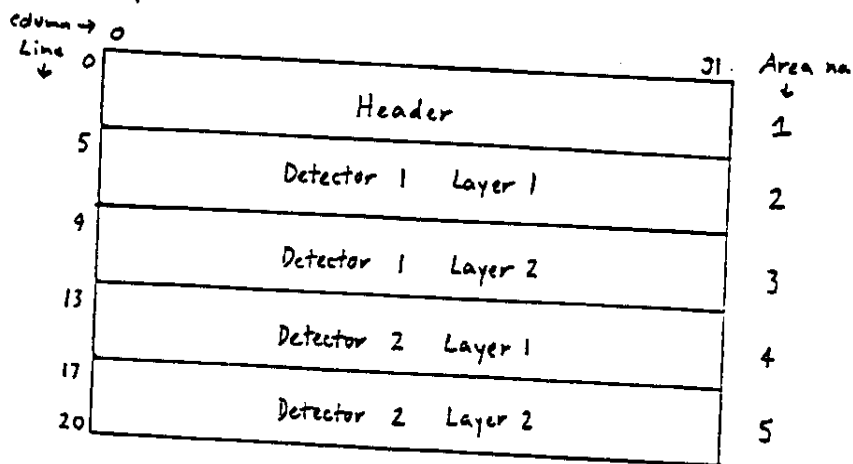
The broadband channels are assigned to the following CSD words of the second line :

words 12-16: D1L1 broadband channels 0-4 resp.
words 17-21: D1L2 broadband channels 0-4 resp.
words 22-26: D2L1 broadband channels 0-4 resp.
words 27-31: D2L2 broadband channels 0-4 resp.

The iron line channel is coded for each detector and layer in line 0, words 6 and 7. Detector 1 is coded in word 6 and detector 2 in word 7; layer 1 is coded in the upper byte, and layer 2 in the lower byte. In each byte, the channel code = $\text{NINT}(10 * (\text{channel} - 50))$, where NINT means nearest integer.

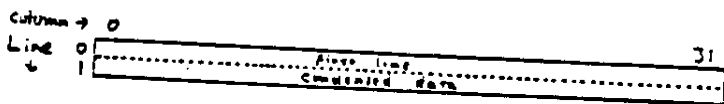
Differences between Integration Unit Format and Spectral Data and Condensed Data Records

Spectral (SPD)



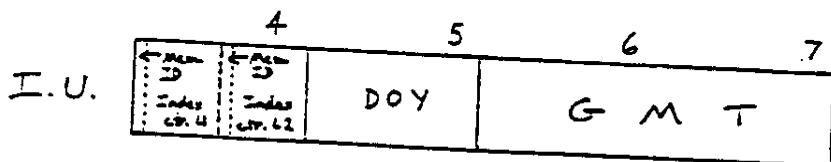
The spectral data record is the same as the I.U. except that the paragraphs are not duplicated in areas 6 and 7, and columns 5, 6, and 7 in line 0 are changed (see below).

Condensed (CSD)

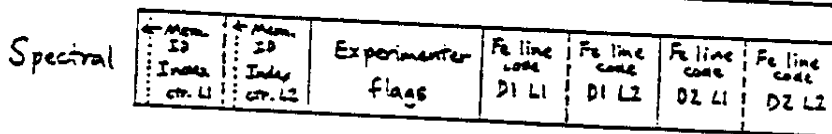


The condensed data record is only two lines. Line 0 is the same as line 0 of the I.U., except columns 4, 5, 6, and 7 (see below). Line 1 is a squeezed and summed data line (also see below).

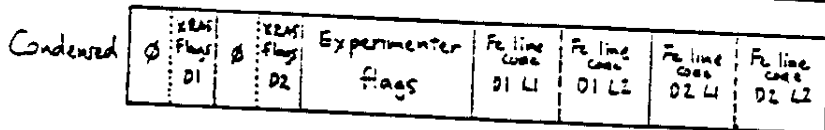
Words 4, 5, 6, and 7 of line 0:



Memory ID for each layer is in high bit of each byte of word 4. Index counter occupies rest of byte.

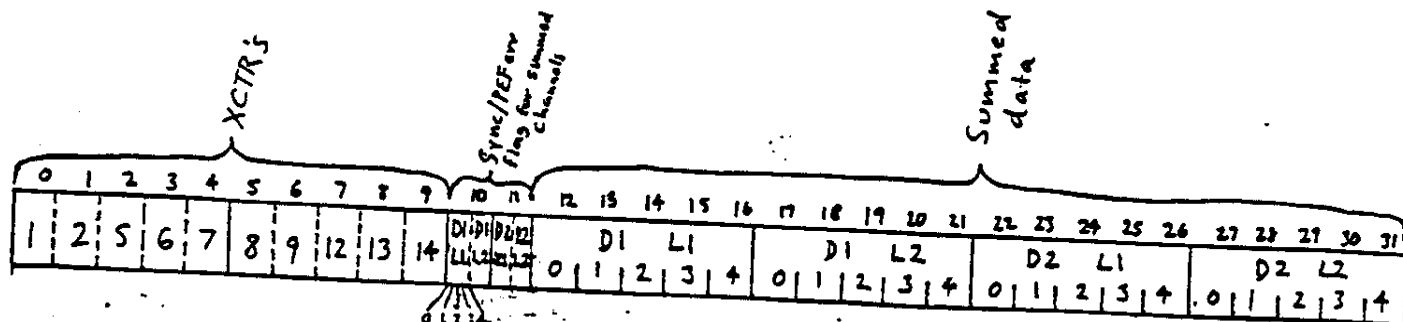


In spectral file, DOY is replaced with experimenters flags set after generation of Spectral file, and iron line channels codes replace the GMT.



In Condensed file, XRAS flags replace memory ID-index counters, as well as changes made to spectral file.

Line 1 of Condensed Data Record



D. Condensed Scan Sum (CSS) record and file structure

CSS is the name of the structure which includes both the CTS (Condensed Time Sum) and the CRS (Condensed Radial Sum) structures, since these two are nearly identical. The format of the CSS record is as follows:

No. of words	Data type	Item
32	As in CSD	Duplication of line 0 of the first CSD record to be added in
32	As in CSD	Duplication of line 0 of the last CSD record to be added in
4	Real*4	In CRS: x- and y-coordinates of center point
4	Integer*4	In CTS: zeroes
10	Integer*2	In CRS: Inner and outer radii x 10,000
10	Integer*2	In CTS: zeroes
10	Integer*2	Duplication of XCTR's of the first CSD record to be added in
8	Real*4	Duplication of XCTR's of the first CSD record to be added in
40	Real*4	Total number of records added into each detector and layer. In CRS this may be fractional. Summed counts for each CSD channel in each detector and layer. In CRS these may be fractional.

The CTS file simply consists of a series of CTS records whose times and data are completely independent. Each run of CTSGEN simply adds one record to the file.

In the CRS file, on the other hand, the records are highly interdependent. All the records in a CRS file have the same start and stop MET's and the same center point. In addition, the outer radius of one record is the inner radius of the next record, so that there are no gaps or overlaps from the center point to the outermost radius. On a run of CRSGEN, if the CRS file does not exist, it asks for the start and stop MET's, center point coordinates, and radii, then it creates all the CRS records at once, and then it adds the data. If the file already exists, it will ask only for start and stop times and then add the new data to the records that are already there. It will also adjust the line 0's and XCTR's if the new data is earlier or later than what has come before.

Format of CSS (Condensed Scan Sum) records and files

CSS is the name of the pattern into which both the CTS (Condensed Time Sum) and CRS (Condensed Radial Sum) records fall.

Duplication of line 0 of the first CSD record summed																			
Duplication of line 0 of the last CSD record summed																			
Cent. RA (CSS only)	Cent. pt. dec (CSS only)	Inner radius (CRS only)	Outer radius (CRS only)	Duplication of XCTR's of the first CSD record summed				Duplication of XCTR's of the last CSD record summed				Tot. D1 L1	Tot. D1 L2	Tot. D2 L1	Tot. D2 L2				
Counts		D1	L1	Counts				D1	L2	Counts		D2	L1	Counts		D2	L2		
0	1	2	3	4	0	1	2	3	4	0	1	2	3	4	0	1	2	3	4

Coordinates of central point of radial sum are real + i. Inner and outer radius of radial sum in arcmin are multiplied by 10,000 and stored as integers. These four positions are zero in the time sum. Totals are real + i and are number of records for each detector and layer that are in the current bin. Counts are also real + i and are summed detector counts. Totals and counts are floating since CSD records may overlap ring boundaries and are then prorated, resulting in fractional increments.

CTS file

Time 1 to time 2	Record 1
Time 3 to time 4	Record 2
Time 5 to time 6	Record 3
.	.
.	.
.	.
Time 2n-1 to time 2n	Record n

First time (start time) is key. Records are independent.

CRS file

Radius 0 to radius 1	Record 1
Radius 1 to radius 2	Record 2
Radius 2 to radius 3	Record 3
.	.
.	.
.	.
Radius n-1 to radius n	Record n

First radius (inner radius) is key. All records in a CRS file have same times and same center point.

E. Spectral Sum (SPS) record and file structure

Analogously to the CSS structure, SPS is the name of the structure which includes both the STS (Spectral Time Sum) and the SRS (Spectral Radial Sum) structures. The format of the SPS record is as follows:

No. of words	Data type	Item
32	As in SPD	Duplication of line 0 of the first SPD record to be added in
32	As in SPD	Duplication of line 0 of the last SPD record to be added in
14	Integer*2	Duplication of XCTR's of the first SPD record to be added in
14	Integer*2	Duplication of XCTR's of the first SPD record to be added in
4	Real*4	RA and dec of target
4	Real*4	In SRS: x- and y-coordinates of center point
4	Integer*4	In STS: zeroes
4	Integer*4	In SRS: inner and outer radii x 10,000
8	Real*4	In STS: zeroes
		Total number of SPD records added into each detector and layer. In SRS these may be fractional.
1024	Real*4	Summed counts for each SPD channel in each detector and layer. In either STS or SRS these may be fractional.

The differences between the STS and SRS file structures are exactly analogous to the differences between the CTS and CRS file structures.

Format of SPS (Spectral Sum) records

Analogous to CSS, SPS is the pattern into which both STS (Spectral Time Sum) and SRS (Spectral Radial Sum) records fall.

Duplication of line # of the first SPD record summed													
Duplication of line # of the last SPD record summed													
Dup. of XCTRS of first SPD record summed						Dup. of XCTRS of last SPD record summed							
01 LI	01 L2	02 LI	02 L2	Targ. RA	Targ. Dec	Cent. RA	Cent. Dec	Inner rad.	Outer rad.	01 LI	01 L2	02 LI	02 L2
Iron line position in sum										Totals			
Summed counts of PHA channels Detector 1 Layer 1													
Summed counts of PHA channels Detector 1 Layer 2													
Summed counts of PHA channels Detector 2 Layer 1													
Summed counts of PHA channels Detector 2 Layer 2													

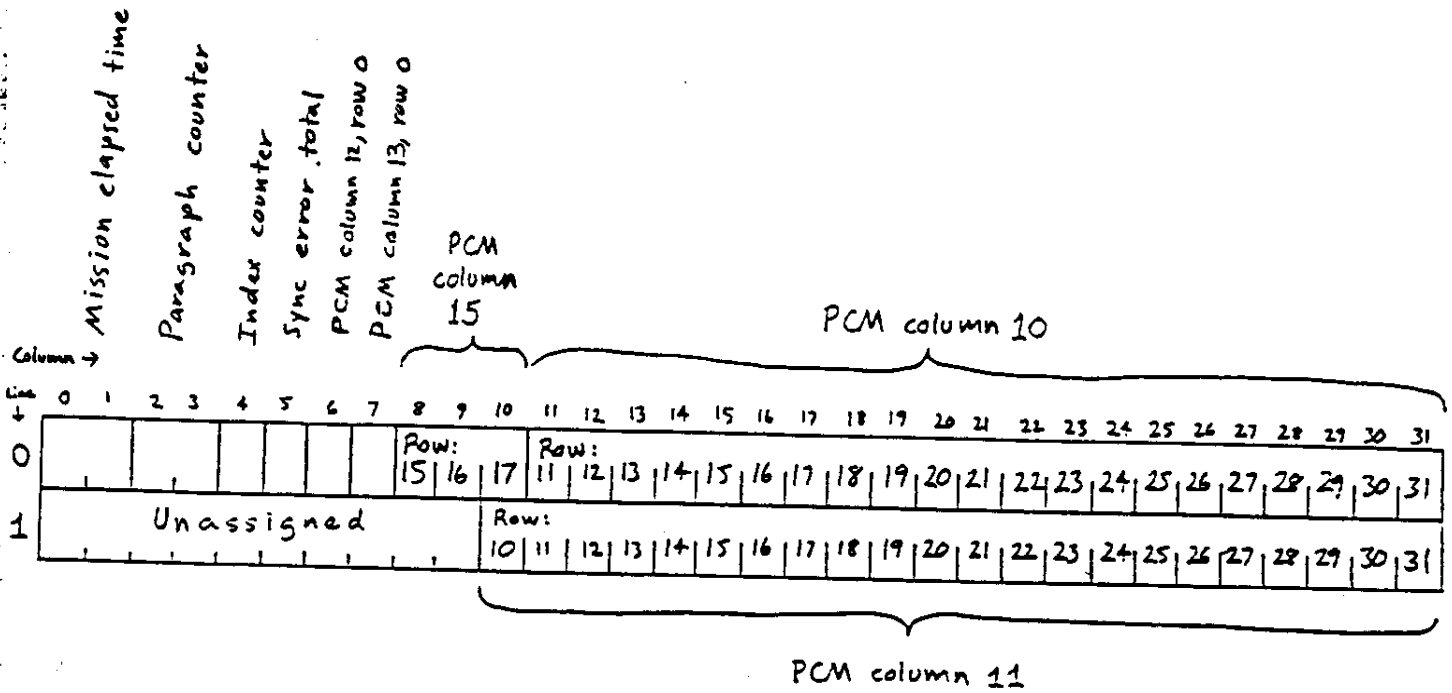
As in CSS, coordinates of target and central point are in real*4, whereas inner and outer radii are in arc minutes times 10,000, stored as integer*4. Coordinates of central point and radii are zero in time sum. Totals and counts are also in real*4. Fractional increments in SPS occur not only from overlapping of ring boundaries but also from channel splitting due to iron line contraction; thus fractional counts occur not only in SRS but also in STS. SPS file structure is same with respect to its records as CSS files.

F. Attitude Control System (ACS) record structure

An ACS record consists of two lines of 31 words each, assigned as follows:

Line 0: words 0- 1: MET
words 2- 3: paragraph counter
word 4 : index counter
word 5 : sync error total
word 6 : PCM column 12, line 0
word 7 : PCM column 13, line 0
words 8-10: PCM column 15, lines 15-17
words 11-31: PCM column 10, lines 11-31
Line 1: words 0- 9: unassigned
words 10-31: paragraph column 11, lines 10-31

ACS Record Format



III. Algorithms

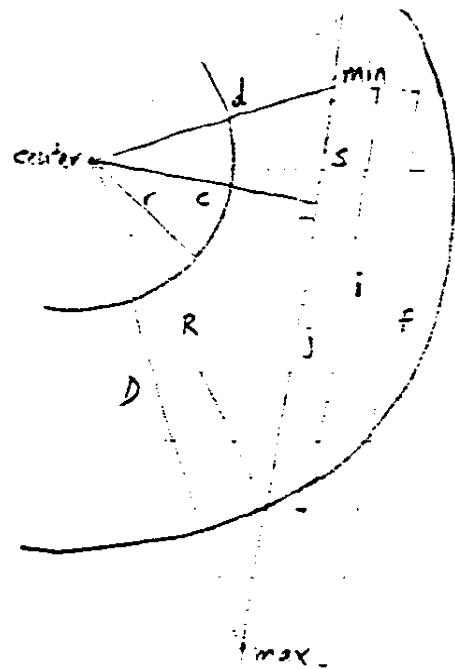
This section contains descriptions of various involved algorithms used in some Spartan programs. This section contains:

- A. Radial summing algorithm used in CRSGENALT and SRSGENALT.
- B. Revised radial summing algorithm used in CRSGEN and SRSGEN.
- C. SPS iron line rebinning algorithm used in SPSADD.

A. Radial summing algorithm (CRSGENACT, SRSGENACT)

Basic strategy is to check a record against every ring. If the record is entirely within a ring, i.e., start and stop times are in the same ring, then add the entire record to the sum; if it is entirely outside the ring, skip adding; if start and stop times overlap ring boundaries, add a portion of the record to both rings. Following is a treatment of the interesting geometrical problem of determining how much of a given record falls into a ring in an overlap.

The scan is assumed to fall on a straight line. From the aspect solution we know the x and y coordinates of the start and stop times, and of course we supply the RA and dec (and from this the x and y are computed) of the center point. The programs calculate which of the start and stop times is closer to the



center point; this is labelled "min" in the diagram. The farther point is, yes, "max". If min is inside the ring but max is outside, then the record overlaps the outer ring boundary; this is shown in the diagram. If max is inside but min is outside, then the record overlaps the inner ring boundary. It is possible that the record could skim a ring by going in and out again, but geometrically this is an unlikely situation and is thus neglected; the data goes entirely to the outer ring.

Secondly, the triangle formed by center, min, and max could be acute or obtuse. We consider the acute case first, as in the diagram.

We assume flat space in all calculations. From the x and y coordinates of the center point and of the start and stop times of the record, the programs calculate the distances from the center point to the start and stop times (called diststart and diststop in the program), and then select which is the lesser of the two (distmin, labelled d in the diagram) and which is the greater (distmax, labelled D). Then we fetch the inner radius of the ring (radin, labelled r), and the outer radius (radout, R). We then determine if $r \leq d \leq R$ (minisin, ie, distmin is within the ring) and then if $r \leq D \leq R$ (maxisir, i.e., distmax is within the ring). If both are in, we add the whole record; if both are out, we take no action; else we have an overlap.

In the latter case we calculate the distance covered by the record (recdist, labelled f). The following derivation shows how we calculate the portion of the record that is within the ring (recin, i).

First we calculate scanspot, labelled s:

$$s^2 + c^2 = d^2 \Rightarrow c^2 = d^2 - s^2$$

$$(f-s)^2 + c^2 = D^2 \Rightarrow c^2 = D^2 - (f-s)^2$$

$$d^2 - s^2 = D^2 - (f-s)^2 = D^2 - f^2 + 2fs - s^2$$

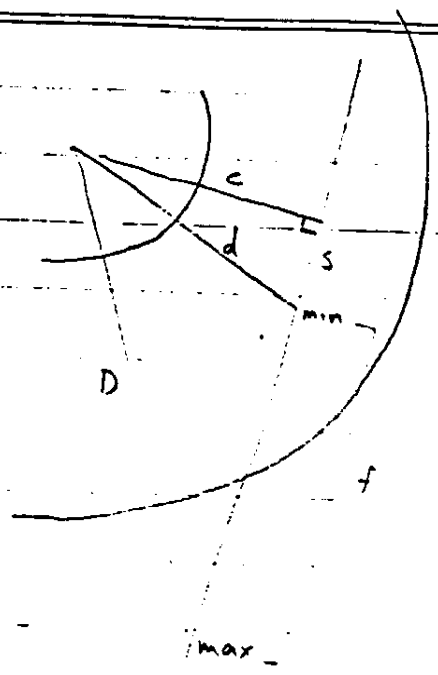
$$d^2 = D^2 - f^2 + 2fs$$

$$2fs = d^2 - D^2 + f^2 \Rightarrow s = \frac{f^2 + d^2 - D^2}{2f}$$

In the obtuse case, we have instead:

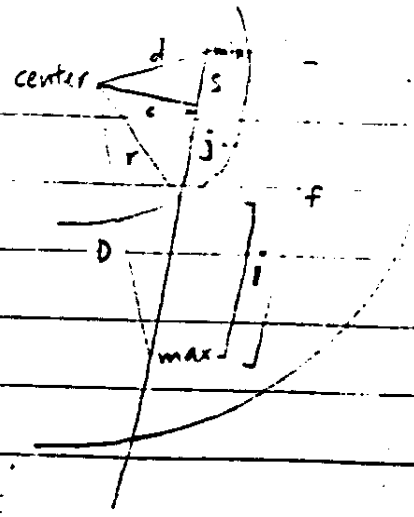
$$s^2 + c^2 = d^2$$
$$(f+s)^2 + c^2 = D^2$$

These equations are identical except for a change in sign of s . Hence if we substitute $-s$ for s , we can use the acute solution for obtuse also. This is done in the programs: if $s > 0$, it is the acute case; if $s < 0$, it is the obtuse case; and if $s = 0$, then the triangle is a right triangle. In all three cases, the same solution for s is used.



The length labelled c is called *censhot* in the program. It is given by $c^2 = d^2 - s^2$ from the first line of the derivation. Now we bifurcate, depending on whether the inner or outer ring boundary is overlapped. If, as in the diagram, the outer radius is overlapped, then $c^2 + j^2 = R^2$, and so $j^2 = R^2 - c^2$ and $i = s + j$.

But if the inner radius is overlapped, then $c^2 + j^2 = r^2$, and so $j^2 = r^2 - c^2$, and $i = f - s - j$.

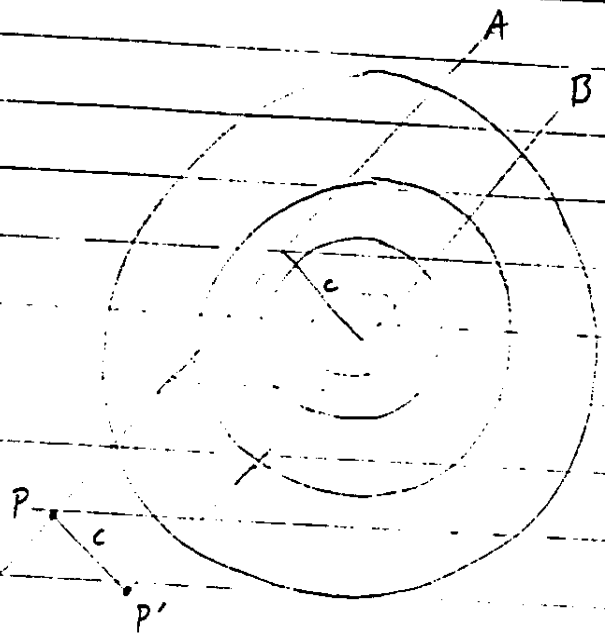


The proportion of the record to add in (factor) is i/f .

B. Revised radial summing algorithm (CRSGEN, SRSGEN)

The radial summing algorithm was modified to employ a line through the target center.

In this case we draw a line B parallel to the scan line A and separated from it by a distance c , called sepline in the programs.



Each point P on A is mapped across to a point P' on B . Then the distance P' is from the center is used to determine what ring P is in. From there we proceed as in the old algorithm: we test for the positions of the endpoints of a CSD or SPD record and add in the portion of that record that falls within the ring.

The new geometric problem is to compute c and to calculate the coordinates of P' .

We draw $PQ \parallel x$ -axis and $QS \perp$ line B .

Now $QP = x$ and $\angle QPS = \theta$, the roll angle. Hence $\sin \theta = \frac{QS}{QP} = \frac{QS}{x}$, so

$QS = x \sin \theta$. R , the point where

line B intersects QS , forms a

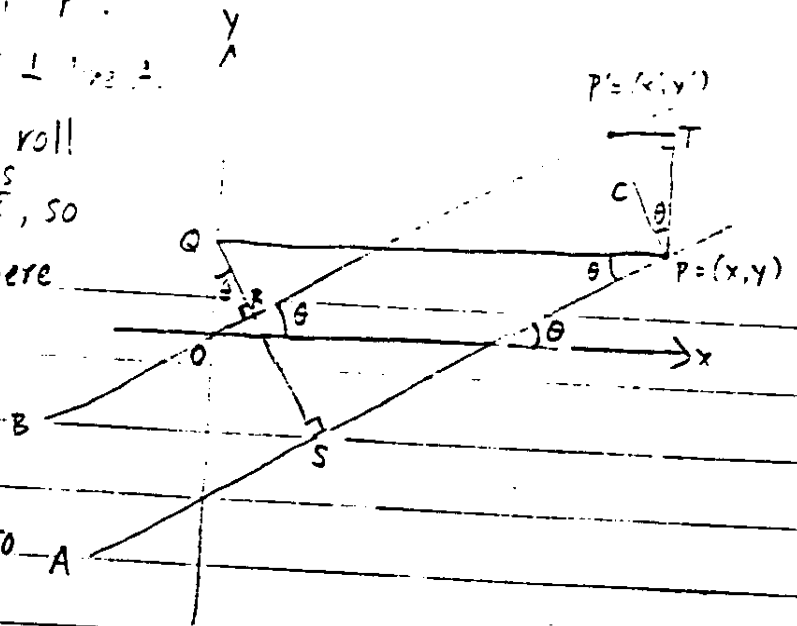
right triangle with Q and O .

Now $QO = y$ and since $\angle PAS = \theta$,

$\angle OQR = \theta$. Hence $\cos \theta = \frac{QR}{QO} = \frac{QR}{y}$, so

$QR = y \cos \theta$. Thus $c = PP' = RS =$

$QS - QR = x \sin \theta - y \cos \theta$



Next we draw T so that $PT \parallel y$ -axis and $P'T \parallel x$ -axis.

$\angle P'PQ = \cos \theta$, and $\angle TPA$ is a right angle, so $\angle TPP' = \theta$. Hence

$\sin \theta = \frac{P'T}{P'P} = \frac{P'T}{c}$ and $\cos \theta = \frac{PT}{P'P} = \frac{PT}{c}$, so $P'T = c \sin \theta$

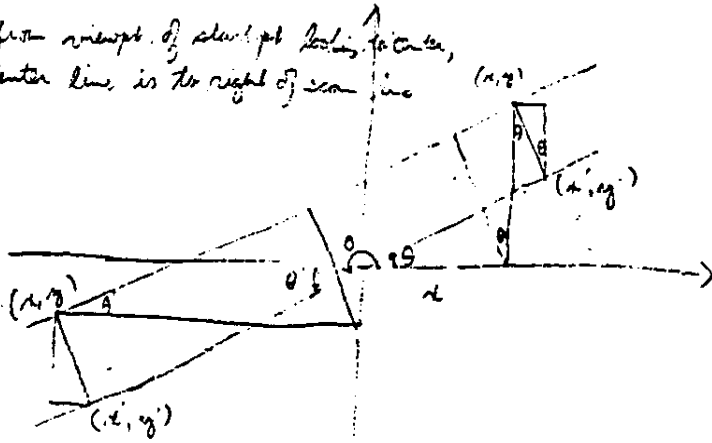
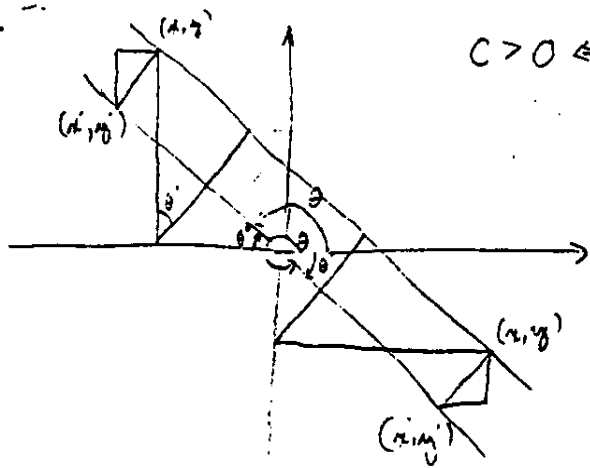
and $PT = c \cos \theta$. We have $P'T = x - x'$, so $x' = x - P'T = x - c \sin \theta$,
and $PT = y' - y$, so $y' = y + PT = y + c \cos \theta$.

There are eight variations on the above algorithm, depending on the quadrant θ is in and which side of B the original line A falls on. It turns out that if you rotate the paper so that P is at the bottom and the origin above it, c is positive if A is to the left of B , and c is negative if A is to the right of B .

If θ is not in the first quadrant, we can define a first-quadrant angle θ' from θ and work with it so that all our lines are positive and all the angles acute. It turns out that in all eight cases the above formulae hold without variation.

On the following page the eight cases are analyzed in detail.

$C > 0 \Rightarrow$ from viewpoint of slant pt looking to center, center line is to right of scan line



II: $\theta' = \pi - \theta$

$$D = |x'| \cos \theta' - |y'| \sin \theta'$$

$$= -x' \cos \theta + y' \sin \theta = C$$

$$x' = x - D \sin \theta' = x - C \sin \theta$$

$$y' = y - D \cos \theta' = y + C \cos \theta$$

IV: $\theta' = 2\pi - \theta$

$$D = |x'| \sin \theta' - |y'| \cos \theta'$$

$$= -x' \sin \theta + y' \cos \theta = -C$$

$$x' = x - D \sin \theta' = x - C \sin \theta$$

$$y' = y - D \cos \theta' = y + C \cos \theta$$

I:

$$D = x' \cos \theta - y' \sin \theta = -C$$

$$x' = x + D \sin \theta = x - C \sin \theta$$

$$y' = y - D \cos \theta = y + C \cos \theta$$

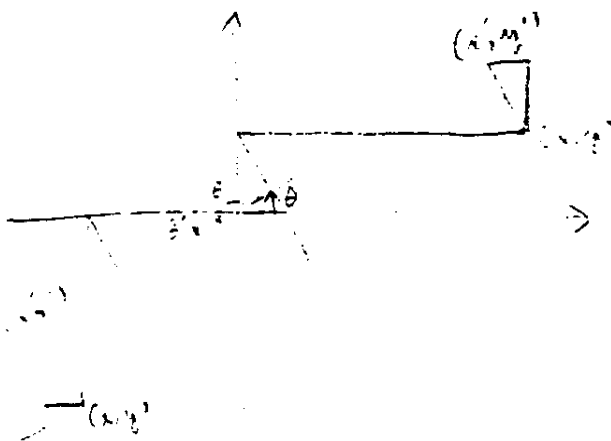
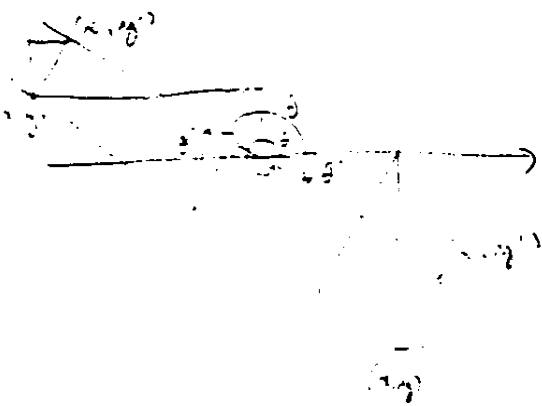
III: $\theta' = \theta - \pi$

$$D = |x'| \sin \theta' - |y'| \cos \theta'$$

$$= x' \sin \theta - y' \cos \theta = C$$

$$x' = x + D \cos \theta' = x - C \cos \theta$$

$$y' = y - D \cos \theta' = y + C \cos \theta$$



I: $\theta' = \pi - \theta$

$$D = |x'| \sin \theta' - |y'| \cos \theta'$$

$$= -x' \sin \theta + y' \cos \theta = -C$$

$$x' = x + D \sin \theta' = x - C \sin \theta$$

$$y' = y + D \cos \theta' = y + C \cos \theta$$

II: $\theta' = 2\pi - \theta$

$$D = |y'| \cos \theta' - |x'| \sin \theta'$$

$$= -y' \cos \theta + x' \sin \theta = C$$

$$x' = x + D \sin \theta' = x - C \sin \theta$$

$$y' = y + D \cos \theta' = y + C \cos \theta$$

I: $D = x' \sin \theta - y' \cos \theta = C$

$$x' = x - D \sin \theta$$

$$y' = y + D \cos \theta$$

III: $D = |y'| \cos \theta' - |x'| \sin \theta' = -C$

$$x' = x - D \sin \theta' = x - C \sin \theta$$

$$y' = y + D \cos \theta' = y + C \cos \theta$$

c. SPS Iron Line Rebinning

The subroutine `Spsadd_rebins` SPD records before adding them to SPS. This is done because of detector gain shifts during the mission, as measured by iron line calibrations throughout the mission. The gain changes so that the iron line steadily decreases in channel number as MET increases.

All the SPS records generated by a run of a program using `Spsadd` contain counts binned with a fixed iron line channel number. By default, for each detector and layer this channel is the iron line position at detector turnon at 02:57:20 MET. Each SPD channel is moved up (higher in channel number) to compensate for the gain having moved the channels down, and then the SPD bin is split into two or three SPS bins.

Channels are proportional to energy, so the SPD channel index, i_{chan} , is increased by multiplying it by the ratio r of the current iron line channel to the fixed SPS iron line. The value of r is at most 1.046. Usually, then the image of an

SPD record under

this multiplication

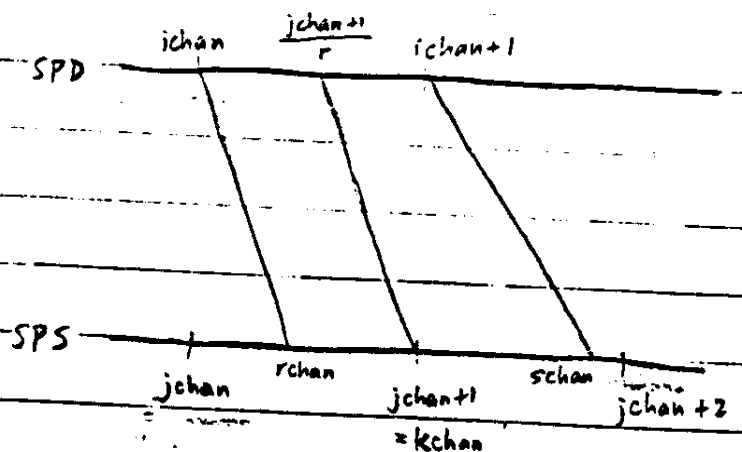
will span two SPS

records. We add the

portion of the SPD record

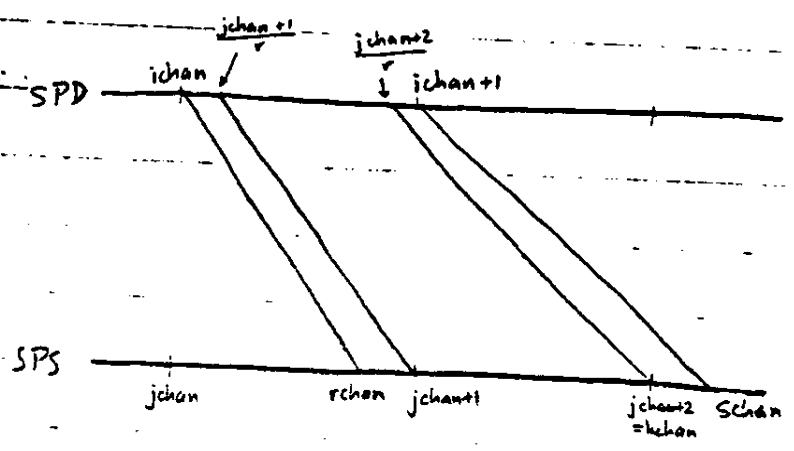
between i_{chan} and $\frac{j_{chan+1}}{r}$

to `SPS(jchan)`. We add



the rest to $SPS(jchan+1)$.

Occasionally it may happen that the image of an SPD record spans three SPD records. In this case $kchan$, the integer part of $schan$, the image of $ichan+1$, is equal to $jchan+2$, rather than $jchan+1$. As before, we would add the portion of the SPD record between $ichan$ and $\frac{jchan+1}{r}$ to $SPS(jchan)$. However, we would add a portion times $\frac{jchan+2}{r} - \frac{jchan+1}{r} = \frac{1}{r}$ to $SPS(jchan+1)$, and the rest to $SPS(jchan+2)$.



V. Miscellaneous

This section contains miscellaneous tables.

Part A is a detailed description of the target-event codes used in the TIMECONV routines in the SPAR library. Nearly all the Spartan programs call these routines to make it possible to enter MET's any of several ways.

Part B is a list of all the target events and the MET's at which they occurred, as indicated by the ACS data. The target-event code for each event is also indicated.

A. Description of target-event codes

The target-event format of the character string is as follows:

The first character is a one letter target code, as follows:

S = Sco X-2	V = Vega
G = Galactic Center	D = Deneb
P = Perseus	H = safehold

The last character is A (arrival/acquisition), D (departure/deacquisition), B (begin), or E (end). The middle characters, if any, are orbit numbers, scan numbers, and/or rotation codes.

On Sco, the following formats are allowed:

SA	Arrival at Sco
S<sweep><scan><B or E>	Beginning or end of sweep-scan
SP<B or E>	Beginning or end of pitch maneuver
SD	Departure from Sco

The sweeps are numbered 1 or 2, and the scans are numbered 1, 2, or 3 (short, long, short). E.g. S12B is the beginning of sweep 1, scan 2.

On the G.C., the following formats are allowed:

G<orbit>A	Arrival at G.C. on given orbit
G<orbit>IR<B or E>	Begin or end of initial roll
G<orbit><scan><B or E>	Begin or end of orbit-scan
G<orbit>FR<B or E>	Begin or end of final roll
G<orbit>D	Departure from G.C. on given orbit

Orbits are numbered 1 to 8 and scans are numbered 1 to 3. E.g. G4A is the time of arrival at G.C. on orbit 4; G42E is the end of scan 2 on orbit 4; G4FRB is the beginning of the final roll on orbit 4.

On Perseus, the following formats are allowed:

P<orbit>A	Arrival at Perseus on given orbit
P<orbit>IR<B or E>	Begin or end of initial roll
P<orbit><sweep><scan><B or E>	Begin or end of orbit-sweep-scan
P<orbit>MR<B or E>	Begin or end of mid roll
P<orbit>FR<B or E>	Begin or end of final roll
P<orbit>DR<B or E>	Begin or end of departure roll
P<orbit>D	Departure from Perseus on given orbit

The "mid roll" is the roll between sweeps; the "final roll" is the roll after sweep 2 which returns the spacecraft to its attitude at arrival; and the "departure roll" is the constant roll after the "final roll" which puts the spacecraft in its departure attitude. Perseus orbit numbers run from 0 to 9, sweep numbers 1 or 2, and scans 1 to 3. An example of scan format is P512B, which is the beginning of orbit 5, sweep 1, scan 2.

At Vega, the following are allowed:

VA	Arrival at Vega
VD	Departure from Vega

At Deneb, the following are allowed:

D<orbit>A	Arrival at Deneb on given orbit
D<orbit>D	Departure from Deneb on given orbit

Orbits are numbered from 0 to 9.

At the safehold, the following are allowed:

H<orbit>A

Arrival at safehold on given orbit

H<orbit>D

Departure from safehold on given orb.

Orbits are numbered from 0 to 9.

This system specifies a time for target event, which is looked up by Codetime to find the actual numerical time. For example, P213B is the begin time of the Perseus scan on science circuit 2, sweep 1, scan 3, which is 06:20:07 = 22807000 msec.

An offset may be applied in the target-event format. For example, P213B+3 means 3 seconds after P213B, or 06:20:10; P213B-10.552 means 10.552 seconds before P213B.

When converting integer millisecond to target-event format, Timecode looks for the nearest event and computes the offset from that event.

Codetime accepts lowercase as well as uppercase characters.

B. TARGET MANEUVER TIMES

Sco X-2

Maneuver	Code	Start MET	Code	Stop MET
<u>Program 18 (orbit 0)</u>				
Arrival	SA	14435 [04:00:35]		-
Short scan (cw)	S11B	14471 [04:01:11]	S11E	14538 [04:02:18]
Long scan (ccw)	S12B	14548 [04:02:28]	S12E	14683 [04:04:43]
Short scan (cw)	S13B	14693 [04:04:53]	S13E	14761 [04:06:01]
2 degree pitch (ccw)	SPB	14861 [04:07:41]	SPE	14863 [04:07:43]
Short scan (cw)	S21B	14893 [04:08:13]	S21E	14960 [04:09:20]
Long scan (ccw)	S22B	14971 [04:09:31]	S22E	15105 [04:11:45]
Short scan (cw)	S23B	15116 [04:11:56]	S23E	15183 [04:13:03]
Departure	SD	15376 [04:16:16]		

Galactic Center

Maneuver	Code	Start MET	Code	Stop MET
<u>Program 57 (orbit 1)</u>				
Arrival	G1A	19821 [05:30:21]		
Initial roll (cw)	G1IRB	19841 [05:30:41]	G1IRE	19847 [05:30:47]
Short scan (cw)	G11B	19960 [05:32:40]	G11E	20116 [05:35:16]
Long scan (ccw)	G12B	20126 [05:35:26]	G12E	20436 [05:40:36]
Short scan (cw)	G13B	20446 [05:40:46]	G13E	20601 [05:43:21]
Final roll (ccw)	G1FRB	20611 [05:43:31]	G1FRE	20617 [05:43:37]
Departure	G1D	20853 [05:47:33]		

Program 58 (orbit 2)

Arrival	G2A	25331 [07:02:11]		
Initial roll (ccw)	G2IRB	25351 [07:02:31]	G2IRE	25432 [07:03:52]
Short scan (cw)	G21B	25470 [07:04:30]	G21E	25626 [07:07:06]
Long scan (ccw)	G22B	25635 [07:07:15]	G22E	25945 [07:12:25]
Short scan (cw)	G23B	25955 [07:12:35]	G23E	26111 [07:15:11]
Final roll (cw)	G2FRB	26121 [07:15:21]	G2FRE	26202 [07:16:42]
Departure	G2D	26363 [07:19:23]		

Program 59 (orbit 3)

Arrival	G3A	30840 [08:34:00]		
Initial roll (ccw)	G3IRB	30860 [08:34:20]	G3IRE	30891 [08:34:51]
Short scan (cw)	G31B	30980 [08:36:20]	G31E	31135 [08:38:55]
Long scan (ccw)	G32B	31145 [08:39:05]	G32E	31455 [08:44:15]
Short scan (cw)	G33B	31465 [08:44:25]	G33E	31620 [08:47:00]
Final roll (cw)	G3FRB	31630 [08:47:10]	G3FRE	31661 [08:47:41]
Departure	G3D	31873 [08:51:13]		

Program 60 (orbit 4)

Arrival	G4A	36350 [10:05:50]		
Initial roll (cw)	G4IRB	36369 [10:06:09]	G4IRE	36426 [10:07:06]
Short scan (cw)	G41B	36490 [10:08:10]	G41E	36644 [10:10:44]
Long scan (ccw)	G42B	36655 [10:10:55]	G42E	36964 [10:16:04]
Short scan (cw)	G43B	36975 [10:16:15]	G43E	37129 [10:18:49]
Final roll (ccw)	G4FRB	37139 [10:18:59]	G4FRE	37195 [10:19:55]
Departure	G4D	37383 [10:23:03]		

Maneuver	Code	Start MET	Code	Stop MET
<u>Program 61 (orbit 5)</u>				
Arrival	G5A	41858 [11:37:38]		
Initial roll (ccw)	G5IRB	41879 [11:37:59]	G5IRE	41936 [11:38:56]
Short scan (cw)	G51B	41999 [11:39:59]	G51E	42154 [11:42:34]
Long scan (ccw)	G52B	42164 [11:42:44]	G52E	42474 [11:47:54]
Short scan (cw)	G53B	42484 [11:48:04]	G53E	42639 [11:50:39]
Final roll (cw)	G5FRB	42649 [11:50:49]	G5FRE	42705 [11:51:45]
Departure	G5D	42892 [11:54:52]		

<u>Program 62 (orbit 6)</u>				
Arrival	G6A	47368 [13:09:28]		
Initial roll (cw)	G6IRB	47389 [13:09:49]	G6IRE	47420 [13:10:20]
Short scan (cw)	G61B	47508 [13:11:48]	G61E	47664 [13:14:24]
Long scan (ccw)	G62B	47674 [13:14:34]	G62E	47983 [13:19:43]
Short scan (cw)	G63B	47993 [13:19:53]	G63E	48149 [13:22:29]
Final roll (ccw)	G6FRB	48159 [13:22:39]	G6FRE	48190 [13:23:10]
Departure	G6D	48402 [13:26:42]		

<u>Program 63 (orbit 7)</u>				
Arrival	G7A	52878 [14:41:18]		
Initial roll (ccw)	G7IRB	52898 [14:41:38]	G7IRE	52917 [14:41:57]
Short scan (cw)	G71B	53018 [14:43:38]	G71E	53173 [14:46:13]
Long scan (ccw)	G72B	53183 [14:46:23]	G72E	53493 [14:51:33]
Short scan (cw)	G73B	53503 [14:51:43]	G73E	53658 [14:54:18]
Final roll (cw)	G7FRB	53668 [14:54:28]	G7FRE	53687 [14:54:47]
Departure	G7D	53911 [14:58:31]		

<u>Program 64 (orbit 8)</u>				
Arrival	G8A	58388 [16:13:08]		
Initial roll (ccw)	G8IRB	58408 [16:13:28]	G8IRE	58477 [16:14:37]
Short scan (cw)	G81B	58528 [16:15:28]	G81E	58683 [16:18:03]
Long scan (ccw)	G82B	58693 [16:18:13]	G82E	59003 [16:23:23]
Short scan (cw)	G83B	59013 [16:23:33]	G83E	59167 [16:26:07]
Final roll (cw)	G8FRB	59177 [16:26:17]	G8FRE	59247 [16:27:27]
Departure	G8D	59421 [16:30:21]		

Perseus Cluster

Maneuver	Code	Start MET	Code	Stop MET
<u>Program 41 (orbit 0)</u>				
Arrival	POA	11046 [03:04:06]		
Initial roll (cw)	POIRB	11170 [03:06:10]	POIRE	11175 [03:06:15]
Short scan (cw)	PO11B	11290 [03:08:10]	PO11E	11449 [03:10:49]
Long scan (ccw)	PO12B	11459 [03:10:59]	PO12E	11778 [03:16:18]
Short scan (cw)	PO13B	11788 [03:16:28]	PO13E	11947 [03:19:07]
Mid roll (cw)	POMRB	11956 [03:19:16]	POMRE	11963 [03:19:23]
Short scan (cw)	PO21B	11983 [03:19:43]	PO21E	12142 [03:22:22]
Long scan (ccw)	PO22B	12151 [03:22:31]	PO22E	12470 [03:27:50]
Short scan (cw)	PO23B	12480 [03:28:00]	PO23E	12639 [03:30:39]
Final roll (ccw)	POFRB	12650 [03:30:50]	POFRE	12660 [03:31:00]
Departure roll (ccw)	PODRB	12860 [03:34:20]	PODRE	12900 [03:35:00]
Departure	POD	12931 [03:35:31]		
<u>Program 42 (orbit 1)</u>				
Arrival	PIA	16563 [04:36:03]		
Initial roll (ccw)	PIIRB	16680 [04:38:00]	PIIRE	16762 [04:39:22]
Short scan (cw)	PI11B	16800 [04:40:00]	PI11E	16959 [04:42:39]
Long scan (ccw)	PI12B	16969 [04:42:49]	PI12E	17288 [04:48:08]
Short scan (cw)	PI13B	17298 [04:48:18]	PI13E	17457 [04:50:57]
Mid roll (cw)	PIMRB	17467 [04:51:07]	PIMRE	17472 [04:51:12]
Short scan (cw)	PI21B	17493 [04:51:33]	PI21E	17652 [04:54:12]
Long scan (ccw)	PI22B	17662 [04:54:22]	PI22E	17980 [04:59:40]
Short scan (cw)	PI23B	17990 [04:59:50]	PI23E	18150 [05:02:30]
Final roll (cw)	PIFRB	18160 [05:02:40]	PIFRE	18237 [05:03:57]
Departure roll (ccw)	PIDRB	18370 [05:06:10]	PIDRE	18410 [05:06:50]
Departure	PID	18441 [05:07:21]		

Maneuver	Code	Start MET	Code	Stop MET
<u>Program 43 (orbit 2)</u>				
Arrival	P2A	22072 [06:07:52]	P2IRE	22228 [06:10:28]
Initial roll (ccw)	P2IRB	22190 [06:09:50]	P211E	22469 [06:14:29]
Short scan (cw)	P211B	22310 [06:11:50]	P212E	22798 [06:19:58]
Long scan (ccw)	P212B	22478 [06:14:38]	P213E	22966 [06:22:46]
Short scan (cw)	P213B	22807 [06:20:07]	P2MRE	22982 [06:23:02]
Mid roll (cw)	P2MRB	22976 [06:22:56]		
Short scan (cw)	P221B	23002 [06:23:22]	P221E	23161 [06:26:01]
Long scan (ccw)	P222B	23171 [06:26:11]	P222E	23490 [06:31:30]
Short scan (cw)	P223B	23500 [06:31:40]	P223E	23659 [06:34:19]
Final roll (cw)	P2FRB	23669 [06:34:29]	P2FRE	23702 [06:35:02]
Departure roll (ccw)	P2DRB	23880 [06:38:00]	P2DRE	23920 [06:38:40]
Departure	P2D	23950 [06:39:10]		
<u>Program 44 (orbit 3)</u>				
Arrival	P3A	27582 [07:39:42]	P3IRE	27748 [07:42:28]
Initial roll (cw)	P3IRB	27699 [07:41:39]	P311E	27978 [07:46:18]
Short scan (cw)	P311B	27819 [07:43:39]	P312E	28307 [07:51:47]
Long scan (ccw)	P312B	27988 [07:46:28]	P313E	28476 [07:54:36]
Short scan (cw)	P313B	28317 [07:51:57]	P3MRE	28492 [07:54:52]
Mid roll (cw)	P3MRB	28486 [07:54:46]		
Short scan (cw)	P321B	28512 [07:55:12]	P321E	28671 [07:57:51]
Long scan (ccw)	P322B	28681 [07:58:01]	P322E	29000 [08:03:20]
Short scan (cw)	P323B	29010 [08:03:30]	P323E	29169 [08:06:09]
Final roll (ccw)	P3FRB	29179 [08:06:19]	P3FRE	29233 [08:07:13]
Departure roll (ccw)	P3DRB	29390 [08:09:50]	P3DRE	29430 [08:10:30]
Departure	P3D	29459 [08:10:59]		

Maneuver	Code	Start MET	Code	Stop MET
<u>Program 45 (orbit 4)</u>				
Arrival	P4A	33091 [09:11:31]		
Initial roll (ccw)	P4IRB	33219 [09:13:39]	P4IRE	33260 [09:14:20]
Short scan (cw)	P411B	33329 [09:15:29]	P411E	33488 [09:18:08]
Long scan (ccw)	P412B	33498 [09:18:18]	P412E	33817 [09:23:37]
Short scan (cw)	P413B	33827 [09:23:47]	P413E	33986 [09:26:26]
Mid roll (cw)	P4MRB	33996 [09:26:36]	P4MRE	34001 [09:26:41]
Short scan (cw)	P421B	34022 [09:27:02]	P421E	34180 [09:29:40]
Long scan (ccw)	P422B	34191 [09:29:51]	P422E	34509 [09:35:09]
Short scan (cw)	P423B	34520 [09:35:20]	P423E	34679 [09:37:59]
Final roll (cw)	P4FRB	34689 [09:38:09]	P4FRE	34742 [09:39:02]
Departure roll (ccw)	P4DRB	34900 [09:41:40]	P4DRE	34940 [09:42:20]
Departure	P4D	34969 [09:42:49]		
<u>Program 46 (orbit 5)</u>				
Arrival	P5A	38601 [10:43:21]		
Initial roll (cw)	P5IRB	38719 [10:45:19]	P5IRE	38746 [10:45:46]
Short scan (cw)	P511B	38838 [10:47:18]	P511E	38997 [10:49:57]
Long scan (ccw)	P512B	39008 [10:50:08]	P512E	39326 [10:55:26]
Short scan (cw)	P513B	39336 [10:55:36]	P513E	39494 [10:58:14]
Mid roll (cw)	P5MRB		P5MRE	
Short scan (cw)	P521B	39531 [10:58:51]	P521E	39690 [11:01:30]
Long scan (ccw)	P522B	39700 [11:01:40]	P522E	40019 [11:06:59]
Short scan (cw)	P523B	40029 [11:07:09]	P523E	40188 [11:09:48]
Final roll (ccw)	P5FRB	40198 [11:09:58]	P5FRE	40231 [11:10:31]
Departure roll (ccw)	P5DRB	40409 [11:13:29]	P5DRB	40449 [11:14:09]
Departure	P5D	40478 [11:14:38]		

Maneuver	Code	Start MET	Code	Stop MET
<u>Program 47 (orbit 6)</u>				
Arrival	P6A	44111 [12:15:11]		
Initial roll (ccw)	P6IRB	44228 [12:17:08]	P6IRE	44243 [12:17:23]
Short scan (cw)	P611B	44348 [12:19:08]	P611E	44507 [12:21:47]
Long scan (ccw)	P612B	44517 [12:21:57]	P612E	44835 [12:27:15]
Short scan (cw)	P613B	44846 [12:27:26]	P613E	45004 [12:30:04]
Mid roll (cw)	P6MRB	45015 [12:30:15]	P6MRE	45020 [12:30:20]
Short scan (cw)	P621B	45040 [12:30:40]	P621E	45200 [12:33:20]
Long scan (ccw)	P622B	45210 [12:33:30]	P622E	45528 [12:38:48]
Short scan (cw)	P623B	45538 [12:38:58]	P623E	45697 [12:41:37]
Final roll (cw)	P6FRB	45708 [12:41:48]	P6FRE	45719 [12:41:59]
Departure roll (ccw)	P6DRB	45919 [12:45:19]	P6DRE	45959 [12:45:59]
Departure	P6D	45988 [12:46:28]		

Program 48 (orbit 7)

Arrival	P7A	49620 [13:47:00]		
Initial roll (cw)	P7IRB	49738 [13:48:58]	P7IRE	49809 [13:50:09]
Short scan (cw)	P711B	49857 [13:50:57]	P711E	50017 [13:53:37]
Long scan (ccw)	P712B	50027 [13:53:47]	P712E	50345 [13:59:05]
Short scan (cw)	P713B	50355 [13:59:15]	P713E	50514 [14:01:54]
Mid roll (cw)	P7MRB	50524 [14:02:04]	P7MRE	50530 [14:02:10]
Short scan (cw)	P721B	50550 [14:02:30]	P721E	50709 [14:05:09]
Long scan (ccw)	P722B	50719 [14:05:19]	P722E	51038 [14:10:38]
Short scan (cw)	P723B	51048 [14:10:48]	P723E	51207 [14:13:27]
Final roll (ccw)	P7FRB	51217 [14:13:37]	P7FRE	51293 [14:14:53]
Departure roll (ccw)	P7DRB	51429 [14:17:09]	P7DRE	51469 [14:17:49]
Departure	P7D	51497 [14:18:17]		

Maneuver	Code	Start MET	Code	Stop MET
<u>Program 49 (orbit 8)</u>				
Arrival	P8A	55130 [15:18:50]		
Initial roll (ccw)	P8IRB	55247 [15:20:47]	P8IRE	55319 [15:21:59]
Short scan (cw)	P811B	55367 [15:22:47]	P811E	55526 [15:25:26]
Long scan (ccw)	P812B	55536 [15:25:36]	P812E	55854 [15:30:54]
Short scan (cw)	P813B	55865 [15:31:05]	P813E	56024 [15:33:44]
Mid roll (cw)	P8MRB	56034 [15:33:54]	P8MRE	56039 [15:33:59]
Short scan (cw)	P821B	56059 [15:34:19]	P821E	56219 [15:36:59]
Long scan (ccw)	P822B	56229 [15:37:09]	P822E	56547 [15:42:27]
Short scan (cw)	P823B	56557 [15:42:37]	P823E	56717 [15:45:17]
Final roll (cw)	P8FRB	56727 [15:45:27]	P8FRE	56792 [15:46:32]
Departure roll (ccw)	P8DRB	56937 [15:48:57]	P8DRE	56977 [15:49:37]
Departure	P8D	57007 [15:50:07]		
<u>Program 50 (orbit 9)</u>				
Arrival	P9A	60640 [16:50:40]		
Initial roll (cw)	P9IRB	60756 [16:52:36]	P9IRE	60772 [16:52:52]
Short scan (cw)	P911B	60876 [16:54:36]	P911E	61035 [16:57:15]
Long scan (ccw)	P912B	61046 [16:57:26]	P912E	61364 [17:02:44]
Short scan (cw)	P913B	61375 [17:02:55]	P913E	61534 [17:05:34]
Mid roll (cw)	P9MRB	61544 [17:05:44]	P9MRE	61549 [17:05:49]
Short scan (cw)	P921B	61569 [17:06:09]	P921E	61728 [17:08:48]
Long scan (ccw)	P922B	61737 [17:08:57]	P922E	62056 [17:14:16]
Short scan (cw)	P923B	62067 [17:14:27]	P923E	62226 [17:17:06]
Final roll (ccw)	P9FRB	62237 [17:17:17]	P9FRE	62258 [17:17:38]
Departure roll (ccw)	P9DRB	62447 [17:20:47]	P9DRE	62487 [17:21:27]
Departure	P9D	62517 [17:21:57]		

Vega

Maneuver	Code	Start MET	Code	Stop MET
Arrival	VA	9709 [02:41:49]		
Departure	VD	10468 [02:54:28]		

Deneb

Maneuver	Code	Start MET	Code	Stop MET
<u>Orbit 0</u>				
Arrival	DOA	10491 [02:54:51]		
Departure	DOD	10980 [03:03:00]		
<u>Orbit 1</u>				
Arrival	D1A	15601 [04:20:01]		
Departure	D1D	16143 [04:29:03]		
<u>Orbit 2</u>				
Arrival	D2A	21110 [05:51:50]		
Departure	D2D	21652 [06:00:52]		
<u>Orbit 3</u>				
Arrival	D3A	26620 [07:23:40]		
Departure	D3D	27161 [07:32:41]		
<u>Orbit 4</u>				
Arrival	D4A	32129 [08:55:29]		
Departure	D4D	32671 [09:04:31]		
<u>Orbit 5</u>				
Arrival	D5A	37639 [10:27:19]		
Departure	D5D	38181 [10:36:21]		
<u>Orbit 6</u>				
Arrival	D6A	43148 [11:59:08]		
Departure	D6D	43690 [12:08:10]		
<u>Orbit 7</u>				
Arrival	D7A	48658 [13:30:58]		
Departure	D7D	49199 [13:39:59]		
<u>Orbit 8</u>				
Arrival	D8A	54167 [15:02:47]		
Departure	D8D	54709 [15:11:49]		
<u>Orbit 9</u>				
Arrival	D9A	59677 [16:34:37]		
Departure	D9D	60219 [16:43:39]		

Safehold

Maneuver	Code	Start MET	Code	Stop MET
<u>Orbit 0</u>				
Arrival	H0A	13559 [03:45:59]		
Departure	H0D	13852 [03:50:52]		
<u>Orbit 1</u>				
Arrival	H1A	19059 [05:17:39]		
Departure	H1D	19323 [05:22:03]		
<u>Orbit 2</u>				
Arrival	H2A	24569 [06:49:29]		
Departure	H2D	24833 [06:53:53]		
<u>Orbit 3</u>				
Arrival	H3A	30078 [08:21:18]		
Departure	H3D	30342 [08:25:42]		
<u>Orbit 4</u>				
Arrival	H4A	35588 [09:53:08]		
Departure	H4D	35852 [09:57:32]		
<u>Orbit 5</u>				
Arrival	H5A	41097 [11:24:57]		
Departure	H5D	41361 [11:29:21]		
<u>Orbit 6</u>				
Arrival	H6A	46607 [12:56:47]		
Departure	H6D	46871 [13:01:11]		
<u>Orbit 7</u>				
Arrival	H7A	52117 [14:28:37]		
Departure	H7D	52381 [14:33:01]		
<u>Orbit 8</u>				
Arrival	H8A	57626 [16:00:26]		
Departure	H8D	57890 [16:04:50]		
<u>Orbit 9</u>				
Arrival	H9A	63136 [17:32:16]		
Departure	H9D	63400 [17:36:40]		

DRAFT

SPARTAN-1 Aspect Solution Summary

by

William A. Snyder

Code 4121.4

E.O. Hulburt Center for Space Research

Naval Research Laboratory

20 October 1987

I. Introduction

A good deal of effort has gone into creating an aspect solution for the SPARTAN-1 observations. Uncertainties on the order of 1 arc minute or less are desired because the FWHM detector field-of-view along the SPARTAN-1 scan direction is 5 arc minutes. Much of the most recent work has centered on the Perseus cluster aspect solution because the pre-flight method chosen for determining aspect had to be abandoned. The Perseus cluster aspect solution cannot be derived strictly from observations but must also include some assumptions about the Attitude Control System (ACS) behavior. The accuracy of any solution is only as good as the observations and assumptions that have gone into it. It is important that everyone understand the process and assumptions that have gone into creating the aspect solution, and this report is intended to provide a summary of that process.

The report is organized as follows: In Section II we describe the method used to determine aspect information from in-flight optical photographs. This method was intended to be used to determine aspect for both the galactic center (G.C.) and Perseus cluster targets. However, it was used only on the G.C. target because the Perseus cluster aspect film was severely fogged due to light scattering into the aspect cameras. The G.C. aspect solution is discussed in Section III and provides a measure of the reliability of the ACS system. In Section IV we discuss the ONESTAR method of determining Perseus cluster aspect from observations of Algol and the assumption of nominal scan orientation. Systematic trends in this solution are discussed and are shown to be understood within the limitations of the assumptions used. We also discuss a modified ONESTAR solution (ONESTARP9) where an additional assumption of uniform scan rate is included, and we argue that this method provides the overall best solution obtainable. In Section V we discuss the relevant errors associated with the P9 solution.

II. SPARTAN-1 Aspect

The method used for determining the SPARTAN-1 galactic center aspect is based on measurement of in-flight star field photographs. In this method the ACS is used to lock the spacecraft optic axis onto a bright stellar object and then a photograph is taken in order to position the optic axis relative to fiducials on the photographic frame. All subsequent photographs then locate the optic axis position on the sky by measuring positions of stars on the frames and noting their relative placement about the optic axis position. A set of photographs were taken during each scan across the target and the aspect solution is determined for all points along the scan by fitting a great circle (approximated by a straight line) to the photographic positions.

For SPARTAN-1 the calibration star was Deneb (α Cyg, see Figure 1). Aspect photographs were taken only while slowly scanning across a target and were not taken while off target. A calibration photograph was taken during each of the 10 orbits the ACS was updated. Two aspect cameras were used to take star-field photographs. The field of view of the aspect cameras were approximately 7° on a side and stars as faint as 9th magnitude could be measured during the 10 second exposure.

A number of steps must be completed before the aspect solution can be determined. The aspect photographs (frames) must first be measured. Two basic results are needed: (1) the centroid of the calibration star (optic axis) must be determined, and (2) the position of reference stars relative to frame fiducials must be measured. All frames were measured at the Manually Operated Measuring Machine (MOMM) at Fermilab. The Fermilab measurements were written to a Vax ASCII data file (LSTSTAR.DAT) and were later converted to "millimeter" coordinates and reformed by the program FERMSTAR for later analysis. Harry Heckathorn directed the photographic measurements and provided the solution for the optic axis position (x_0 , y_0) as a function of orbit. He also computed the aspect solution for each of the galactic center frames. The optic axis coordinates for both detectors are shown in Figure 2 as a function of orbit. [These values were later independently derived with the CAMCAL program.] A clear shift in optic axis position is seen in each

camera as the mission proceeds and the amount of shift roughly corresponds to 60 arc seconds for both detectors. The nature of the shift is unclear but may be related to thermal effects. The choice of x_0 and y_0 used for deriving the aspect for a particular target was determined by linear interpolating between calibration measurements. Although we used Heckathorn's solution for the G.C. photographs the solutions obtained with our own in-house program (PICPOS) are in good agreement.

To determine position as a function of time a time value must be assigned to each frame measurement. The shutter open and close time for each of the photographs was determined from the flight data while it was being processed on the Eclipse computer. This information was recorded only once each paragraph (roughly 0.4 seconds) so that on average each frame time is uncertain by approximately 0.2 seconds. The shutter midpoint time was assigned to each photograph because all star positions were measured at their center. The program CAMERGE merged the shutter times with the appropriate aspect frame measurement. This merged data was stored in a Camera data file (with Vax file extension "CAM"). This file was then read by SKYPOS to determine the aspect for each of the scans.

The program SKYPOS fits a straight line to the data. To determine the aspect solution the start and stop time of the scan must be entered. These times were recorded to the nearest second and were determined by visually inspecting an ACS data file with ACS PLOT and noting the appropriate transition time of the Program Step Counter. [Each maneuver performed by the ACS requires an instruction from the onboard flight computer. Each of these instructions is performed in sequence and when executed produces a voltage shift of 0.5 volts in the Program Step Counter. By counting half-volt shifts it is possible to determine when a particular instruction was executed.]

Camera frames with times between the start and stop time were then extracted from the camera file and their best fit Ra's and Dec's transformed to a spherical coordinate system (x,y) centered on the target. The "official" target positions for various flight maneuvers are stored in a DATA statement in the subroutine TARGETS. The position of the Perseus cluster is RA = 49.12500, DEC = 41.32556 (this position is slightly different than the

published radio position for NGC 1275) and the G.C. target position is $Ra = 265.68750$, $Dec = -28.95000$. The coordinate system is aligned so that the positive y axis is parallel to the local DEC great circle and the positive x axis is oriented along increasing RA. Close to the target the (x,y) coordinate system is Euclidean to a very good approximation (e.g., the linear and angular distances differ by less than 2 arc seconds over 2 degrees). The aspect solution is then obtained by fitting linear functions of time to both the x and y components of the frame measurements (see Figure 3). A common positional uncertainty is assigned to each point during the fit. The magnitude of the uncertainty that produces an acceptable fit (i.e., chi-square approximately equal to the number of data points) provides a measure of the aspect error. A comparison of the offset between adjacent scan end points also provides a similar estimate. The best fit polynomial coefficients are written to an aspect file (with Vax file extension "ASP"). This aspect file is used to integrate the aspect solution into the Experimenter Tape (ET) at a later time. The aspect position is stored on tape in the (x,y) coordinate system. The transformation to Ra and Dec is straightforward if the target position is known. The target name is stored in each tape record.

III. The Galactic Center Solution

A schematic of the G.C. aspect solution based on connecting camera 2 frame positions is shown in Figure 4 and a more detailed view of the scan end points derived from the SKYPOS fits are given in Figure 5. Overall spatial scale and orientation have been preserved from orbit to orbit in Figure 5 with major tick marks denoting 1 arc minute intervals. The start and stop points for each G.C. observation (i.e., orbit) have been plotted in the large rectangle in the center of the figure. The Ra axis increases to the right in the figure and the Dec axis increases toward the top. The smaller boxes that surround the central rectangle show the start and stop points for various scan segments. Relative orientation and scale have been preserved for each set of points with the points placed roughly in the direction of scan (the scan direction is shown as an arrow from pointing from point A). Aspect photographs from camera 2 were also taken at various times while the spacecraft was sitting at points D and E and those positions are shown as a plus (+) in the figure. The time interval separating points B and C and points D and E was 10 seconds.

Inspection of Figure 5 shows that while the ACS system generally performed very well during the mission some unexpected systematic trends are evident in the data. The displacement of the actual starting location (point A) from the intended location (the G.C.) changes at about 1 arc minute per orbit in the direction of decreasing declination. There is an approximate 1.5-2.0 arc minute random scatter about this drift. Another interesting feature is that point F (the end of the G.C. scans) does not appear to be randomly displaced about point A. If the arrow from point A represents "noon" on a clock then point F is generally located at 2 or 3 o'clock. This suggests the presence of a net non-zero force perpendicular to the scan direction. The average displacement perpendicular to the scan direction is ~ 1 arc minute and occurred over a 641 second time interval. This displacement corresponds to an effective drift rate of 5.6 arc minutes per hour which is within the gyro specs and was probably caused by gyro drift.

The relative displacement of point C relative to point B and point E relative to point D was apparently random and probably reflects aspect solution uncertainties. The magnitudes of these displacements are plotted in Figure 6 and no obvious trends are evident in the data. The average end point displacement is on the order of 40 arc seconds. This value corresponds very closely to the 30 arc second error used in SKYPOS to obtain an acceptable chi-square fit to the photographic aspect. This indicates that the galactic center aspect solution is probably accurate to within ~ 30 -40 arc seconds.

The scan rate derived for each orbit is shown in Table 1. The average rate is 0.00648 ± 0.00007 deg/s (sample deviation; the error in the mean is 0.00003 deg/s) and there is no evidence for a systematic trend in the data. The scan rate is constant to within 0.46% of the average value. The average observed rate may be slightly (0.5%) larger than planned (0.00644 deg/s) although the planned (i.e., nominal) value lies just outside the mean error limits.

A comparison of observed and planned scan angles is shown in Table 2. The average deviation for this set of points about the planned value is 0.15 ± 0.12 degrees (error in the mean). This non-zero difference is small but may be related to the southward displacement in acquisition of the intended

galactic center target. The planned scan angle can only be obtained if the spacecraft is properly oriented before beginning the roll maneuver to bring the spacecraft to the planned orientation. Any error in target acquisition would change the spacecraft orientation and this change would be reflected as an apparent shift in scan angle. The mean southward displacement of ~5 arc minutes would produce an apparent offset in scan angle of 0.18° . This is comparable to the observed value of 0.15° and we therefore conclude that the ACS roll maneuvers were executed as planned.

In summary, the photographic aspect solution for the galactic center indicates that while there were small unexpected variations in spacecraft performance the ACS system performed its major functions of target acquisition, scan orientation, and constancy of scan rate remarkably well. Scan angles were positioned to within 0.2° of their intended value, individual scan rates were the same to within 0.5%, and the average scan rate was close to nominal.

IV. The Perseus Cluster ONESTAR Solutions

The Perseus cluster was only 30° from the Sun at the time of observation and the aspect frames for this target were in all cases heavily fogged. No stars were visible on most frames, but on orbits 0, 4, and 5 one star (Algol, β Per) was visible on the majority of camera 1 frames.

It was thought that it might be possible to detect Algol and other stars on all the other camera 1 frames if the frames could be digitized and the images processed to extract faint features. All the camera 1 frames were electronically digitized at 30 arcsecond resolution using a Perkin-Elmer PDS 1010M microdensitometer. Although it proved impossible to extract new stars from the digitized images the digitization process produced a valuable data base that made it possible to easily inspect and manipulate images using the UV Branch PDP-11 image processing software.

An inspection of the Algol images suggested that the relative pixel displacement of Algol on frames taken during any orbit were to a good approximation repeated on other orbits. This repeatability is not surprising

if the spacecraft ACS and camera timing mechanism worked as intended or at least were repeated from one orbit to the next. The measured pixel locations for Algol on orbits 0, 4, and 5 are listed in Table 3. [Only the x pixel values are given because the y pixel coordinates do not noticeably change during a scan.] We will show later that this assumption of exact repeatability is probably not strictly true and introduces small but significant errors into the aspect solution on arc minute scales.

Kevin Carmody used this repeatability feature of the Algol image offset to electronically superimpose images in order to increase the signal to noise ratio of the Algol signal. On every orbit images within that orbit were added after first shifting the frames by the average pixel amount measured in Table 3. Because the images were superimposed onto frame #1 this summation effectively enhanced the Algol signal for the first frame of each orbit. A well defined stellar image was noted on 8 of the 10 orbit summations while weaker signals were seen in the remaining 2 (orbit 1 and 7). The pixel locations of the superimposed Algol images are shown schematically in Figure 7.

Careful inspection of Figure 7 will reveal that the Algol positions define a semicircle whose centroid (denoted by C in the figure) is offset from the calculated optic axis position (denoted by O) by ~ 8 pixels (4 arc minutes). The formal error is on the order of 2 pixels (1 arc minute). A computed centroid for the first frame of the G.C. scans is also shown. A casual interpretation would suggest that the optic axis is offset from the roll axis by approximately 4 arc minutes, a value which is considerably larger than the 30 arc seconds measured on the ground. However, the G.C. and Perseus centroids should be shifted to the right approximately 13 pixels to correct for scan motion that occurs during the 25.5 seconds between the start of the scan (the real roll axis position) and the time frame #1 was taken. When this is done the difference in Perseus centroid from the expected optic axis position is ~ 3.6 pixels (1.8 arc minutes) in the vertical direction and ~ 5.4 (2.7 arc minutes) in the horizontal (or scan) direction. This apparent 3.2 arc minute offset is not real and is produced by an ~ 5 arc minute scatter in the ACS acquisition of the Perseus target. Fitting a circle to the Algol frames effectively assumes that the roll maneuver occurs at a fixed point in

space (i.e., that the angular offset of Algol from the roll axis has a fixed radius). However, there is a clear 5 arc minute shift in this position as inferred from the computed aspect solution (see Figure 14). Thus the angular distance of Algol from the roll (i.e., optic) axis is not constant and a centroid obtained by fitting the Algol positions to a circle which has a fixed radius should be offset from the true roll axis by an amount which is equal to half the change in roll (i.e., optic) axis displacement (2.5 arc minutes). The Perseus aspect solution is computed under the assumption that the optic axis is aligned with the spacecraft roll axis. The results obtained here are consistent with that assumption.

By measuring the position of Algol for the first frame of each orbit it is possible to determine the angular distance the optic axis is from Algol for that frame. This single measurement localizes the frame #1 aspect solution to a circle on the sky centered on β Per. This positional uncertainty can be reduced to a single point if one assumes that the spacecraft orientation was as planned during the scan. The galactic center aspect solution verified that this was a good assumption within the uncertainty of the measurement ($\sim 0.2^\circ$). The aspect solution for the other frames can then be derived by "unshifting" the frames by their superimposed distance. This is the underlying principle used in the ONESTAR Perseus cluster aspect solution. The aspect solution for each frame is then written to a Camera file and the general aspect solution is obtained with SKYPOS.

The basic geometry of the problem and the equations used to determine the right ascension and declination of the first camera frame are shown in Figure 8. The important parameters in these equations are λ which is the angular offset of Algol from the optic axis position, θ which is the angle Algol makes with the spacecraft scan direction as measured on the aspect photographs (see also Figure 9), and η which is the intended scan angle. These quantities must be precisely known if an aspect solution of arc minute uncertainty is to be obtained.

A precise derivation of these quantities requires five coordinate transformations (see Figure 9). The pixel coordinate measurements of Algol must first be transformed to millimeter values in order to determine the

(millimeter) offset of Algol from the optic axis (remember, the optic axis coordinates x_0 and y_0 are known only in millimeters). This transformation involves a slight ($\sim 0.2^\circ$) rotation and a coordinate axis reassignment (i.e., $\Delta y_{\text{mm}} = -\Delta x_{\text{pix}}$, $\Delta x_{\text{mm}} = \Delta y_{\text{pix}}$). A third coordinate system (x, y) is centered on the optic axis and is aligned parallel to $(x_{\text{mm}}, y_{\text{mm}})$ but with $x \parallel y_{\text{mm}}$ and $y \parallel x_{\text{mm}}$ (Figure 9). The angular offsets λ and θ_1 are determined in this coordinate system using a plate scale (camera focal length) determined by Harry Heckathorn. The (x, y) coordinate system is itself slightly misaligned ($\langle \theta_{\text{mis}} \rangle = -0.41^\circ$) with the spacecraft scan axis (x_s, y_s) . The angle θ is given by $\theta = \theta_1 + \theta_{\text{mis}}$. This slight misalignment has only been recently uncovered. Those familiar with the Perseus scan analysis will remember that the best fit transit centroid of the Perseus cluster center as determined with an aspect solution that did not include this misalignment was found to be offset from NGC 1275 by ~ 1 arc minute and excluded NGC 1275 at over 99% confidence (see Figure 10). This offset could ONLY be removed by adding an ad hoc roll angle misalignment of -0.3° . The camera misalignment explains the magnitude of this offset. The angle $\langle \theta_{\text{mis}} \rangle$ was determined by measuring the change in star positions observed on long G.C. scans. The misalignment angle was determined by calculating $\theta_{\text{mis}} = \arctan (\Delta y_{\text{mm}} / \Delta x_{\text{mm}})$ for a set of stars. The average misalignment angles measured for 15 stars in each G.C. orbit are listed in Table 4. Although the present aspect solution uses an average of these values we note that orbits 1 and 8 differ significantly from the average. This reason for this difference is not known.

The angle η , the angle the scan axis makes with the local Ra small circle, is defined in the celestial (Ra, Dec) coordinate system. These angles were chosen before flight and the ACS was programmed to maneuver to the proper spacecraft attitude. Programmed into the ACS was the roll angle that was needed to produce the correct angle η under the ASSUMPTION that the roll was performed at the intended target position. The planned scan angle is obtained only if the spacecraft is at the proper attitude before beginning the roll. If the ACS doesn't perform exactly as planned and the roll is initiated at a point other than the intended target position then the final spacecraft attitude is different than planned and the value of η will change. Put more simply the scan angle assumes a planned value only if the roll occurs at a particular celestial declination. In a sense this forms a Catch 22. One

cannot solve the aspect solution without assuming a given value for η , but η will change depending upon the correct aspect solution. Fortunately the situation isn't quite that bad. Small offsets in target acquisition change the scan angle only slightly and hardly produce any change in aspect near scan center (i.e., near photo #1). However, the error in aspect caused by small differences in η becomes more pronounced as one proceeds off scan center. This is one reason the aspect solution becomes poorer the closer it approaches the end of a scan. Errors in η can be reduced by iterating toward a solution. First an aspect solution is created assuming the pre-flight scan angles (see Table 5). When this was done it was noticed that most scans intersected at a point $\sim 0.1^\circ$ North of the intended target position (the coordinate origin). This northward displacement will tend to produce a change in scan angle η of -0.07° . A second aspect solution (Figure 11) is then created with all scan angles adjusted by this amount. The solution was stopped at this point although in principle the iterations could continue.

The aspect solution shown in Figure 11 (P7.ASP) was produced by ONESTARP7. Earlier versions of ONESTAR (P1-P6) were superseded as more detailed and correct analysis was incorporated. We don't intend to recount in detail all the program changes but a brief summary of the major milestones are in order. ONESTARP3 was produced by Kevin Carmody and used the Algol pixel coordinate values as originally measured on each of the frame summations. From an inspection of this solution it was apparent that at least one and possibly two scans were incorrectly positioned. The ONESTARP4 solution "corrected" these problems by shifting the measured positions of Algol for the two discrepant scans so that their scan pattern matched the pattern for the remaining scans. [These scan shifts were later readjusted for the P9.ASP aspect solution. The need for these scan shifts is described more fully in Appendix A.] The P4.ASP aspect file was the last aspect solution produced by Kevin Carmody before leaving NRL. It was the first program to incorporate into the solution the spherical geometry of the system. ONESTARP5 was essentially a copy of ONESTARP4 except it was possible to adjust roll angle and plate scale (focal length). The roll angle adjustment of -0.3° needed to align scan centroids and NGC 1275 was discovered with this program. ONESTARP6 corrected an error in scan angle (η) but contained an error of its own. ONESTARP7 corrected this error but it contained no correction for camera misalignments. As a

consequence the Perseus cluster centroid is offset from NGC 1275 (just as it had been in all earlier solutions) but relative scan positions are correct.

However, a close inspection of the P7 aspect solution displays some systematic trends that we believe are not real and can be related to an incorrect assumption inherent in the ONESTAR method. We have plotted in Figure 12 the angular offsets of adjacent scan end points as a function of orbit. Although on average the scan end point differences are only slightly larger than observed in the galactic center solution (see Figure 6) there are clear trends in the Perseus displacements that are not apparent in the galactic center solution. Another disturbing trend in the P7 solution is an apparent increase in scan rate during the mission (see Table 6). The scan rate is calculated to be 0.00447 deg/s during orbit #0 and increases linearly to 0.00454 deg/s during orbit 9. Although the difference in rate is comparable to the scatter measured in the galactic center solutions there is no evidence for a systematic change in G.C. rate. We believe that both the systematic trend in scan rate and the end point misalignment are tied to the assumption that Algol pixel offsets are EXACTLY repeated from orbit to orbit.

It is important to note that the camera clock, which controlled shutter openings and closings, sped up during the mission. The camera clock ran 1.6% faster during orbit 9 as compared to orbit 0 (that is, $\Delta T_0 = 1.016 \Delta T_9$). The change in clock rate over time was approximately linear and was probably caused by thermal heating. The assumption of constant pixel separation means that the arc lengths (ΔL) separating frames are the same for all orbits. Because the computed scan rate is given by $SR = \Delta L / \Delta T$, we expect that $SR_0 = \Delta L / \Delta T_0 = 0.984 \Delta L / \Delta T_9 = 0.984 SR_9$. This ratio is equal to the observed change in calculated P7 rates and means that the change in rate is not real.

A change in camera clock rate coupled with a constant scan rate would also explain why there is a systematic trend in scan end point displacements. The Algol frame offsets were computed by superimposing images only from orbits 0, 4, and 5. If the scan rate were constant and if images were available from all orbits we would expect that the summed image would be more elongated than that obtained with the present summation. This would shift the image center so that $\langle \Delta L_{all} \rangle$ would be greater than $\langle \Delta L_{0,4,5} \rangle$. It is not surprising,

therefore, that the largest total discrepancy in scan end points occur at the end of the mission where there were no scan summations (see Figure 12).

It is likely, therefore, that the scan rate was constant during the mission and that a better overall aspect solution is possible by including this assumption into the solution. The overall best estimate of the rate is probably obtained by averaging the scan rates measured for orbits 0, 4, and 5. This value is 0.00451 deg/s which is 1% larger than planned.

The assumption of a constant scan rate was used to create both the P8 and P9 aspect solutions. The ONESTARP8 program uses the ONESTARP7 algorithm to calculate the aspect solution for frame #1 only. A constant nominal (i.e., planned) scan rate is then assumed to directly determine the aspect solution. SKYPOS is not used and the ASP file is created directly by ONESTARP8. This program produces a Perseus map comparable to maps made with P7.ASP. ONESTARP9 was used to create P9.ASP and uses the ONESTARP8 algorithm to calculate the aspect for frame #1. It also assumes a constant scan rate to determine the aspect solution directly but uses the average value of 0.00451 deg/s. This program updates ONESTARP8 to include scan angle adjustments caused by target acquisition errors and corrects for camera misalignment with the spacecraft coordinate system. The P9 aspect solution is shown in Figure 13 and a schematic of the scan start (and stop) point is presented in Figure 14. This aspect solution is the latest and most understood solution available.

V. Errors Associated with the P9.ASP Solution

There are only 3 derived quantities (λ , θ , and η) used to determine the Perseus cluster aspect solution. Only the displacement (λ) of Algol from the optic axis depends on coordinate scale. The angle η is specified at the time of aspect solution while the angle θ depends only on the angular relationships of the different coordinate systems. Errors in either η or θ will tend to produce a systematic rotation of the aspect solution scan pattern about the Algol position while errors in λ will tend to push the scan pattern closer to or further from β Per. The assumption of a constant scan rate assures that the angular scale of the scan pattern remains independent of any of these quantities. Thus small errors in λ , η , and θ all tend to produce systematic

shifts in the absolute placement of the scan pattern on the sky, but do not effect in a major way the placement of one scan relative to another. This explains why the Perseus mapping has not been very sensitive to the details of the aspect solution.

The positional uncertainty for frame #1 can be derived in a straightforward manner. The choice of plate scale (camera focal length) is derived directly from the G.C. aspect solution and is known to great accuracy. Uncertainties in this value produce a positional error of less than a few arc seconds (Heckathorn, private communication). The measured uncertainties in optic axis (x_0, y_0) position are on the order of 10-20 arc seconds (the general scatter of points about a smooth trend in Figure 2). The measured uncertainty in the pixel location of Algol on the digitized images is less than one pixel or ~ 30 arc seconds. Added in quadrature these errors produce an uncertainty on the order of 35 arc seconds. In addition to these errors there are also shifts produced by uncertainties in the measured or assumed values for θ and η . Errors in θ are dominated by uncertainties in camera misalignment from the scan direction. From Table 4 this uncertainty is on the order of 0.2° . Variations in η are caused by individual scan displacements about the 0.1° northern average. An uncertainty of 0.05° would change η by 0.035° . The total angular uncertainty, therefore, is almost surely less than 0.25° . Because the angular distance to Algol is on the order of 2.2° this angular uncertainty can produce a shift of approximately 35 arc seconds in the position of the optic axis on the sky. The total positional error for frame #1 (i.e., the scan center) is then $\sqrt{(35^2 + 35^2)} \approx 50$ arc seconds.

The aspect uncertainty increases with distance from scan center because of possible errors in scan rate and scan orientation. A 1% error in scan rate produces an 0.4 arc minute shift in position at the end of a scan. This error is strictly a function of scan radius and errors introduced while scanning away from scan center are corrected for when the scan is reversed. A small error in scan rate will not greatly change the position centroid of the cluster because the transit point occurs near scan center. Errors in coordinate system alignment also become more important with distance from scan center. An uncertainty of 0.2° in coordinate alignment will produce an 0.2 arc minute uncertainty perpendicular to the scan direction at the end of a

scan. At the end of a scan the region of uncertainty is elliptical but can be approximated by a circular region 0.3 arc minute (20 arc seconds) in radius. Thus the total positional error probably increases to ~90 arc seconds at the end of a scan.

In addition to these well understood uncertainties there are at least three other sources of error that are more difficult to quantify. The measured position of the summed Algol image for the first camera frame is probably influenced at some level by the pixel shifts chosen to add frames. We have already argued that these shifts are probably not strictly appropriate for the later orbits. It is possible, therefore, that the superimposed image of Algol may depend somewhat on orbit. This difference could produce a systematic shift in image centroid of about 1/2 pixels. It is not clear whether this source of error will produce a slight systematic or random shift in the aspect solution.

The two other sources of error are related to assumptions about the ACS. Unlike that observed on the galactic center the Perseus cluster scans are assumed to have no component of motion perpendicular to the scan direction. While this is probably an incorrect assumption we expect the error to be small (less than 1 arc minute) and mainly in a direction perpendicular to the scan. Our solution also assumes that the scan rate is constant and this is almost surely not the case. If the scan rate were constant observations of the Perseus cluster would begin and end at the same point. This means that the observed count rate should be the same at the beginning and end of an observation. In no case has this been observed to be true. As shown in Figure 15 the count rate is always significantly different and is consistent with the end point falling short of where it began. This slow-down of the scan rate is probably caused by gyro drift and based on the galactic center aspect solution probably does not cause an error greater than 1 arc minute at the end of the observation. It is not clear how significant this error really is because other uncertainties may tend to average this error over the length of the scan.

Although we have determined that the positional uncertainty at the center of the scan may be on the order of 60 arc seconds, this estimate may be

somewhat conservative. Shown in Figure 16 is the 90% confidence positional centroid for the Perseus cluster using the P9 aspect solution. The chi-square for the fit was 25 for 18 degrees of freedom and assumed a positional error of 30 arc seconds for each point. Much of this chi-square was contributed by one scan (scan 10, see Appendix A). An even smaller chi-square value would be produced if an error of 60 arc seconds were assumed. The good agreement in Figure 16 of the 90% confidence positional centroid of the Perseus cluster centroid and NGC 1275 suggests that our absolute placement of the aspect solution on the sky is probably accurate to within 1 arc minute at scan center.

Acknowledgments

This report would not have been possible without the hard work and help of many individuals. Because of their very close association with this project, Harry Heckathorn and Kevin Carmody deserve special recognition. Harry Heckathorn supervised the film measurement at Fermi Lab, participated in the film digitization, provided the G.C. aspect solution, and provided valuable counsel. Kevin Carmody conceived and developed the ONESTAR method for determining aspect and developed a more user friendly working environment for the PDS microdensitometer. His programming expertise, hard work and counsel were invaluable to the project.

Appendix A: Modification of some Algol Pixel Locations

The measured pixel locations of the summed Algol image for each orbit are shown in Figure 7 and the ONESTARP3 aspect solution using these positions is given in Figure 17. From an inspection of this figure it is clear that compared to the other scans the aspect solution for orbit 70 is considerably misplaced from that of orbit 71. A position centroid for the narrow Perseus cluster component derived from this solution shows that the observed transit for orbit 70 is considerably different than predicted. Because the summed Algol image is not very clear on some orbits it seems likely that the measured position of Algol for orbit 70 is incorrect.

Rather than discarding the data from this orbit it was decided to modify the aspect solution for orbit 70 by changing the position of Algol relative to orbit 71. Kevin Carmody changed the position of Algol on orbits 70 and 10 and these positions have been used for the ONESTARP7 solution (Figure 11). Because it remains unclear how these changes were determined it was decided to recalculate these modifications for the P9 solution.

The basic question to be addressed is how to determine the bad from the good Algol measurements. Shown in Table 7 are the best fit parameters assuming that the Algol images in Figure 7 define a circle about some centroid. While we have argued that this is not strictly true this approximation is adequate for the purpose at hand. For each Algol measurement we have calculated the distance in pixels the image is from the best fit centroid, the deviation of this value from the best fit radius, and the angle the image subtends in the pixel coordinate system. Also shown in the table are the angular differences between adjacent orbits. In general, adjacent orbits are displaced 5.89° from each other and the difference between observed and best fit radius is small (0-2 pixels).

Orbits 70, 10, and 11 are exceptions to this general pattern. The large difference in observed to expected radius for orbit 70 clearly singles out that measurement as bad and this measurement can be corrected by merely changing its centroid distance. The small angular difference between orbits

10 and 11 suggests that one or both of the measurements are likely to be wrong but because they both have radii close to the best fit value no correction to any single measurement is obvious. For this reason we have not changed the pixel values for the orbit 1 measurements in the P9 solution. A comparison of the observed and predicted transits of the Perseus cluster center suggests that orbit 10 is probably incorrectly placed. The misalignment of 101 arc seconds can be corrected before analysis by adjusting the aspect solution so that observed and predicted transit times agree exactly.

The pixel position for orbit 70 was changed for the P9 solution as follows:

$$\begin{aligned}\theta_{70} &= \theta_{71} - \theta_{ave} \\ &= 47.0996 - 5.8869 = 41.2127^\circ\end{aligned}$$

$$\begin{aligned}\Delta x_{pix} &= R_{ave} * \cos(\theta_{70}) & \Delta y_{pix} &= R_{ave} * \sin(\theta_{70}) \\ &= 269.32 * \cos(41.2127) & &= 269.32 * \sin(41.2127) \\ &= 202.60 & &= 177.44\end{aligned}$$

$$\begin{aligned}x_{pix70} &= x_{cen} + \Delta x_{pix} & y_{pix70} &= y_{cen} + \Delta y_{pix} \\ &= 470.80 + 202.60 & &= 508.40 + 177.44 \\ &= 673.40 & &= 685.84\end{aligned}$$

Table 1

Measured Galactic Center Scan Rates

<u>Orbit</u>	<u>Scan Times (MET)</u>	<u>Sweep Rate (deg/s)</u>
1.1	05:32:40 - 05:35:16	0.0065
1.2	05:35:26 - 05:40:36	0.0065
1.3	05:40:46 - 05:43:21	0.0065
2.1	07:04:30 - 07:07:06	0.0065
2.2	07:07:15 - 07:12:25	0.0065
2.3	07:12:35 - 07:15:11	0.0064
3.1	08:36:20 - 08:38:55	0.0065
3.2	08:39:05 - 08:44:15	0.0065
3.3	08:44:25 - 08:47:00	0.0066
4.1	10:08:10 - 10:10:44	0.0065
4.2	10:10:55 - 10:16:04	0.0065
4.3	10:16:15 - 10:18:49	0.0064
5.1	11:39:59 - 11:42:34	0.0065
5.2	11:42:44 - 11:47:54	0.0065
5.3	11:48:04 - 11:50:39	0.0064
6.1	13:11:48 - 13:14:24	0.0066
6.2	13:14:34 - 13:19:43	0.0065
6.3	13:19:53 - 13:22:29	0.0064
7.1	14:43:38 - 14:46:13	0.0066
7.2	14:46:23 - 14:51:33	0.0065
7.3	14:51:43 - 14:54:18	0.0064
8.1	16:15:28 - 16:18:03	0.0065
8.2	16:18:13 - 16:23:23	0.0064
8.3	16:23:33 - 16:26:07	0.0064
	Mean rate:	0.00648
	Sample deviation:	0.00006
	Error in Mean:	0.00003

Table 2

Galactic Center Roll Angles

<u>Orbit</u>	<u>Planned Angle</u>	<u>Observed Angle</u>	<u>O - P</u>
1.1	219.9998	220.0147	+0.0149
1.2		220.3134	+0.3136
1.3		219.6743	-0.3255
2.1	309.9497	309.8345	-0.1152
2.2		310.0906	+0.1409
2.3		309.7910	-0.1587
3.1	258.5497	258.2340	-0.3157
3.2		258.9237	+0.3740
3.3		259.0724	+0.5227
4.1	168.5997	168.4437	-0.1560
4.2		169.0441	+0.4444
4.3		168.3580	-0.2417
5.1	284.2497	283.8834	-0.3663
5.2		284.6169	+0.3672
5.3		284.2447	-0.0050
6.1	194.2997	194.6867	+0.3870
6.2		195.0727	+0.7730
6.3		194.8395	+0.5398
7.1	245.6997	245.7979	+0.0982
7.2		246.3280	+0.6283
7.3		246.1956	+0.4959
8.1	155.7497	155.4002	-0.3495
8.2		156.2967	+0.5470
8.3		155.7854	+0.0357

Mean O - P : +0.1520
Sample deviation: 0.3540
Error in Mean: 0.1214

Table 3

Algol Pixel Offsets

<u>Frame</u>	<u>Orbit</u>					
	<u>01</u>	<u>11</u>	<u>40</u>	<u>41</u>	<u>50</u>	<u>51</u>
2	-22	-22	-22	-20	-20	-21
3	-56	-55	-54	-53	-52	-53
4	-55	-56	-55	-55	-55	-54
5	-12	-14	-13	-14	-15	-12
6	+33	+30	+31	+31	+33	+32
7	-	+73?	+74	+74	+76	+75
8	+76	+75	+78	+80	+82?	+80
9	+52	+51	+55	+57	+59?	+58
10	+24	+20	+28	+28	+33?	+31

Average Offset (Good Frames Only)

<u>Frame Number</u>	<u>Offset</u>
2	-21.17 ± 0.98
3	-53.83 ± 1.47
4	-55.00 ± 0.63
5	-13.33 ± 1.21
6	+31.67 ± 1.21
7	+74.75 ± 0.96
8	+77.80 ± 2.28
9	+54.60 ± 3.05
10	+26.20 ± 4.27

Table 4

Camera 1 Misalignment (degrees)

Star	Orbit							
	<u>1</u>	<u>2</u>	<u>3</u>	<u>4</u>	<u>5</u>	<u>6</u>	<u>7</u>	<u>8</u>
1	-	-0.3754	-0.7624	-0.3047	-0.3893	-0.6489	-0.4722	-0.2450
2	-0.1311	-0.4422	-0.4489	-0.4023	-0.3377	-0.6735	-0.7923	-0.4936
3	-0.1549	-0.4252	-0.4946	-0.3802	-0.5699	-0.7996	-0.5338	-0.5280
4	-0.1447	-	-0.6629	-	-0.7020	-	-0.3837	-
5	-0.1241	-0.4937	-0.5547	-	-0.5444	-	-0.1123	-
6	-0.1960	-0.6842	-0.4887	-0.4937	-0.5764	-	-0.2078	-0.4279
7	-0.3194	-0.2180	-0.4383	-0.3298	-0.3696	-0.8173	-	-0.4224
8	-0.4345	-0.4610	-0.4684	-0.3364	-0.3669	-0.8848	-0.2614	-0.2294
9	-0.2908	-0.0348	-0.4162	-	-0.4468	-0.7623	-0.2571	-0.3723
10	-0.1728	-0.3922	-	-0.2931	-0.5548	-0.8739	-0.1082	-0.2809
11	-0.1442	-0.3174	-0.3827	-0.3083	-0.7051	-0.8265	-0.4630	-0.0922
12	+0.0153	-0.6821	-0.2614	-0.4381	-0.4507	-0.9221	-0.3239	-0.2300
13	-0.1952	-	-	-0.4715	-0.5699	-0.8279	-0.1689	-0.4236
14	-0.0444	-0.3556	-0.3813	-0.4943	-0.4204	-0.7758	-0.3512	+0.0014
15	-0.1465	-	-0.4028	-0.4019	-0.4232	-0.8721	-0.1546	-0.3103
μ	-0.1774	-0.4068	-0.4741	-0.3876	-0.4951	-0.8071	-0.3279	-0.3125
σ	0.1121	0.1785	0.1286	0.0745	0.1177	0.0825	0.1911	0.1545
σ_μ	0.0299	0.0515	0.0357	0.0215	0.0304	0.0238	0.0511	0.0429

$$\langle \mu \rangle = -0.4189 \pm 0.0210 (\sigma_\mu) \\ \pm 0.2149 (\sigma)$$

Table 5

Nominal Perseus Cluster Roll Angles

<u>Orbit</u>	<u>Roll Angle</u>
0	43.342 37.717
1	133.342 127.717
2	88.342 82.717
3	358.342 352.717
4	110.842 105.217
5	20.842 15.217
6	65.842 60.217
7	335.842 330.217
8	122.092 116.467
9	32.092 26.467

Table 6

Computed Perseus Cluster Long Scan Rates

<u>Orbit</u>	<u>Scan Times (MET)</u>	<u>Sweep Rate (deg/s)</u>
0	03:10:59 - 03:16:18 03:22:31 - 03:27:50	0.00447 0.00447
1	04:42:49 - 04:48:08 04:54:22 - 04:59:40	0.00448 0.00448
2	06:14:38 - 06:19:58 06:26:11 - 06:31:30	0.00449 0.00449
3	07:46:28 - 07:51:47 07:58:01 - 08:03:20	0.00450 0.00450
4	09:18:18 - 09:23:37 09:29:51 - 09:35:09	0.00450 0.00451
5	10:50:08 - 10:55:26 11:01:40 - 11:06:59	0.00452 0.00452
6	12:21:57 - 12:27:15 12:33:30 - 12:38:48	0.00452 0.00453
7	13:53:47 - 13:59:05 14:05:19 - 14:10:38	0.00453 0.00453
8	15:25:36 - 15:30:54 15:37:09 - 15:42:27	0.00453 0.00454
9	16:57:26 - 17:02:44 17:08:57 - 17:14:16	0.00454 0.00454
	Mean rate:	0.00451
	Sample deviation	0.00002
	Error in mean	0.00001

Table 7

Algol Pixel Centroid

<u>Orbit</u>	<u>Xpix</u>	<u>Ypix</u>	<u>R</u>	<u>R-Rave</u>	<u>Theta</u>	<u>Del Theta</u>
00	708.45	375.75	272.16	2.84	330.8309	
01	717.35	402.35	268.39	-0.93	336.7257	5.8948
10	352.45	267.45	268.45	-0.87	243.8406	
11	372.45	260.75	266.46	-2.86	248.3403	4.4997
20	555.05	252.05	269.84	0.52	288.1932	
21	577.95	264.15	266.72	-2.60	293.6866	5.4934
30	727.45	593.45	270.38	1.05	18.3344	
31	716.55	620.55	270.13	0.81	24.5300	6.1956
40	452.35	236.85	272.18	2.86	266.1131	
41	477.95	239.35	269.14	-0.18	271.5223	5.4092
50	739.85	489.65	269.70	0.38	356.0135	
51	739.55	518.35	268.93	-0.39	2.1203	6.1068
60	645.55	305.35	267.89	-1.43	310.7161	
61	665.95	326.95	266.47	-2.85	317.0834	6.3673
70	688.75	699.25	289.70	20.38	41.2073	
71	656.05	707.75	272.14	2.82	47.0996	5.8923
80	402.15	247.45	269.83	0.51	255.2608	
81	427.45	245.35	266.60	-2.72	260.6419	5.3811
90	731.15	440.25	269.12	-0.20	345.3312	
91	737.25	468.95	269.35	0.03	351.5781	6.2469

Best Fit Circle

$$\langle \text{Theta} \rangle = 5.8869 \pm 0.4011$$

$$x_{\text{cen}} = 470.80$$

$$y_{\text{cen}} = 508.40$$

$$R_{\text{ave}} = 269.32$$

Figure Captions

- Figure 1 - A reproduction of one of the calibration photographs taken of the Deneb (α Cyg) star field. The field-of-view is approximately 7° on a side. The optic axis lies at the center of the Deneb image. Also shown are the frame fiducials as measured at Fermi Lab.
- Figure 2 - The position of the optic axis (x_0, y_0) measured on each orbit in a coordinate system centered on Fiducial #1 and aligned with the positive X axis pointed toward Fiducial #4. The measurements are in millimeters. The position of the optic axis was observed to drift approximately one arc minute during the mission. The nature of this drift is unknown but may be related to thermal effects.
- Figure 3 - A schematic of the SKYPOS method used to determine the aspect solution for the galactic center observations.
- Figure 4 - A schematic of the G.C. scan pattern. Circles denote the position of the optic axis determined from camera 2 photographs. The inferred scan pattern is approximated by the straight lines connecting these points.
- Figure 5 - A schematic of the start and stop end points for each of the galactic center scans. The specification of scan end points is shown in the lower left corner of the figure.
- Figure 6 - The magnitude of the G.C. aspect scan end point offsets for points b and c and d and e of Figure 5. The average offset of 0.4 arc minutes provides a measure of the aspect solution accuracy.
- Figure 7 - The relative position of the summed Algal image for each Perseus cluster observation. The centroid of these images (the roll axis) is denoted by C and the computed position of the optic axis is denoted by O. These points coincide when the Algal centroid is corrected for scan motion model distortion (see text).

Figure 8 - The spherical geometry and basic equations used in the ONESTAR method for determining Perseus cluster aspect.

Figure 9 - The various coordinate systems used to solve the Perseus cluster aspect.

Figure 10 - The circles represent the 90% confidence transit centroids of the narrow and broad Perseus cluster components derived with an aspect solution that incorrectly assumed camera and spacecraft coordinates were aligned. The effect of adding an ad hoc correction to the assumed roll angle for each orbit is shown.

Figure 11 - The Perseus cluster aspect solution derived with ONESTARP7 after adding -0.07° to each of the planned scan angles. This correction is necessary in order to properly account for the $\sim 0.1^\circ$ northward displacement of the scans from the intended target.

Figure 12 - The magnitudes of the Perseus cluster scan end point offsets derived from the ONESTARP7 solution. Unlike the G.C. solution (see Figure 6) there are clear trends in the data that suggest the aspect solution may be unreliable on arc minute scales.

Figure 13 - The Perseus aspect solution obtained with ONESTARP9 which assumes the scan rates are constant.

Figure 14 - The end point(s) for the start and stop position of the P9 Perseus cluster aspect solution. This figure is equivalent to the central panel of Figure 5 but only one point is plotted for each orbit because of the constant scan rate assumption.

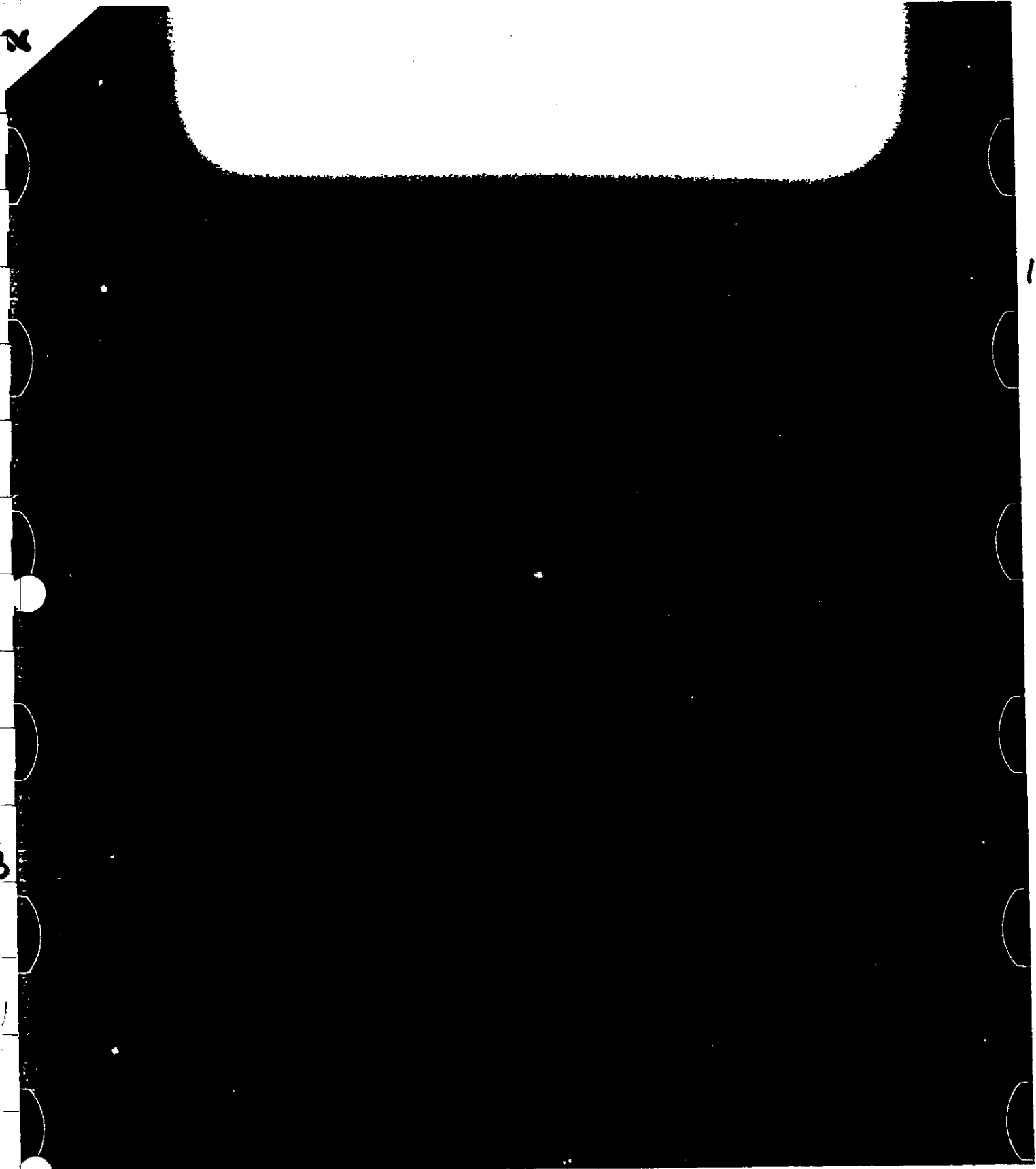
Figure 15 - The observed 1-10 keV count rate for the beginning and end of one of the Perseus cluster observations. The arrows indicate the region of comparison. The count rate difference indicates that the observation end points do not coincide.

Figure 16 - The 90% and 99% confidence positional error box for the Perseus cluster narrow component obtained with the P9 aspect solution. The position of NGC 1275 is indicated.

Figure 17 - The ONESTAR3 aspect solution obtained by using all the measured Algol pixel positions. Note that orbit 70 is considerably displaced from orbit 71 suggesting that the pixel position measured on that orbit is in error.

Figure 1

Z XEN-0.1



FIDUCIALS #1 + #4 IN GROUVE
USE FIDUCIALS #2 + #3 IN REDUCTIONS

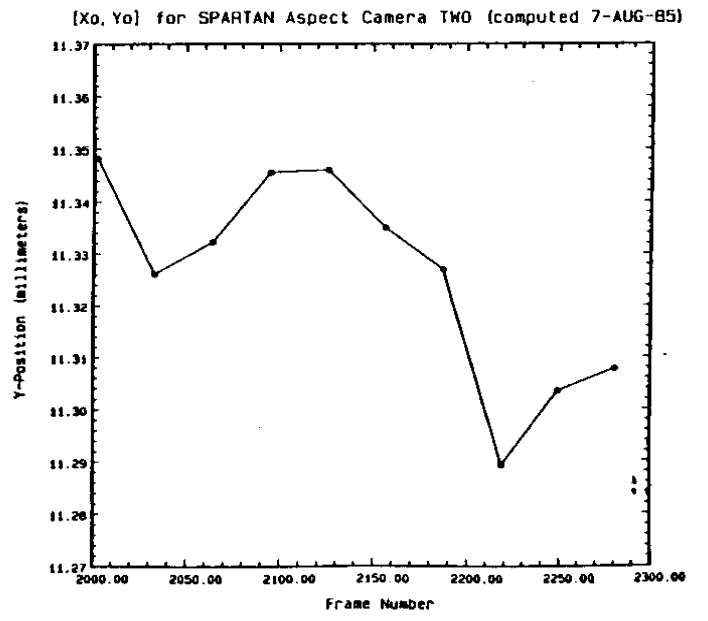
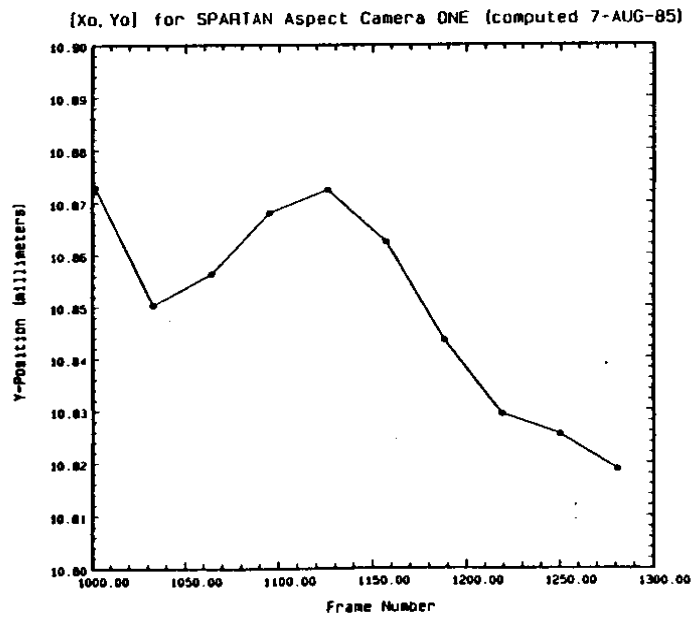
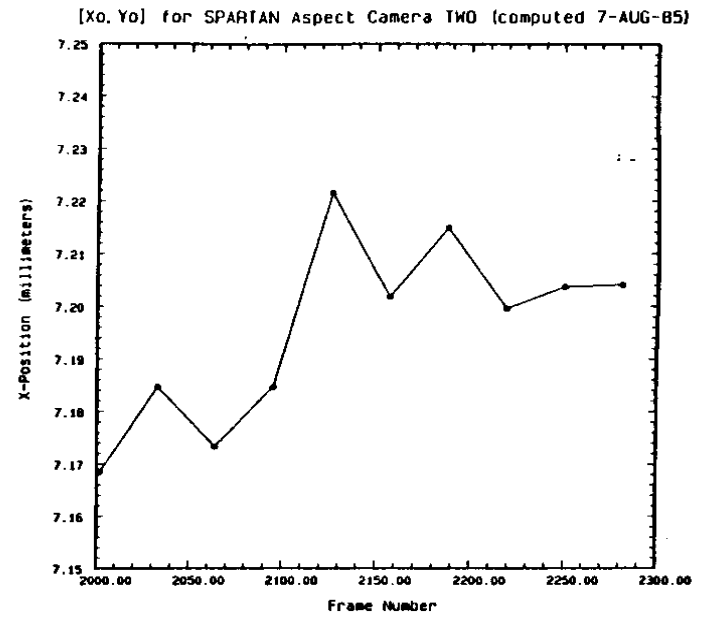
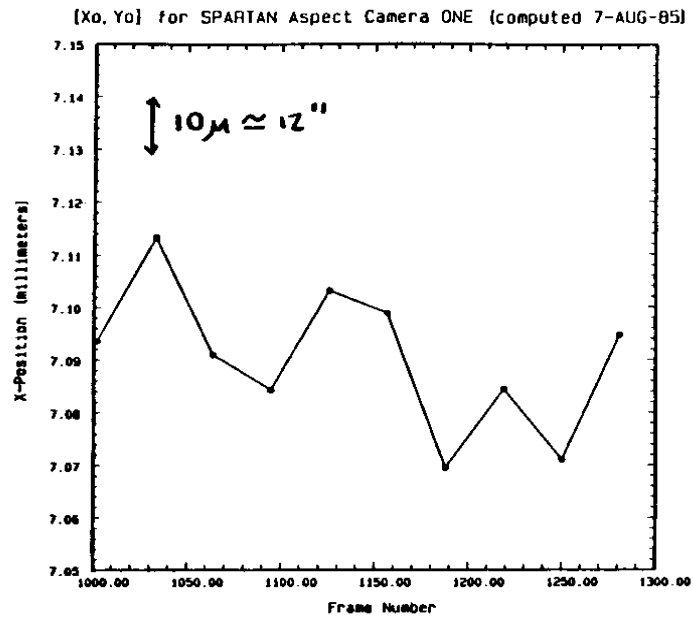


Figure 2

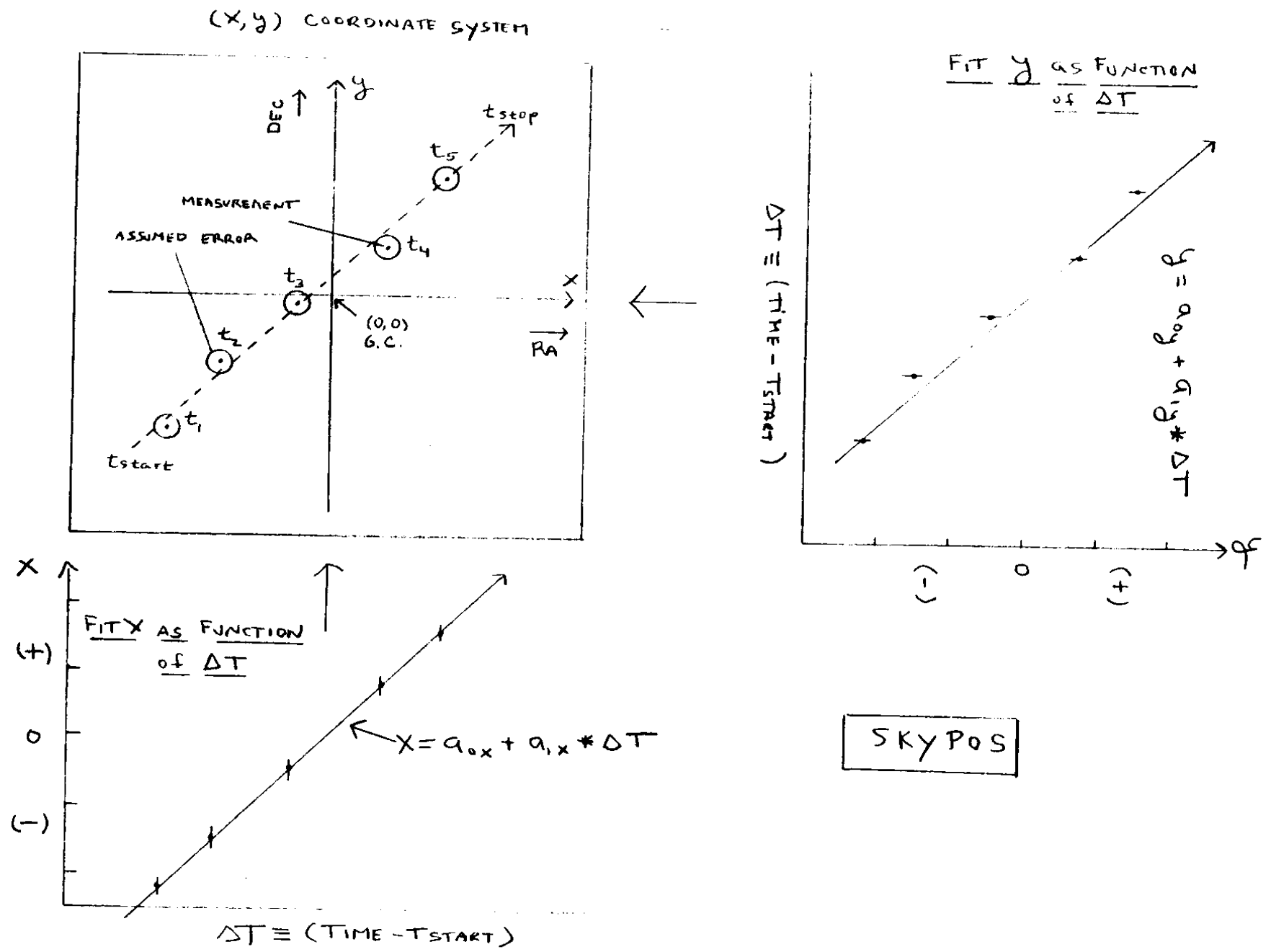


Figure 3

Spartan I Aspect Solution: Galactic Center Field, Camera TWO

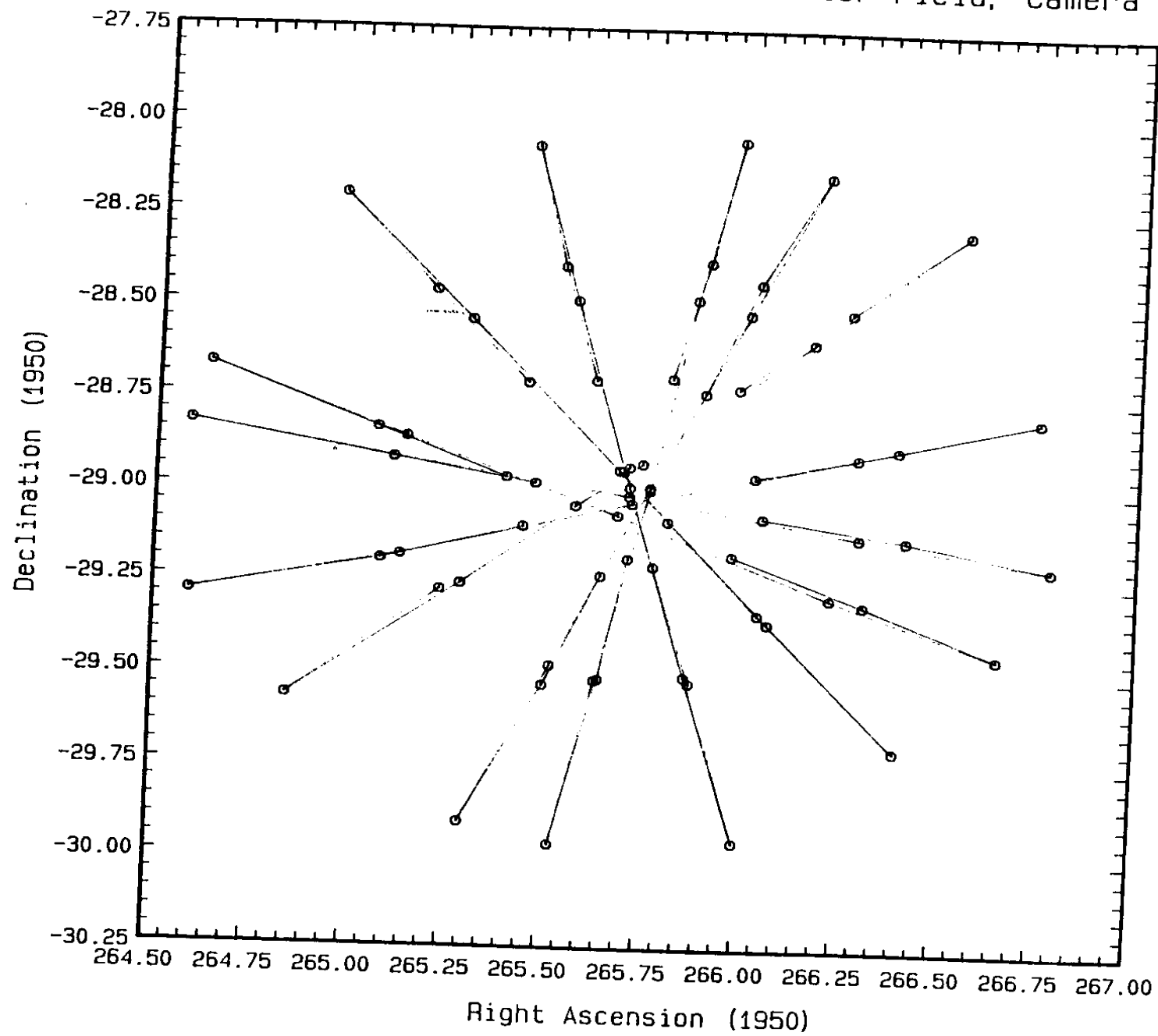


Figure 4

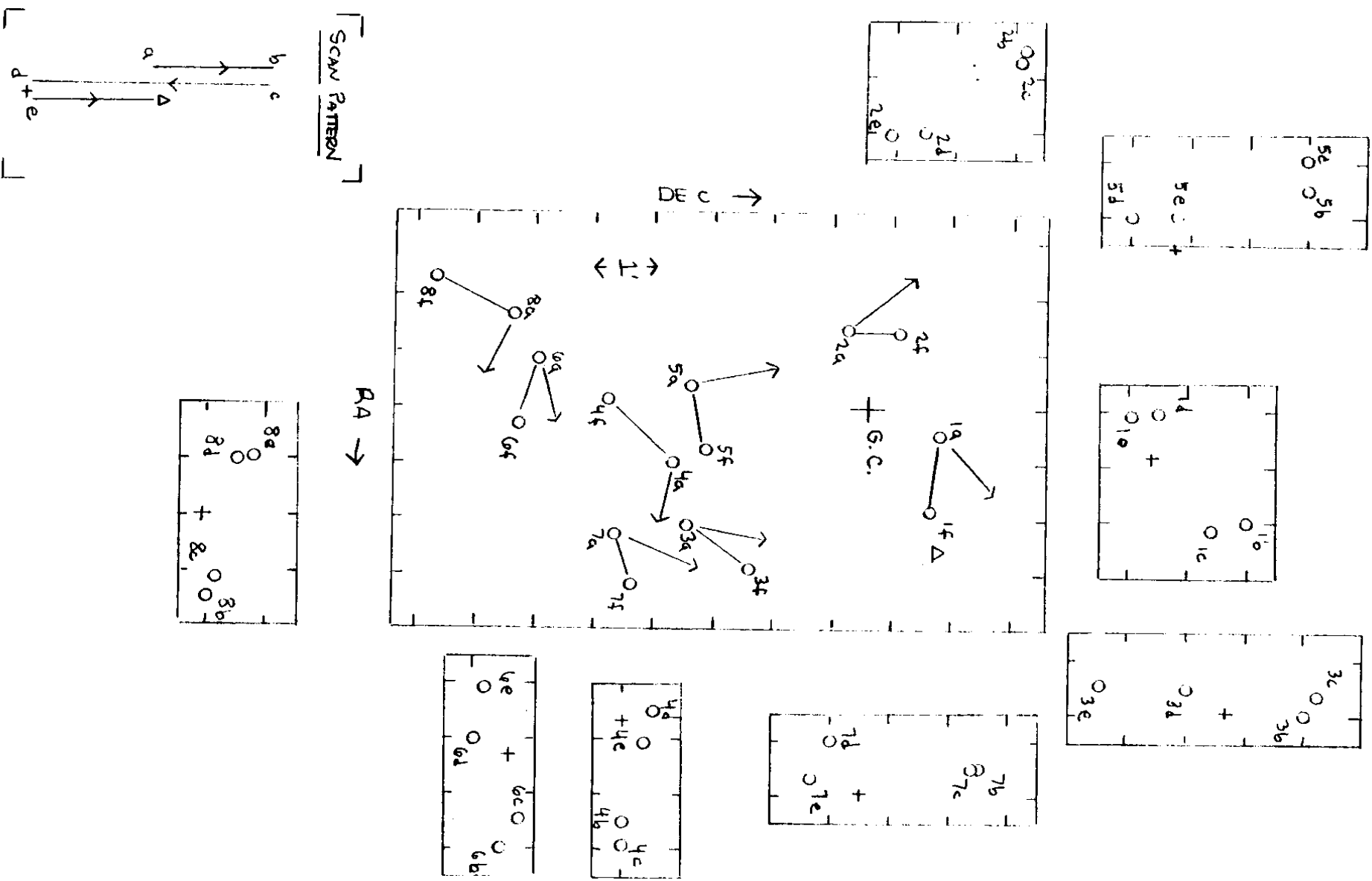


Figure 5

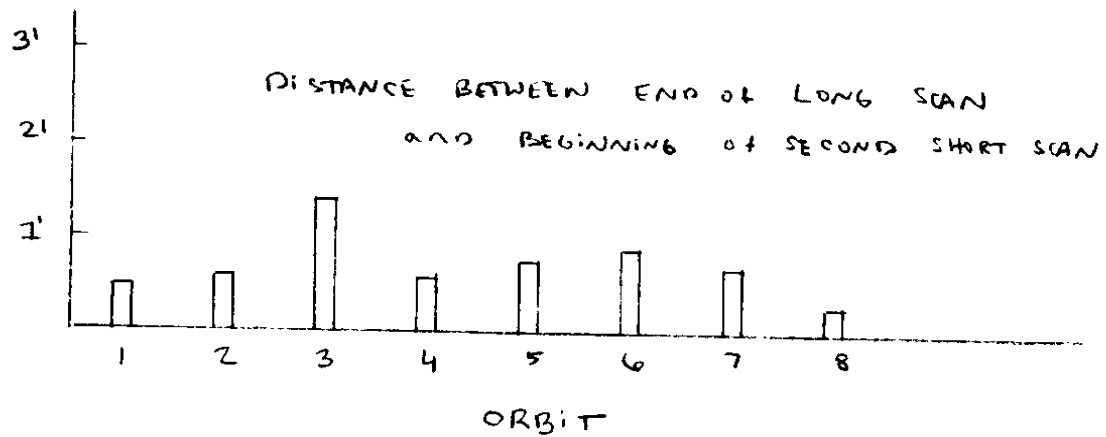
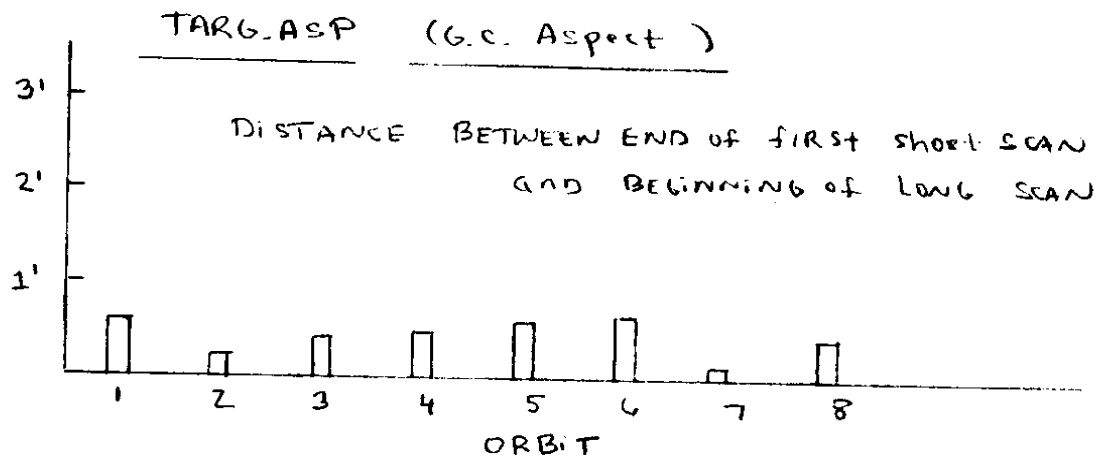


Figure 6

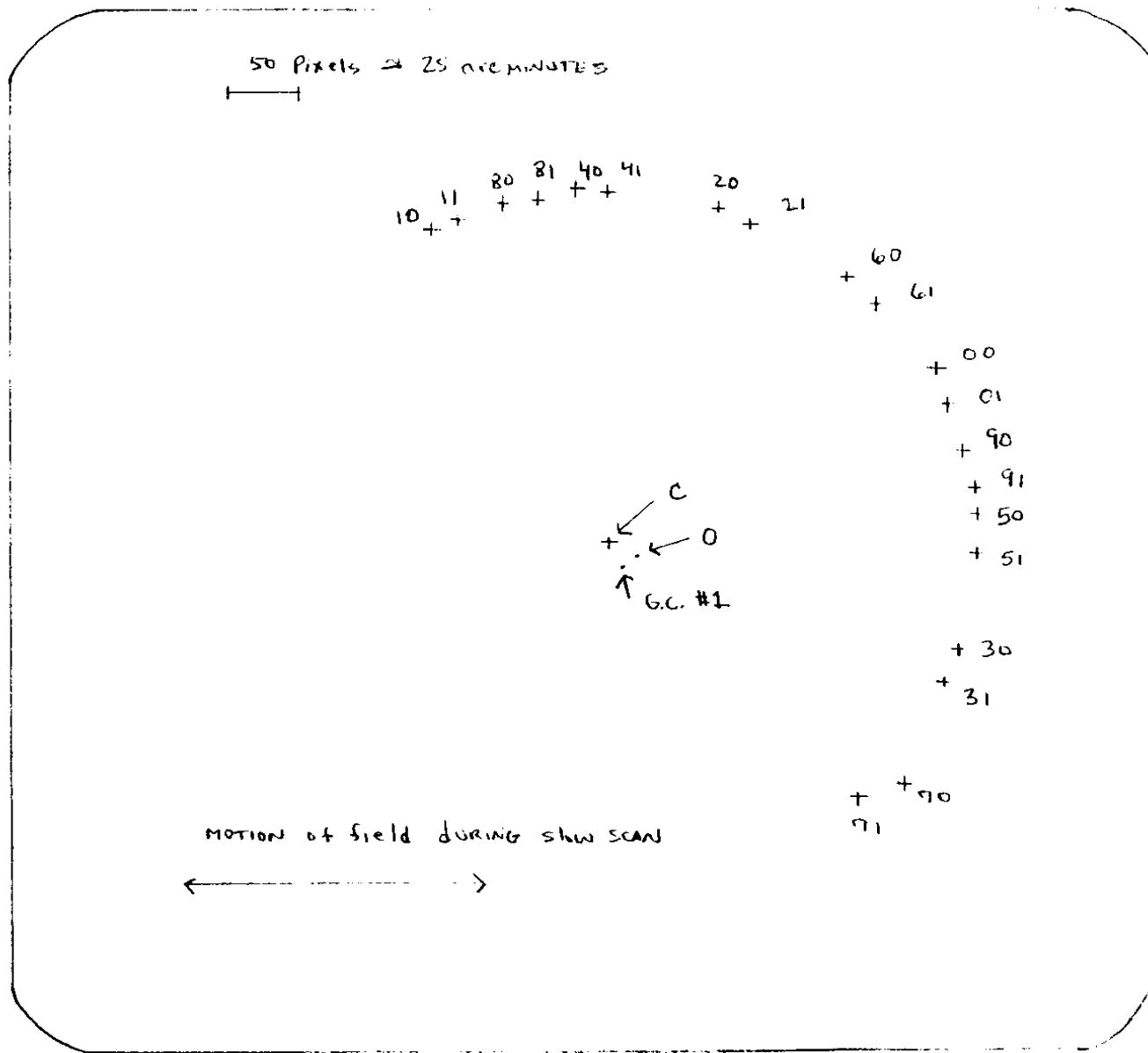


Fig 1
x

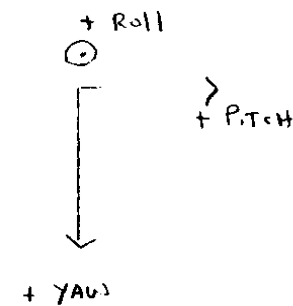
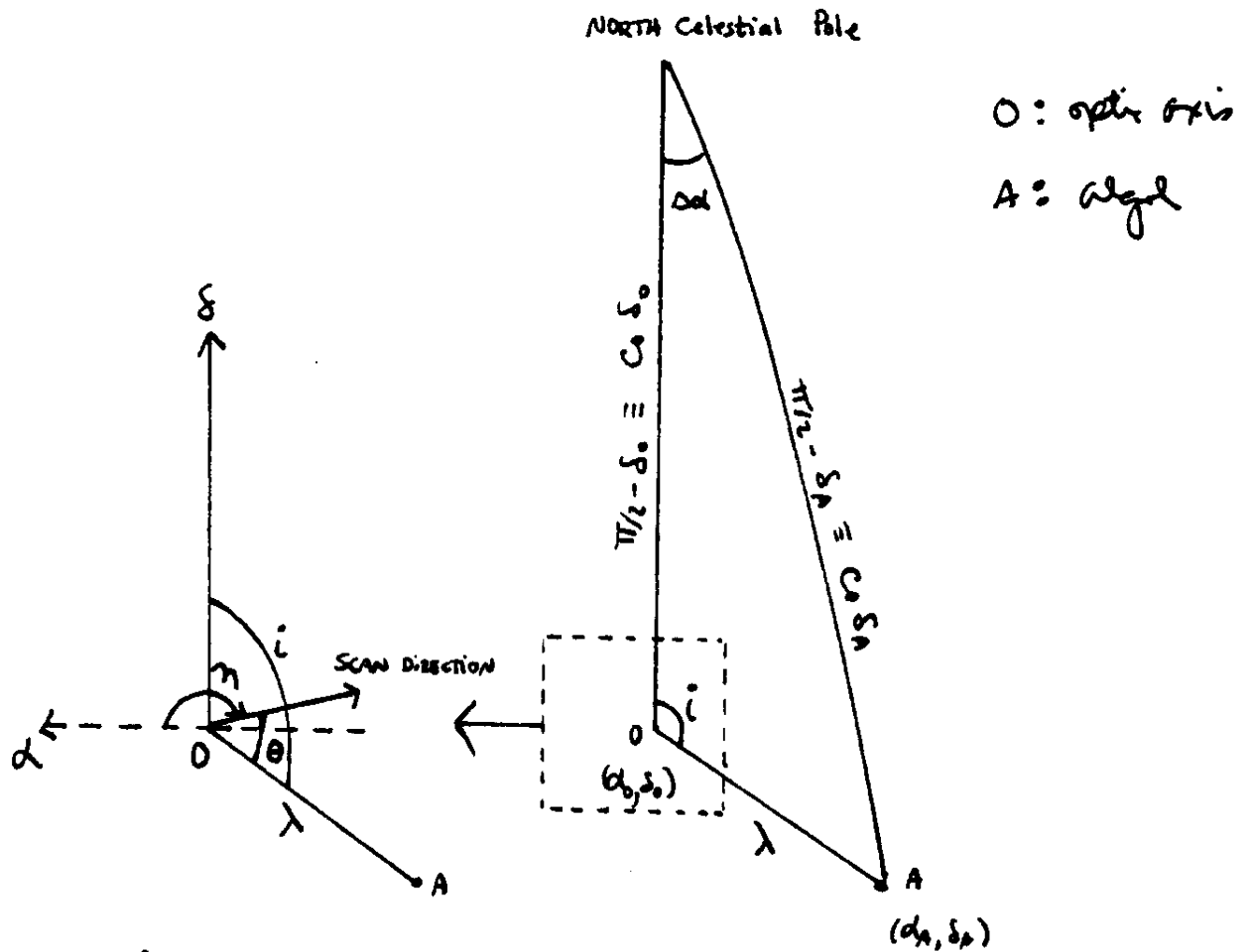


Fig 4
x

Figure 7

Figure 8



$$i = \theta + [\pi/2 - (\pi - m)]$$

$$i = \theta + \eta - \pi/2$$

law of sines

$$\frac{\sin A}{\sin a} = \frac{\sin B}{\sin b}$$

$$\frac{\sin \Delta \alpha}{\sin \lambda} = \frac{\sin i}{\sin(\pi/2 - \delta_A)} = \frac{\sin i}{\cos \delta_A}$$

from SINEG (p. 49, p. 23)

$$\cos \frac{1}{2}(A+B) = \tan \frac{c}{2}$$

$$\cos \frac{1}{2}(A-B) = \tan \frac{1}{2}(a+b)$$

$$\cos \frac{1}{2}(i + \Delta \alpha) = \tan \frac{1}{2} \cos \delta_0$$

$$\cos \frac{1}{2}(i - \Delta \alpha) = \tan \frac{1}{2}(\lambda + \cos \delta_A)$$

$$\therefore \cos \delta_0 = 2 \tan^{-1} \left[\frac{\cos \frac{1}{2}(i + \Delta \alpha) \tan \frac{1}{2}(\lambda + \cos \delta_A)}{\cos \frac{1}{2}(i - \Delta \alpha)} \right]$$

and $\delta_0 = \pi/2 - \cos \delta_0$

$$\therefore \Delta \alpha = \sin^{-1} \left[\frac{\sin \lambda \sin i}{\cos \delta_A} \right]$$

and $\alpha_0 = \alpha_A + \Delta \alpha$

ONESTAR COORDINATE SYSTEMS

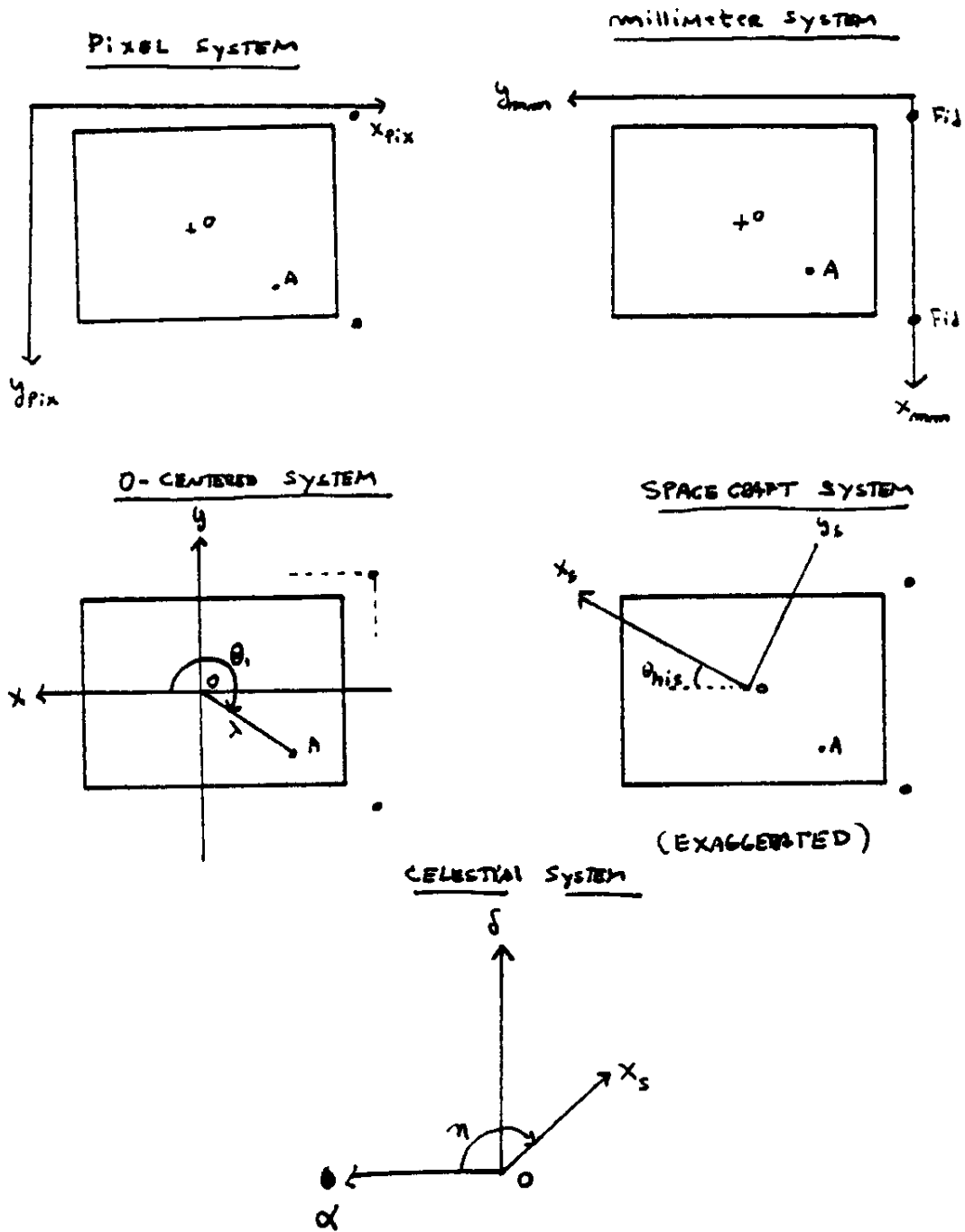


Figure 9

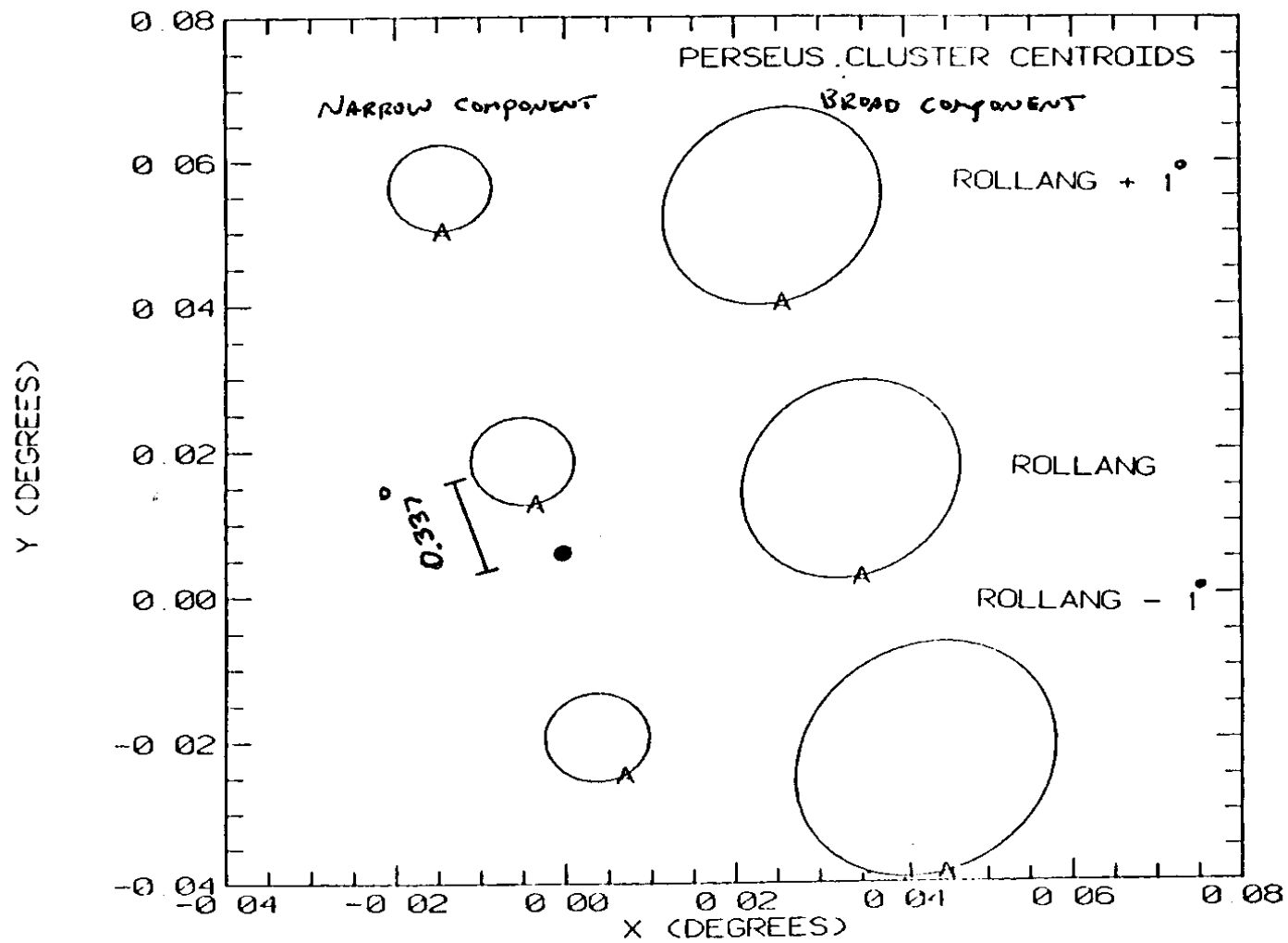


Figure 10

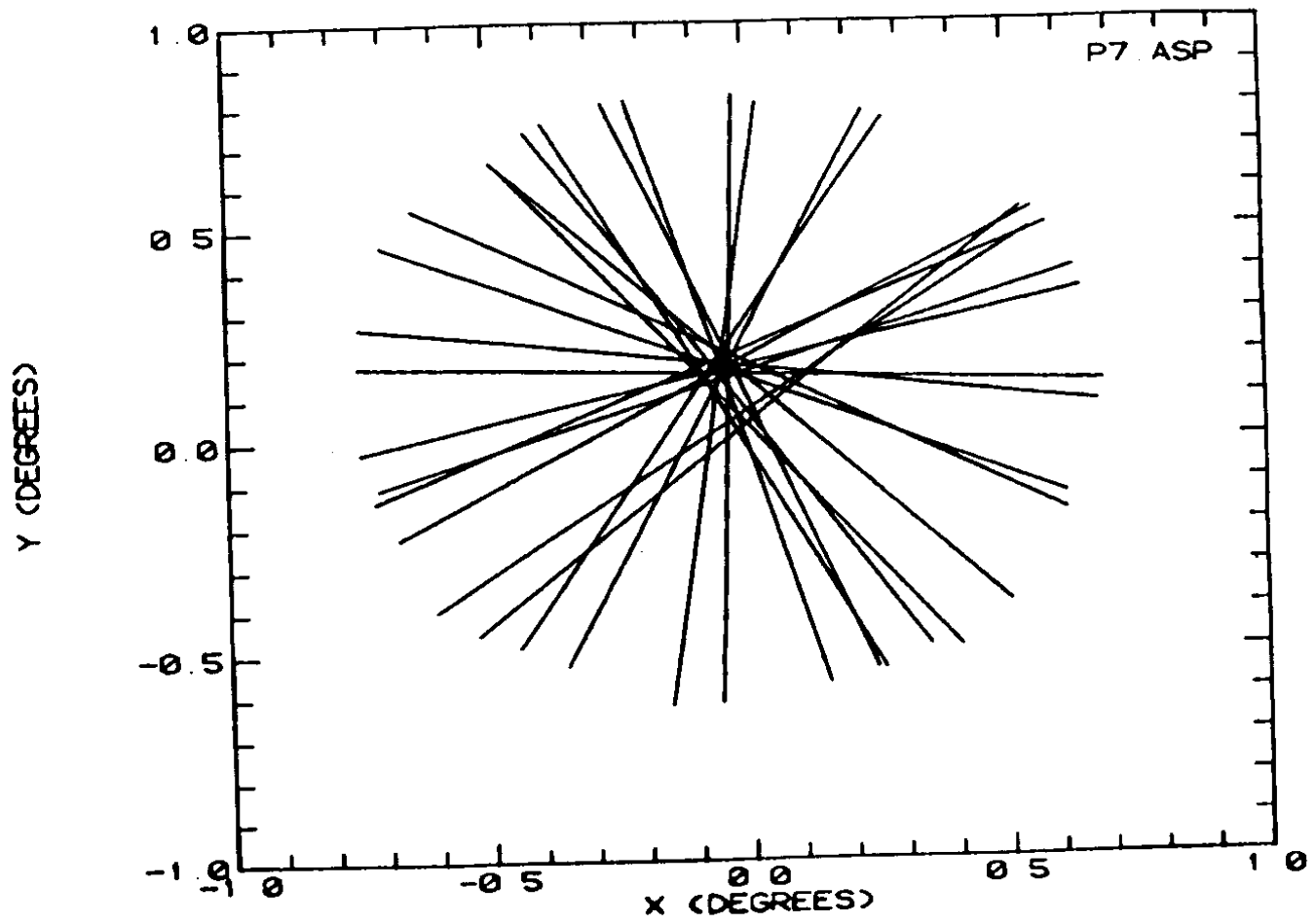


Figure 11

P7. ASP

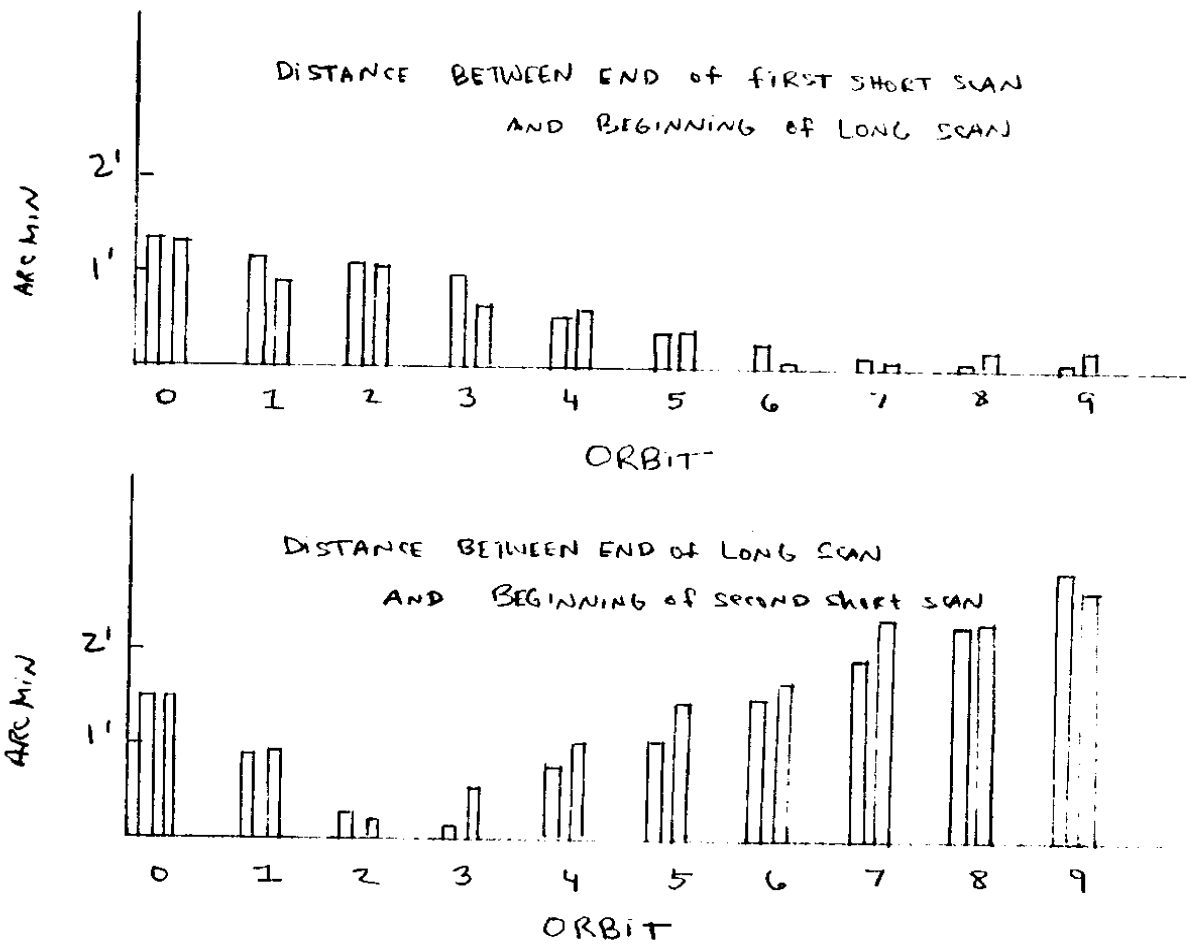


Figure 12

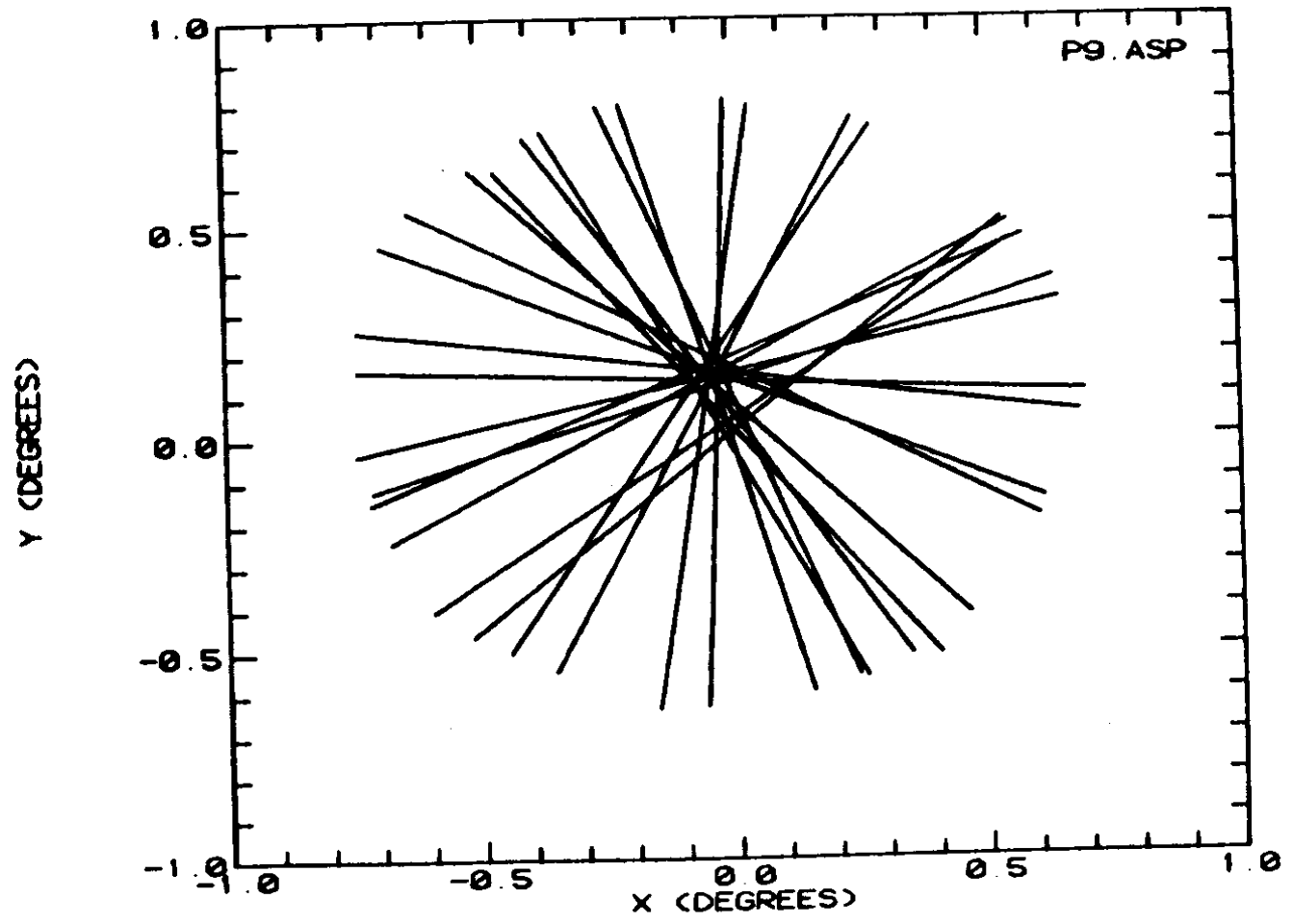


Figure 13

P9 START (STOP) POINTS

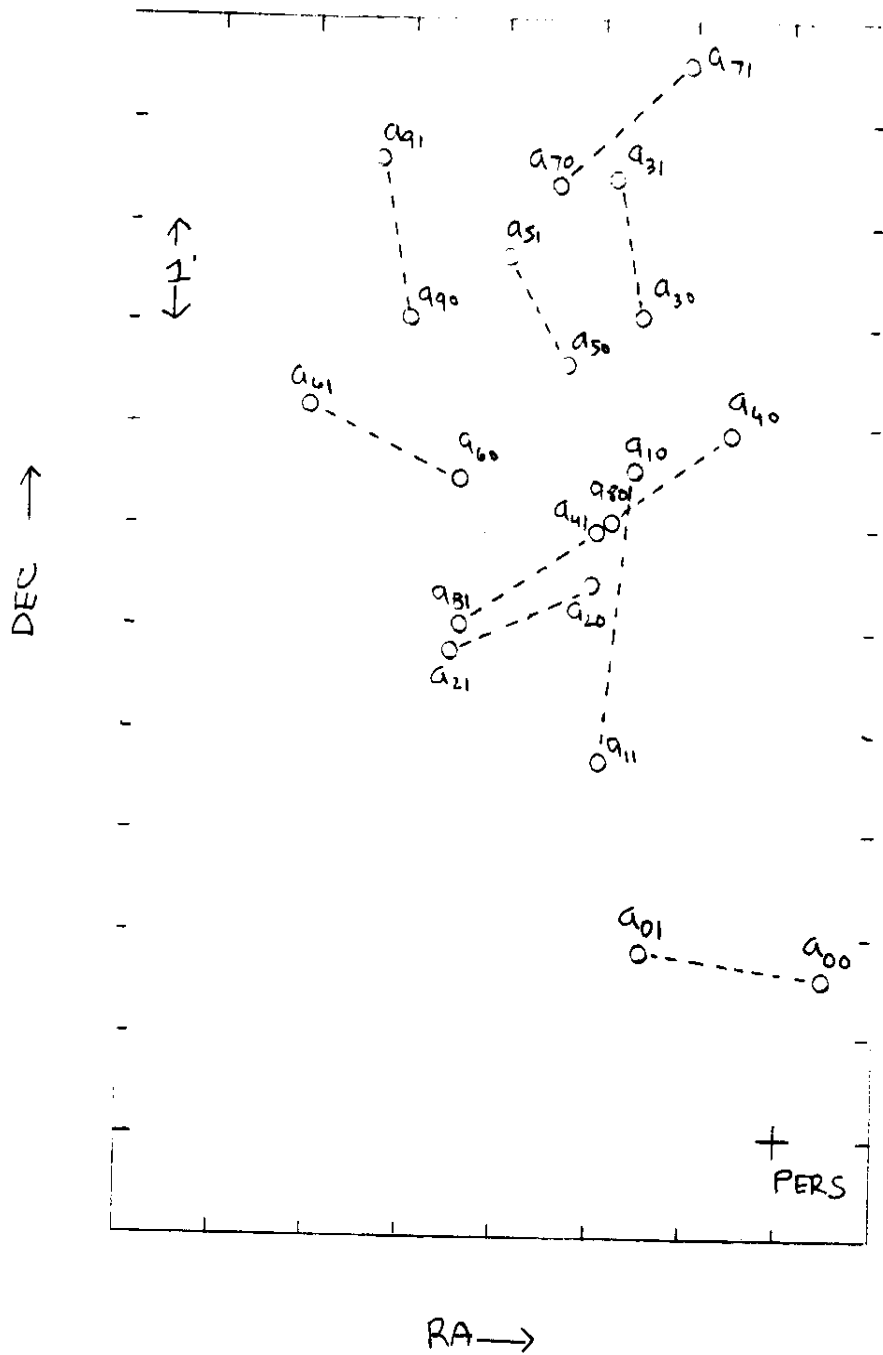


Figure 14

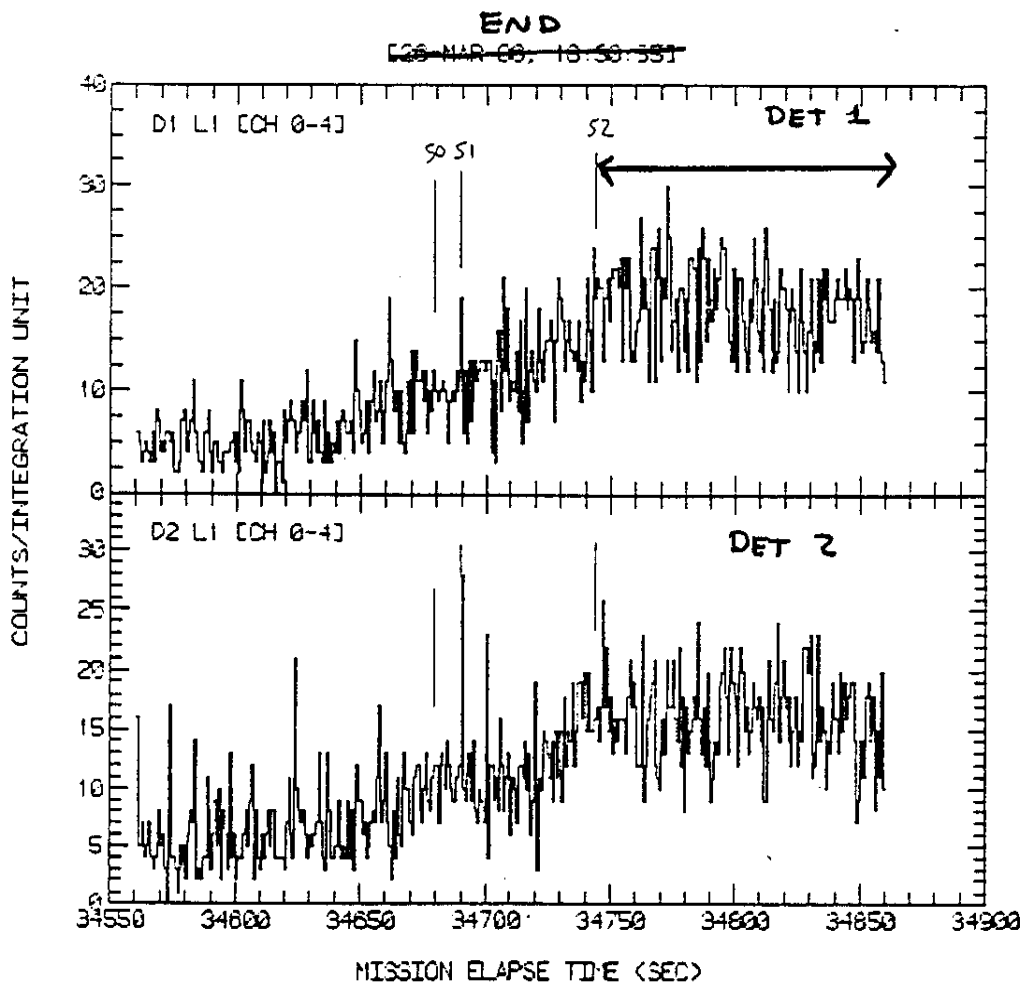
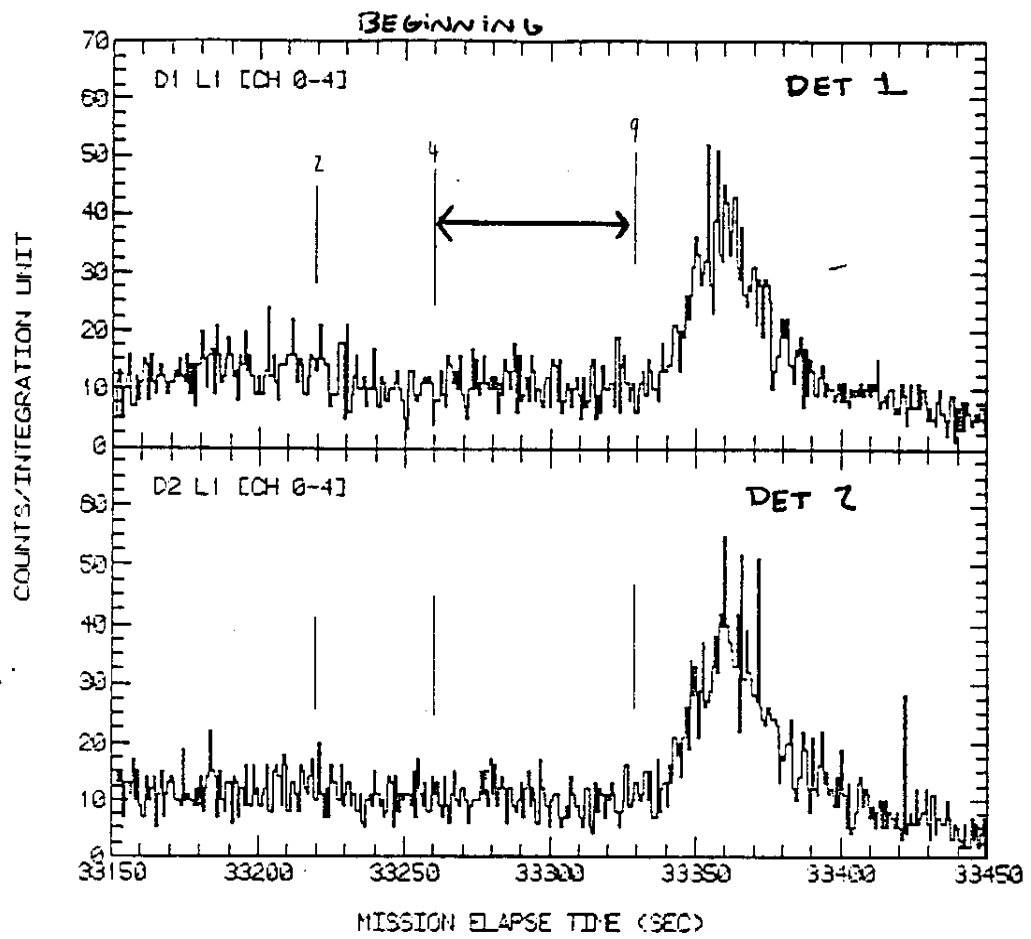


Figure 15

CONTOUR LEVELS:
A = 30.380
B = 34.970

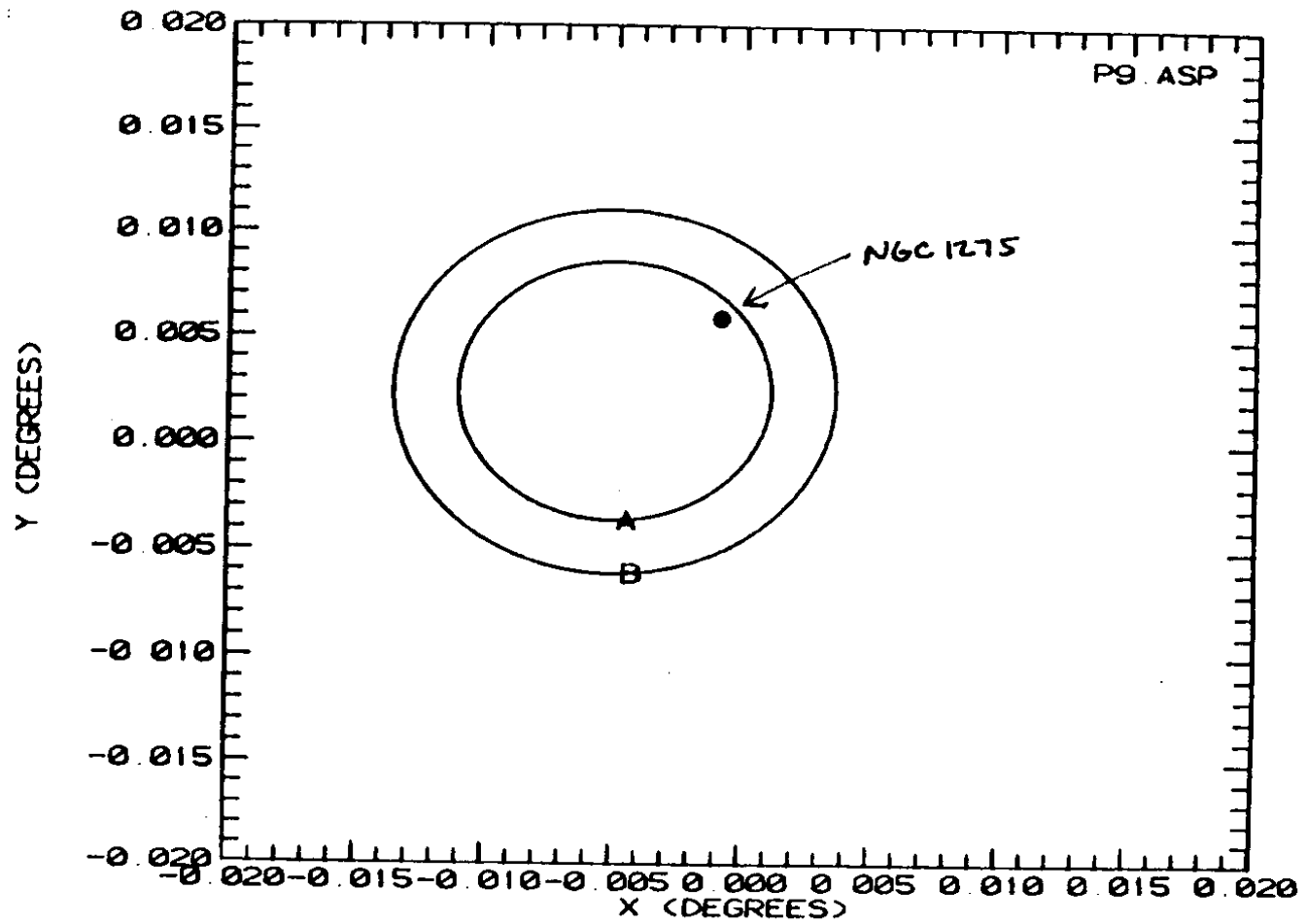


Figure 16

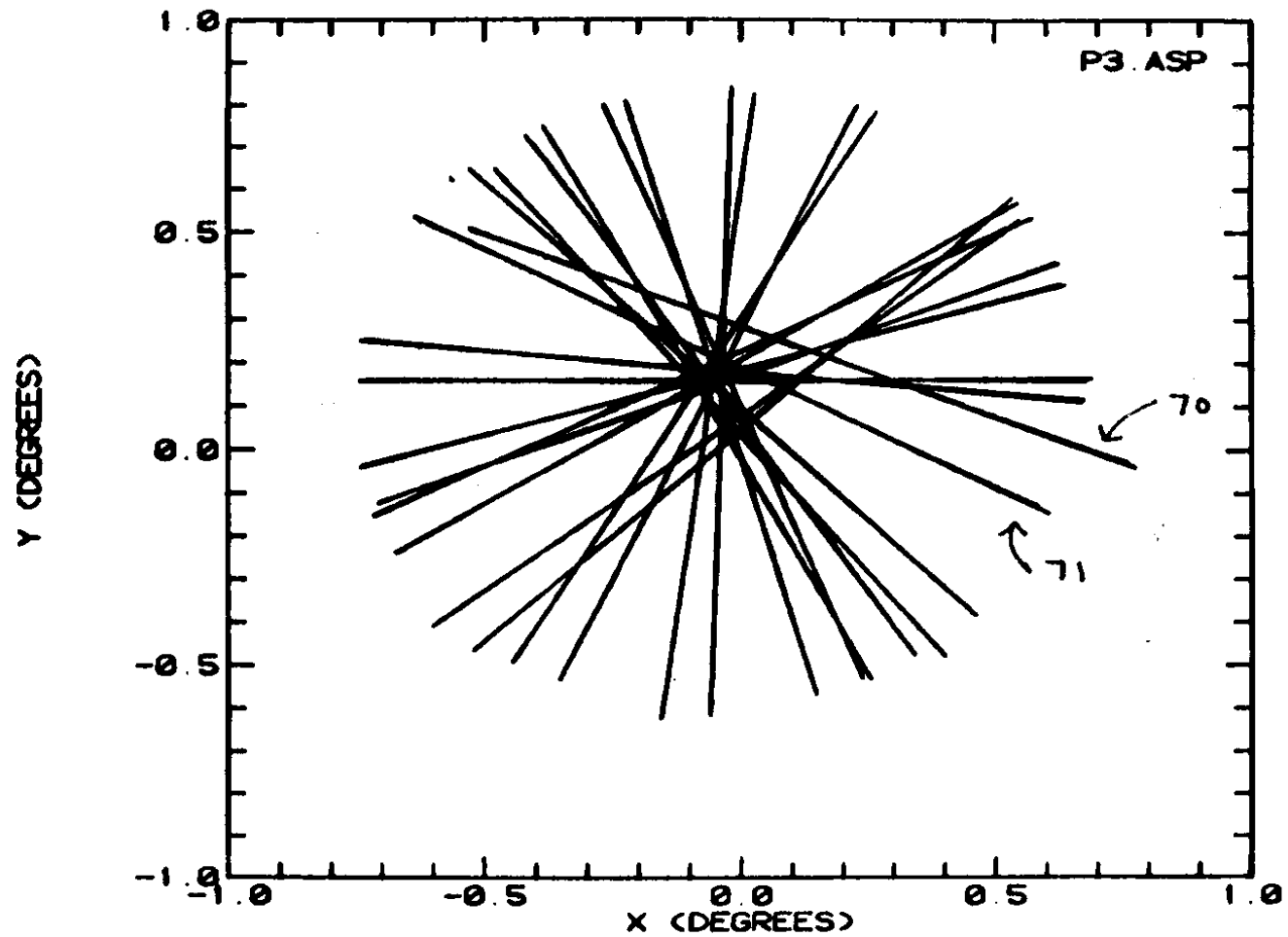


Figure 17



The Spartan 1 Mission

R. G. CRUDDACE AND G. G. FRITZ
E.O. Hulburt Center for Space Research

D. J. SHREWSBERRY
NASA Goddard Space Flight Center

D. C. BRANDENSTEIN, J. O. CREIGHTON, G. GUTSCHEWSKI,
S. W. LUCID, S. R. NAGEL, AND J. M. FABIAN
NASA Johnson Space Center

D. ZIMMERMAN
NASA Kennedy Space Center

E. E. FENIMORE
Los Alamos National Laboratory

C. GROSS
McDonnell Douglas Corporation

July 11, 1989

REPORT DOCUMENTATION PAGE				Form Approved OMB No. 0704-0188	
1a. REPORT SECURITY CLASSIFICATION UNCLASSIFIED			1b. RESTRICTIVE MARKINGS		
2a. SECURITY CLASSIFICATION AUTHORITY			3. DISTRIBUTION / AVAILABILITY OF REPORT		
2b. DECLASSIFICATION / DOWNGRADING SCHEDULE			Approved for public release; distribution unlimited.		
4. PERFORMING ORGANIZATION REPORT NUMBER(S) NRL Report 9207			5. MONITORING ORGANIZATION REPORT NUMBER(S)		
6a. NAME OF PERFORMING ORGANIZATION Naval Research Laboratory		6b. OFFICE SYMBOL (if applicable) 4120	7a. NAME OF MONITORING ORGANIZATION		
6c. ADDRESS (City, State, and ZIP Code) Washington, DC 20375-5000			7b. ADDRESS (City, State, and ZIP Code)		
8a. NAME OF FUNDING / SPONSORING ORGANIZATION (See page ii)		8b. OFFICE SYMBOL (if applicable)	9. PROCUREMENT INSTRUMENT IDENTIFICATION NUMBER		
8c. ADDRESS (City, State, and ZIP Code) Washington, DC 20546			10. SOURCE OF FUNDING NUMBERS		
			PROGRAM ELEMENT NO.	PROJECT NO.	TASK NO.
			WORK UNIT ACCESSION NO. DN480-104		
11. TITLE (Include Security Classification) The Spartan 1 Mission					
12. PERSONAL AUTHOR(S) (See page ii)					
13a. TYPE OF REPORT Final		13b. TIME COVERED FROM 1980 TO 1985	14. DATE OF REPORT (Year, Month, Day) 1989 July 11		15. PAGE COUNT 18
16. SUPPLEMENTARY NOTATION					
17. COSATI CODES			18. SUBJECT TERMS (Continue on reverse if necessary and identify by block number)		
FIELD	GROUP	SUB-GROUP			
			Space science X-ray astronomy		
			Spartan program Space shuttle		
19. ABSTRACT (Continue on reverse if necessary and identify by block number)					
<p>This report documents the first Spartan mission. The Spartan program, an outgrowth of a joint Naval Research Laboratory (NRL)/National Aeronautics and Space Administration (NASA)-Goddard Space Flight Center (GSFC) development effort, was instituted by NASA for launching autonomous, recoverable payloads from the space shuttle. These payloads have a precise pointing system and are intended to support a wide range of space-science observations and experiments.</p> <p>The first Spartan, carrying an NRL X-ray astronomy instrument, was launched by the orbiter Discovery (STS 51G) on June 20, 1985 and recovered successfully 45 h later, on June 22. During this period, Spartan 1 conducted a preprogrammed series of observations of two X-ray sources—the Perseus cluster of galaxies and the center of our galaxy. The mission was successful from both an engineering and a scientific viewpoint. Only one problem was encountered—the attitude control system (ACS) shut down earlier than planned because of high-attitude control-system gas consumption. A preplanned emergency mode then placed Spartan 1 into a stable, safe condition and allowed a safe recovery.</p> <p style="text-align: right;">(Continues)</p>					
20. DISTRIBUTION / AVAILABILITY OF ABSTRACT <input checked="" type="checkbox"/> UNCLASSIFIED/UNLIMITED <input type="checkbox"/> SAME AS RPT <input type="checkbox"/> DTIC USERS			21. ABSTRACT SECURITY CLASSIFICATION UNCLASSIFIED		
22a. NAME OF RESPONSIBLE INDIVIDUAL Raymond G. Cruddace			22b. TELEPHONE (Include Area Code) 202-767-2344		22c. OFFICE SYMBOL 4129

8a. NAME OF FUNDING/SPONSORING ORGANIZATION

Office of Space Science and Applications
National Aeronautics and Space Administration

12. PERSONAL AUTHOR(S)

Cruddace, R.G., Fritz, G.G., Shrewsbury, D.J., Brandenstein, D.C., Creighton, J.O., Gutschewski, G., Lucid, S.W., Nagel, S.R., Fabian, J.M.*, Zimmerman, D., Fenimore, E.E., and Gross, C.†

*Now with ANSER, Arlington, Virginia

†Now at Tel Aviv University

19. ABSTRACT (Continued)

This report describes the events of the mission and presents X-ray maps of the two observed sources, which have been produced from the flight data.

CONTENTS

INTRODUCTION	1
THE SPARTAN 1 PAYLOAD	1
THE SPARTAN 1 MISSION	4
THE SCIENTIFIC RESULTS	8
CONCLUSIONS	12
ACKNOWLEDGMENTS	12
REFERENCES	12



Frontispiece — Spartan 1



Frontispiece — Spartan 1

THE SPARTAN 1 MISSION

INTRODUCTION

Spartan is a program introduced by the National Aeronautics and Space Administration (NASA) to facilitate scientific research using the space shuttle. Inspired by the sounding-rocket program, Spartan employs autonomous payloads, each equipped with a precise pointing system and deployed by the shuttle orbiter in Earth orbit. After performing a preprogrammed series of measurements, which for most missions are astronomical observations, the Spartan payload is retrieved by the orbiter after 2 days and returned to Earth.

The development of the Spartan concept started in 1976 in a collaborative effort by the Naval Research Laboratory (NRL) and the Goddard Space Flight Center (GSFC). The results of early studies are described in Refs. 1 through 3. Development of the first flight payload (Spartan 1) started in 1980 and accelerated in 1982, when Spartan 1 was placed on the flight manifest for the August 1984 launch of STS 41F. The complete Spartan team was then assembled consisting of persons from GSFC, NRL, the Johnson Space Center (JSC), and the Kennedy Space Center (KSC). GSFC was responsible for payload development and testing, and NRL executed a similar scientific-instrument function, performing X-ray astronomical observations. The Perseus cluster of galaxies and the center of our own galaxy were selected for study. JSC and KSC assumed responsibility for integrating Spartan 1 into the orbiter and for developing the techniques needed to deploy and retrieve the payload in orbit. A shuttle malfunction postponed the Spartan 1 flight for 10 months, and it finally flew in June 1985 on STS 51G, on board the orbiter Discovery. In this report, we describe Spartan 1, its flight, and some of the scientific results.

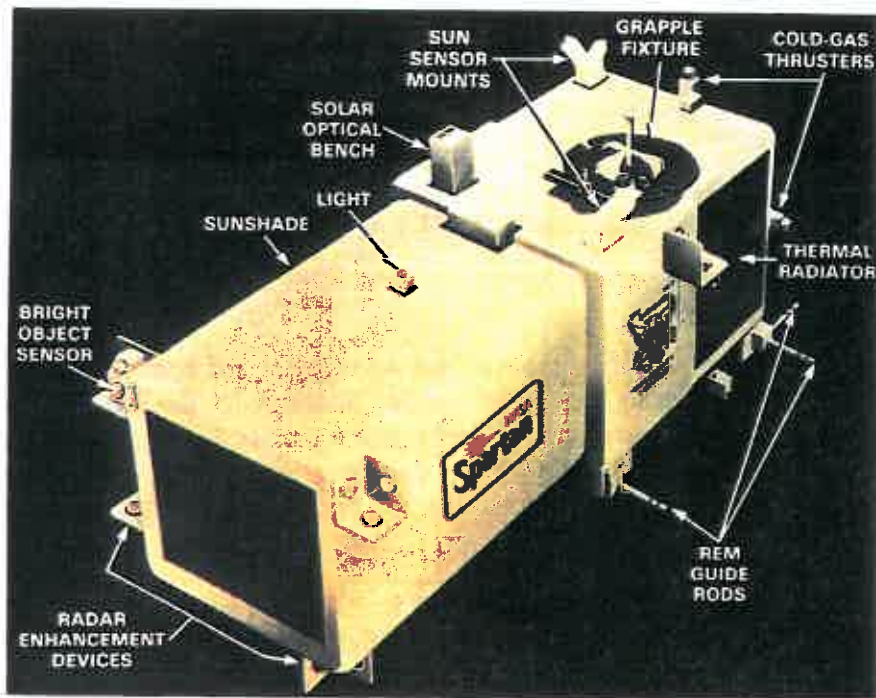
THE SPARTAN 1 PAYLOAD

Figure 1(a) shows the major features of Spartan 1. The long rectangular sunshade was designed to shield the X-ray detectors, a startracker, and two aspect cameras from direct sunlight during daylight observations. The principal payload subsystems are in the rectangular body behind the sunshade. Figure 1(b) shows the payload mounted on the support structure in the orbiter bay. The photograph was taken during the installation operation in the Orbiter Processing Facility at KSC.

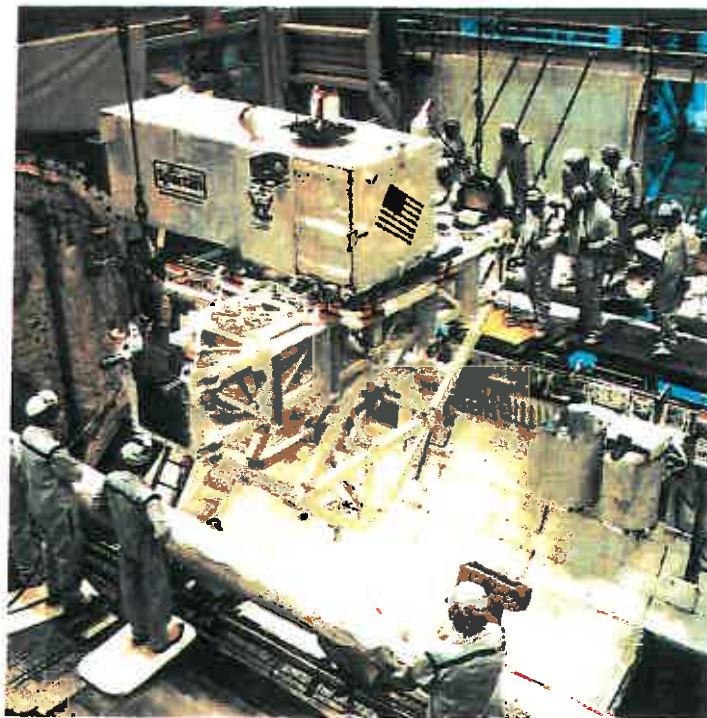
Figure 2(a) shows the payload during final assembly at KSC. The lower section contains the payload functional control system (PFCS), the attitude control system (ACS) and three 28 V silver-zinc batteries (one a reserve) with a total capacity of 700 A.h. Scientific instruments consisting of two large, finely collimated, X-ray proportional counters, are being lowered into the upper section. These detectors are sensitive to X-rays in the 1 to 15 keV band, have an aperture with a collecting area of 1320 cm², and are collimated to view a slit on the sky 5-arcmin wide (full width, half maximum (FWHM)) and 3° long (FWHM). Figure 2(b) shows the detectors—two 35-mm cameras and a startracker—mounted on a flat rectangular structure, the "optical bench."

Manuscript approved February 21, 1989.

CRUDDACE, FRITZ, SHREWSBERRY, BRANDENSTEIN, CREIGHTON, GUTSCHEWSKI,
LUCID, NAGEL, FABIAN, ZIMMERMAN, FENIMORE, AND GROSS

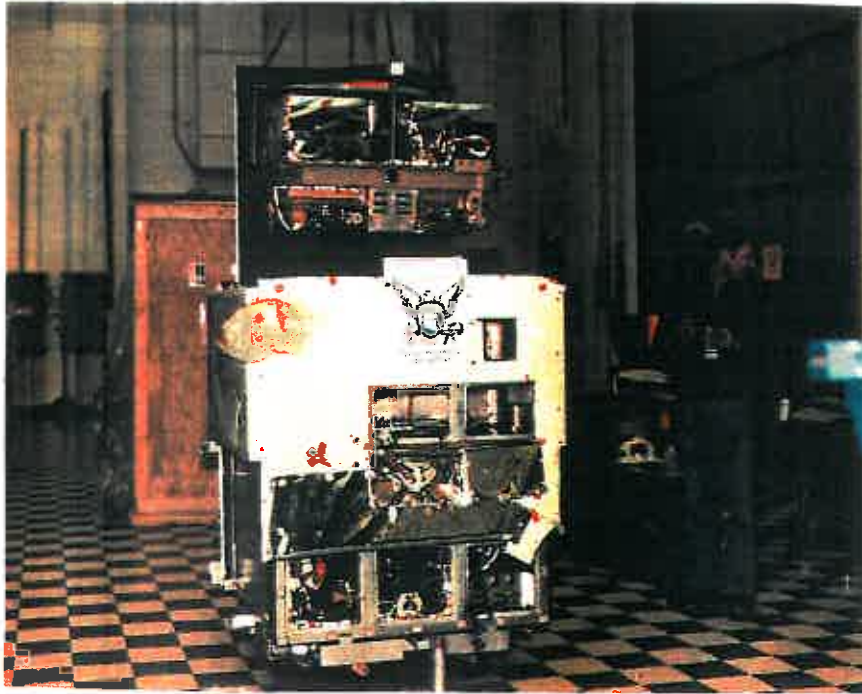


(a)

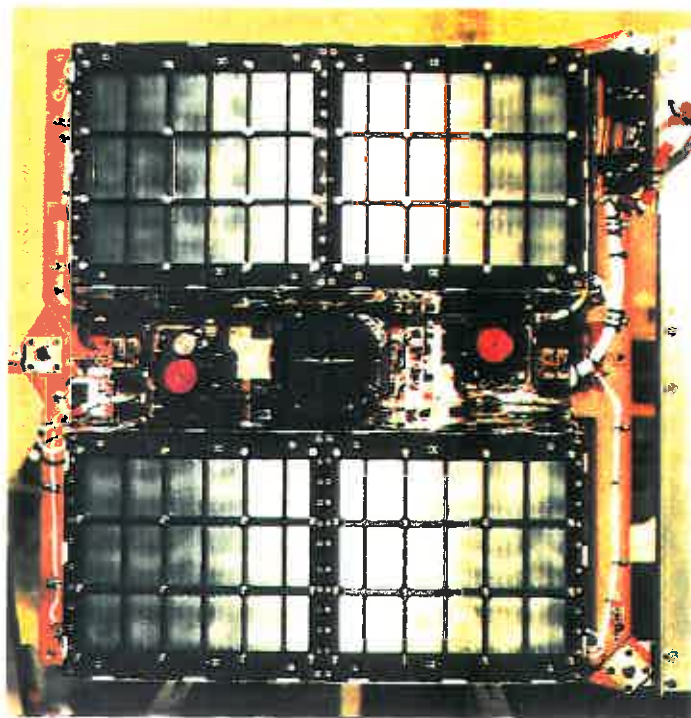


(b)

Fig. 1 -- (a) The Spartan 1 payload; (b) Spartan 1 installed on its support structure
in the Orbiter Processing Facility at the Kennedy Space Center



(a)



(b)

Fig. 2 -- (a) The Spartan 1 payload being assembled at the Kennedy Space Center. The X-ray detectors are being lowered into the payload; (b) Front view of the apertures of the two finely-collimated X-ray detectors. Visible in between are the covered apertures of the startracker and two 35-mm aspect cameras.

Several important external characteristics of Spartan 1 are evident in Fig. 1—the grapple fixture, which is engaged by the arm of the shuttle remote manipulator system (RMS); the structure remote engage mechanism (REM), which mates with the support bridge in the orbiter; various ACS gas thrusters and solar attitude sensors; reflectors to enhance ground tracking by radar; and the thermal surfaces. These surfaces include a multilayer insulation blanket painted white on the outside and thermal radiator surfaces of aluminized Teflon to reject heat from the payload electronics. Spartan 1 is 126 by 42 by 48 in., and it weighs 2222 lb.

The basic PFCS functions are timing, power switching, data encoding, and data storage. The internal clock, which starts at deployment, is used to time payload shutdown in free flight after the conclusion of the observations. Ten modes are selected by the power switching system—one for free flight configuration, one for minimum reserve shutdown (MRS) mode, and the rest for preflight and in-orbit checks. The MRS mode, designed for an emergency, is entered when either the battery voltage or ACS gas pressure falls below preset threshold values. This was, in fact, activated during the mission. The data encoding system is a sounding rocket, pulse-code modulated (PCM) unit, operating at 12500 bits/s. The PCM encoder is programmed to accept a combination of analog and digital signals, the latter including event counts and parallel- and serial-digital data. The encoded data are stored by a Bell and Howell MARS 1400 tape recorder, with a capacity of 10^{10} bits.

For attitude control, the ACS uses gas jets supplied with argon regulated to 60 psia. The pneumatic system stores argon at 3000 psia in two 1615 in³ tanks identical to those employed by the astronaut manned-maneuvering unit (MMU). The jets, with thrust of 0.2 lbf-ft, respond to commands formulated by using one of three inputs:

- computer-generated steering signals and the outputs of a three-axis, rate-integrating gyroscope assembly,
- star-tracker output, or
- output of the solar attitude sensors.

The startracker is located between the two X-ray detectors and is aligned with the detector-view axis. The principal solar-attitude sensors have a view axis orthogonal to the star-tracker axis (Fig. 1). The complete astronomical observing sequence is stored in a microcomputer capable of storing 1000 commands, which takes control of the payload during free flight. It controls the pointing maneuvers and several functions in the scientific instrument including high-voltage turn-on, aspect-camera operation, and calibration of the X-ray detectors.

THE SPARTAN 1 MISSION

Spartan 1's scientific goal was to study the structure of the Perseus cluster and the galactic center by obtaining detailed X-ray emission maps. These surveys were made by sweeping the slit field of view of the detectors in many directions across each source. For the Perseus cluster, each scan was 86.0 arcmin long, and the scan rate was 16.2 arcmin per minute. A computer constructed each image postflight by using techniques familiar in medical X-ray tomography. The free-flight operations of Spartan 1 were optimized under numerous technical constraints to maximize this X-ray observing time. One such constraint was the prior deployment of three communications satellites—MORELOS, ARABSAT, and TELSTAR—so that Spartan 1 operations did not begin until mission-elapsed time (MET) 5^d 1^h 35^m.

All signals to Spartan 1 were sent by a crew member on the aft flight-deck (AFD) who used a hand-held unit resembling a pocket calculator. Binary-coded signals were transmitted along a single, twisted-wire-pair cable leading from the AFD to the orbiter. Table 1 summarizes the four basic instructions sent to the payload in preparation for undocking and deployment. During the self check, Spartan 1 powered itself up and internally conducted a series of PFCS, ACS, battery, and scientific instrument checks. These checks were all positive, whereupon Spartan 1 informed the crew member by means of the APC that it was ready for flight.

Table 1 — Preparation of Spartan 1 for Free Flight

Time before	Function
2 ^h 54 ^m	Turn on ACS computer and gyro heaters
2 ^h 39 ^m	Send "program select" code to register changes in launch day and deployment time
1 ^h 55 ^m	Start self check
1 ^h 24 ^m	Place payload in standby mode: power to ACS computer and gyros heaters only

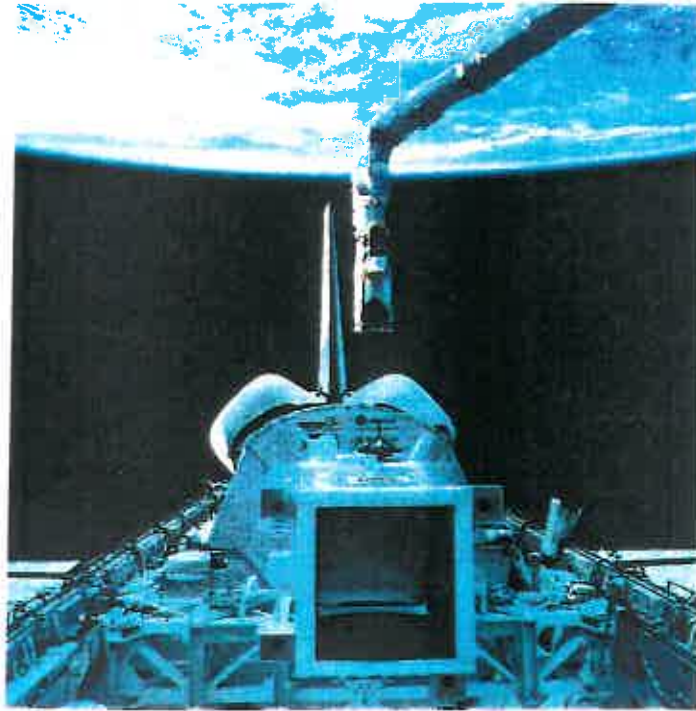
At this point, the crew unlatched Spartan 1 from its support structure and grappled it by use of the RMS (Fig. 3(a)). The RMS then extracted the payload and held it over the orbiter bay as depicted in Fig. 3(b). This was designed to align the startracker within 2° of the star Vega and to point the "solar optical bench" (Fig. 1) at the sun. Spartan 1 was released 3 min after sunrise at MET 3^d 4^h 29^m, or precisely 16^h 2^m 1^s UT on June 20, 1985 (Fig. 3(c)). The release initiated an immediate power-up of the payload followed 30 s later by enabling of the ACS gas system. After 2.5 min, Spartan 1 performed a pirouette maneuver, a rotation of 45° clockwise, then counterclockwise about an axis through the grapple fixture. The pirouette lasted 90 s. It informed the crew that the ACS was performing correctly and that Spartan 1 could continue its mission. Discovery then performed two burns (1 and 2 ft/s), to effect a safe separation from the payload.

Spartan 1 now entered a critical phase of its flight, namely acquisition by the ACS of an inertial reference frame. This had to be delayed a full orbit, however, to avoid confusing the solar attitude sensors with reflections from the orbiter bay. Table 2 summarizes the steps taken in the acquisition procedure.

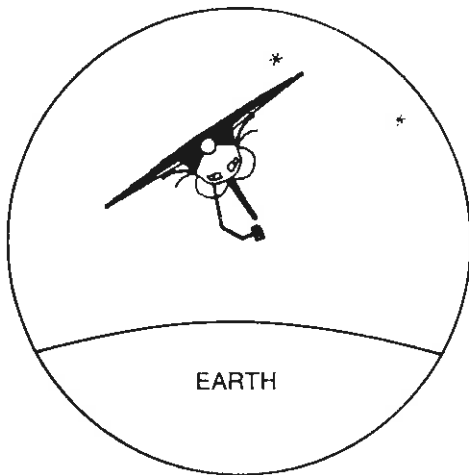
Table 2 — Spartan 1 Attitude Acquisition

Time after deployment	Function
1 ^h 59 ^m	Solar-optical bench locks onto the sun
2 ^h 36 ^m	Night pass: startracker locks onto Vega: gyro update in two axes
2 ^h 54 ^m	Maneuver 23°.8 to Deneb
2 ^h 55 ^m	Startracker locks onto Deneb: update third gyro axis

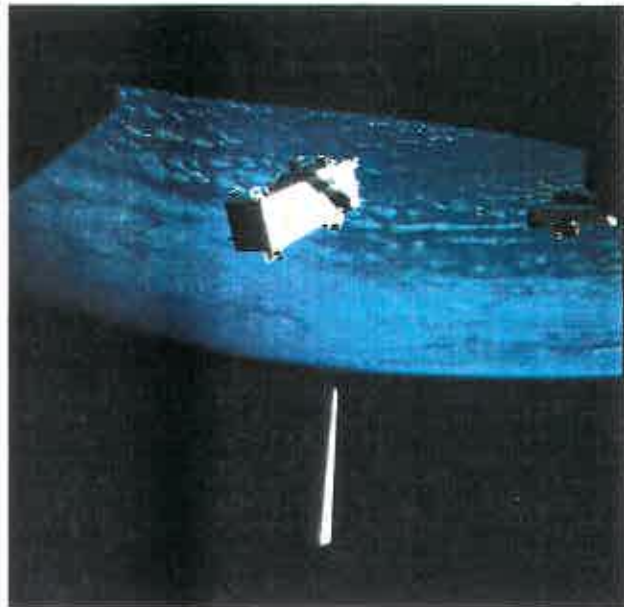
CRUDDACE, FRITZ, SHREWSBERRY, BRANDENSTEIN, CREIGHTON, GUTSCHEWSKI,
LUCID, NAGEL, FABIAN, ZIMMERMAN, FENIMORE, AND GROSS



(a)



(b)

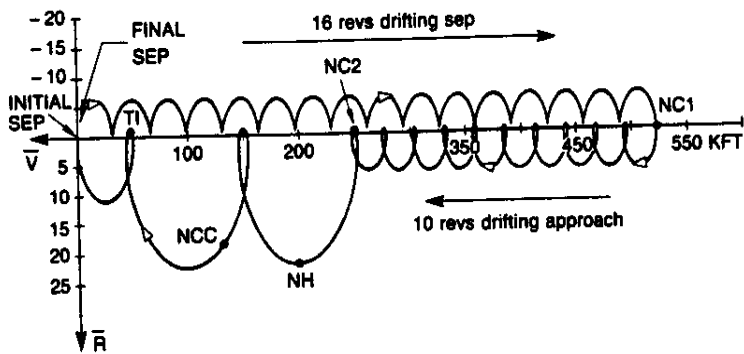


(c)

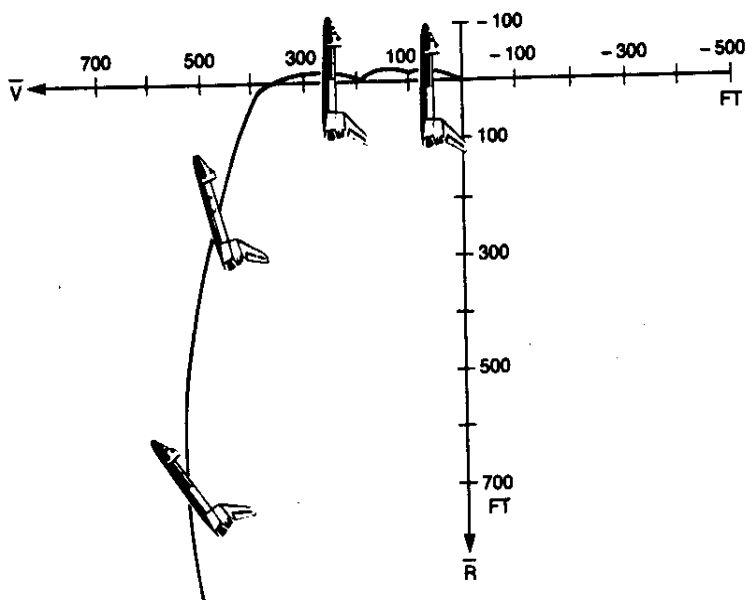
Fig. 3 -- (a) Undocking of Spartan 1 during the STS 51G mission; (b) Orientation of Discovery and position of Spartan 1 at deployment; (c) Spartan 1 after release by the orbiter RMS (visible at right).

With this critical phase completed, Spartan 1 embarked on a preprogrammed, 23-h program of X-ray observations. This program repeated the same pattern each orbit—one scan of the Perseus cluster, one of the galactic center, and a repeat of the last three steps of Table 2—using the stars Altair and Deneb to update the ACS gyro reference. The only change from orbit to orbit was the direction of scanning each X-ray source.

Meanwhile, Discovery slowly drifted away from Spartan 1 (Fig. 4(a)), reaching a maximum separation of 92 nmi at about MET 4^d 5^h, or 16 orbits (~ 24 h) after deployment. The payload was tracked by C-band radar from the ground allowing the JSC mission control team to accurately compute both its Earth-centered position vector and the Discovery-Spartan state vector to plan the rendezvous maneuvers. Table 3 chronicles the orbiter reaction control system (RCS) burns and tracking activities (Fig. 4(a)), which brought Discovery from a range of 92 nmi to the final rendezvous stages at a range of a few miles.



(a)



(b)

Fig. 4 — (a) The motion of Discovery with respect to Spartan 1. ∇ is the direction of orbital motion, and \bar{R} is the vector toward Earth. (The orbiter's NC1, NC2, NCC, and TI burns are described in the text.) (b) The approach of Discovery to Spartan 1 during the final rendezvous phase. As in (a), Spartan 1 is always at the origin.

Table 3—Rendezvous of Discovery with Spartan 1

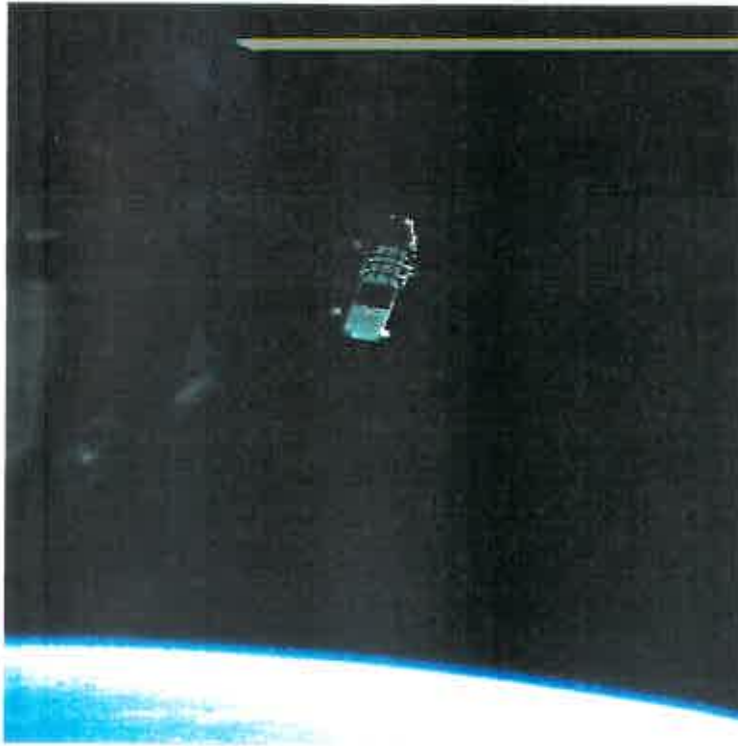
Mission-elapsed time (MET)	Activity	Purpose
4 ^d 5 ^h 21 ^m	NC - 1 burn: 5.1 ft/s: range 92 nmi	Initiate slow approach to Spartan 1
4 ^d 20 ^h 41 ^m	NC - 2 burn: range 35 nmi	Accelerate approach
4 ^d 21 ^h 09 ^m	Spartan 1 acquisition by the Crew Optical Alignment System (COAS)	Tracking and data input to orbiter computers
4 ^d 21 ^h 59 ^m	Spartan 1 acquisition by orbiter K-band radar: range 20 nmi	Tracking and data input to orbiter computers
4 ^d 22 ^h 47 ^m	NCC burn: 1.25 ft/s	Correct out-of-plane velocity difference between Discovery and Spartan 1
4 ^d 23 ^h 45 ^m	TI burn range: 8 nmi	Set up final rendezvous trajectory

After the TI burn, Discovery entered the critical phase of the rendezvous under manual control by the mission commander, who relied primarily on visual sighting of Spartan 1. Figure 4(b) illustrates Discovery's attitude and trajectory in this phase. On approaching the payload, the crew reported that Spartan 1 was in a stable attitude but had an incorrect orientation. Figure 5(a) shows the view of Spartan 1 from the AFD at this time, indicating that the payload had shut itself down prematurely and entered the MRS mode. Postflight analysis revealed that this occurred 17^h 32^m after deployment because of a low-pressure signal from the ACS gas-supply system. The data revealed unexpected noise in the ACS rate-gyro signal, which had caused excessive gas-valve action during maneuvering. The problem was corrected before the second mission.

Regrappling of Spartan 1 by use of the RMS was achieved successfully by the crew in a difficult and unrehearsed operation in which the RMS worked at the limit of its reach. The operator could not see the grapple fixture directly but relied instead on the RMS wrist television monitor. This option was selected to avoid a crew-intensive fly-around maneuver, which had yet to be tried in a shuttle mission. The regrappling occurred as scheduled at 13^h31^m55^s UT on June 22, 1985, 45.5 h after deployment. Figure 5(b) shows Spartan 1 being returned to the orbiter bay.

THE SCIENTIFIC RESULTS

When MRS occurred, 17^h 32^m after deployment, Spartan 1 had completed 10 scans of the Perseus cluster and 8 scans of the galactic center. In both sets of observations, enough information was obtained to permit excellent X-ray maps to be constructed of the two sources. The results are displayed in Fig. 6.



(a)



(b)

Fig. 5 — (a) Orientation of Spartan 1 at rendezvous. This orientation was unexpected because there was a premature payload shutdown late in its mission; (b) Spartan after recovery, on the end of the RMS.

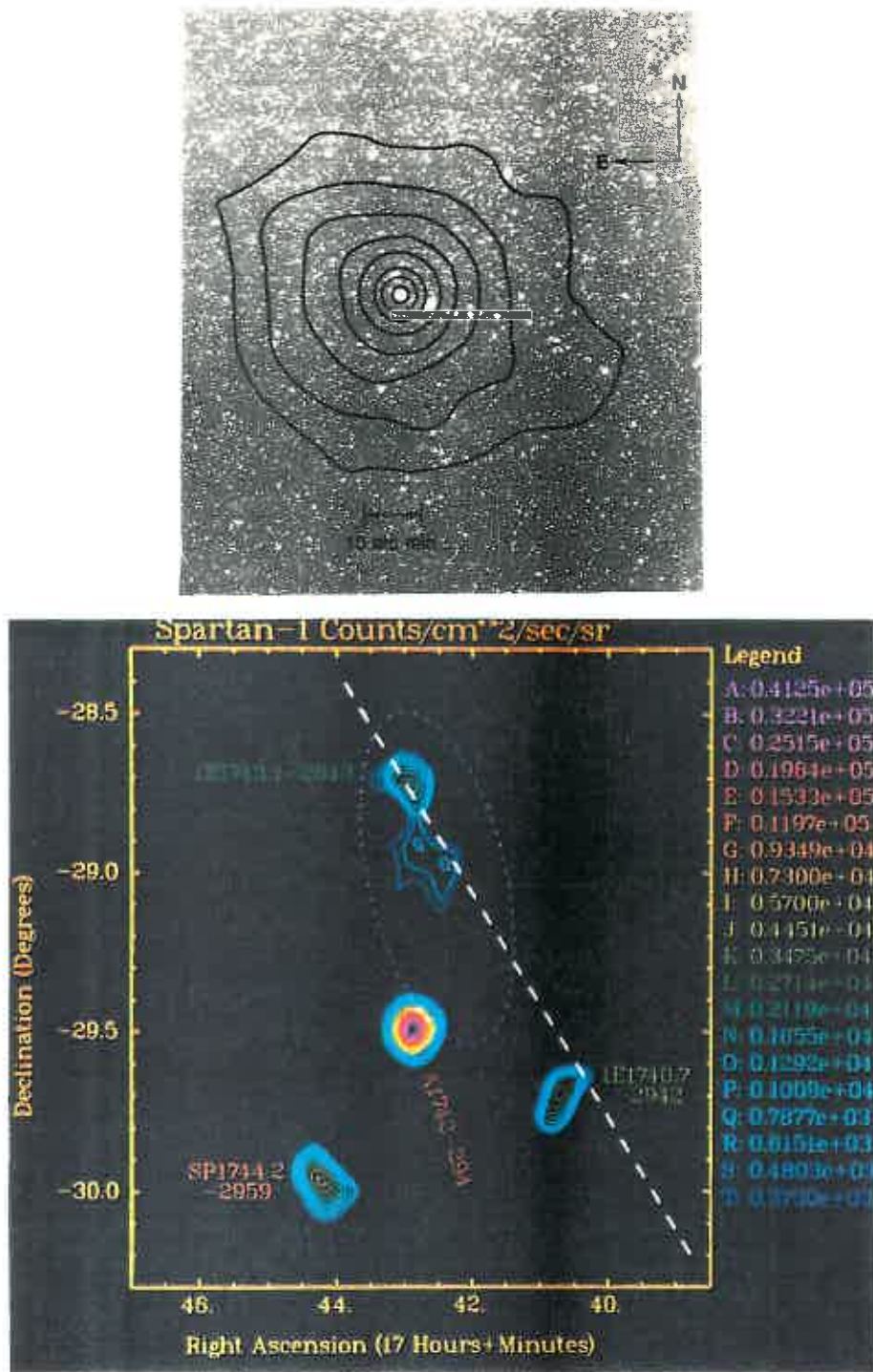


Fig. 6 -- (a) Diffuse X-ray emission from hot gas ($\sim 10^8$ K) in the Perseus cluster of galaxies. Cluster galaxies, which have fuzzy images, may be identified throughout the field but are more numerous near the center. The contours are loci of constant surface brightness, which change by a factor 2.25 between adjacent contours; (b) X-ray sources at the galactic center discovered by Spartan 1. The dashed ellipse delineates an area of weak diffuse emission. The contours within the ellipse are produced by a number of weak X-ray sources surrounding the nucleus of the galaxy. The straight dashed line is the plane of the galaxy.

The contours of X-ray surface brightness shown in Fig. 6(a) have been superposed on an optical picture of the sky taken from the Palomar sky survey. Numerous galaxies, which can be distinguished from stars by their fuzzy appearance and the absence of diffraction spikes, are evident to the eye, and careful inspection has revealed thousands of galaxies in this cluster in Perseus, known to astronomers as Abell 426. As is the case in most clusters of galaxies in the universe, the gravitational well of the cluster is filled with a very hot gas ($\sim 10^8$ K), which is revealed predominantly by its X-ray emission. It is of great interest to astrophysicists to study the spatial distribution of this emission, for three reasons:

- to elucidate the origins of the gas, for it is not yet clear what proportion has been shed or stripped from galaxies, and what proportion is the remnant of the primordial gas from which galaxies formed,
- the gas distribution responds to the shape of the potential well, so that the X-ray contours yield information about the distribution of mass in the cluster. For example, the contours in Fig. 6(a) reveal a slight elongation in a roughly EW direction. This may relate to a prominent chain of galaxies in the Perseus cluster running WSW from the center, and
- astrophysicists continue to puzzle over the mass required to create the potential well, because it exceeds by a large margin the mass we can account for as galaxies and gas. Some invisible ("dark") matter of unknown origin pervades the cluster. Measurements of the radial density and temperature gradients in the hot gas allow the distribution of this dark matter to be measured.

The special feature of the Spartan 1 instrument has been its ability to measure the density and temperature of the intracluster gas out to large radii, in the case of Perseus to more than 40 arcmin (Fig. 6(a)). Earlier imaging observations have been unable to reach so far from the cluster center or to measure radial temperature profiles.

The Spartan 1 map of the galactic center (Figure 6(b)) examines a very small region within only 100 pc of the "galactic nucleus." The density of stars increases very rapidly as the nucleus is approached. The nucleus is thought to be the site of a compact object, a black hole, having a mass of between 10^3 and 10^6 solar masses. The spectral characteristics of the northern-most source (1E1743.1-2843) and the three relatively bright sources to the south suggest that they may be members of familiar classes of X-ray sources. A1742-294 and SP1742.2-2959 probably belong to the class of burst or "quasi-periodic oscillator" (QPO) sources, whereas 1E1743.1-2843 and 1E1740.7-2942 reveal harder X-ray spectra and more absorption intrinsic to the source; they are suspected of being binary X-ray pulsars.

The region to the south of 1E1743.1-2843, the patch of emission roughly at the center of the dashed ellipse, is of special interest for it contains the galactic nucleus. This region comprises a number of faint sources that could not be resolved fully by Spartan 1. However, it is clear from comparing the Spartan 1 results with the observations made by the Einstein Observatory in 1979 that these sources are variable. The region may comprise many faint sources that are continually brightening and dimming. Of particular significance is one source that may be the nucleus itself, and it is clear that this source has faded significantly between 1979 and 1985.

In addition to the sources described, Spartan 1 detected weak diffuse emission from a disk-shaped region lying within the dashed ellipse shown in Fig. 6(b). Its dimensions are approximately

CRUDDACE, FRITZ, SHREWSBERRY, BRANDENSTEIN, CREIGHTON, GUTSCHEWSKI,
LUCID, NAGEL, FABIAN, ZIMMERMAN, FENIMORE, AND GROSS

80 × 180 pc. Although we know from the Spartan 1 data that the spectrum of this emission is similar to that of the discrete sources, its origin has yet to be determined.

CONCLUSIONS

The principal conclusion to be drawn from the Spartan 1 mission is that exciting scientific research on a modest scale may be performed effectively and economically using the space shuttle. The prerequisites are a minimum of paperwork and superfluous management, and a close working relationship among the shuttle crew, the engineers, and the scientists. Enthusiasm and professional skill were 90% of the success of Spartan 1.

The homework has been done in not just the Spartan program but also in complementary programs such as the Getaway Special (GAS) canisters and the Hitchhiker/SPOC attached payload systems. It remains to capitalize on this investment, for there is no shortage of scientific instruments waiting to be flown.

ACKNOWLEDGMENTS

We acknowledge the consistent and solid support throughout the Spartan 1 program of the Office of Space Science and Applications at NASA Headquarters and the efforts of many engineers at GSFC, KSC, JSC, and NRL, who worked together to make Spartan 1 so successful.

REFERENCES

1. R.G. Cruddace, G.G. Fritz, and S. Shulman, "SPEAR: Small Payload Ejection and Recovery for the Space Shuttle," *Astronautics and Aeronautics*, p. 42, Jan. 1977.
2. D.J. Olney, and R.G. Cruddace, "Free-flying Shuttle Payloads, an Extrapolation of Sounding Rocketry into the Shuttle Era," AIAA Paper No. 79-0485, 1979.
3. R.G. Cruddace, G.G. Fritz, and D.J. Shrewsberry, "Space Research and Spartan," AIAA Paper No. 85-0502, 1985.

D83166
 JUNE 20 + JUNE 21, 1985

HEX DUMP OF 16520

VAX SWAPPED

VSPO

0 1 2 3

4 5 6/20
 BYTES AB=171-6/20

FILE 1	RECORD 1	13568	BYTES AB=171-6/20							
(0)	41435155	01000000	1413AB00	B9447103	11840000	51000000	52000000	00000000	00000000	00000000
(40)	00000000	00000000	00000000	00000000	000067F9	1901070F	00000000	0000E801	19FC0000	00000000
(80)	00000000	00000000	00000000	00000000	00000000	0000F001	19FC0000	00000000	00000000	00000000
(120)	00000000	00000000	00000000	00000000	00000000	00000000	00000000	00000000	00000000	00000000
(160)	00000000	00009904	99040000	00000000	00000000	00000000	00000000	00000000	02000200	03000300
(200)	02000200	06000100	02000400	03000300	01000700	00000000	00000000	00000000	00000000	00000000
(240)	00000000	00000000	00000000	00000000	00000000	00000000	00000000	00000000	00000000	00000000
(280)	00000000	00000000	00000000	00000000	00000000	00000000	00000000	00000000	00000000	00000000
(320)	FE000000	00000000	00000000	00000000	00000000	00000000	00000000	00000000	00000000	00000000
(360)	00000000	00000000	00000000	00000000	00000000	00000000	00000000	00000000	00000000	00000000
(400)	00000000	00000000	00000000	00000000	00000000	00000000	00000000	00000000	00000000	00000000
(440)	00000000	00000000	00000000	00000000	00000000	00000000	00000000	00000000	00000000	00000000
(480)	00000000	00000000	00000000	00000000	00000000	00000000	00000000	00000000	00000000	00000000
(520)	00000000	00000000	00000000	00000000	00000000	00000000	00000000	00000000	00000000	00000000
(560)	00000000	00000000	00000000	00000000	FE000000	00000000	00000000	00000000	00000000	00000000
(600)	00000000	00000000	00000000	00000000	00000000	00000000	00000000	00000000	00000000	00000000
(640)	00000000	00000000	00000000	00000000	00000000	00000000	00000000	00000000	00000000	00000000
(680)	00000000	00000000	00000000	00000000	00000000	00000000	00000000	00000000	00000000	00000000
(720)	00000000	00000000	00000000	00000000	00000000	00000000	00000000	00000000	00000000	00000000
(760)	00000000	00000000	00000000	00000000	00000000	00000000	00000000	00000000	00000000	00000000
(800)	00000000	00000000	00000000	00000000	00000000	00000000	00000000	00000000	FE000000	00000000
(840)	00000000	00000000	00000000	00000000	00000000	00000000	00000000	00000000	00000000	00000000
(880)	00000000	00000000	00000000	00000000	00000000	00000000	00000000	00000000	00000000	00000000
(920)	00000000	00000000	00000000	00000000	00000000	00000000	00000000	00000000	00000000	00000000
(960)	00000000	00000000	00000000	00000000	00000000	00000000	00000000	00000000	00000000	00000000
(1000)	00000000	00000000	00000000	00000000	00000000	00000000	00000000	00000000	00000000	00000000
(1040)	00000000	00000000	00000000	00000000	00000000	00000000	00000000	00000000	00000000	00000000
(1080)	00000000	00000000	FE000000	00000000	00000000	00000000	00000000	00000000	00000000	00000000
(1120)	00000000	00000000	00000000	00000000	00000000	00000000	00000000	00000000	00000000	00000000
(1160)	00000000	00000000	00000000	00000000	00000000	00000000	00000000	00000000	00000000	00000000
(1200)	00000000	00000000	00000000	00000000	00000000	00000000	00000000	00000000	00000000	00000000
(1240)	00000000	00000000	00000000	00000000	00000000	00000000	00000000	00000000	00000000	00000000
(1280)	00000000	00000000	00000000	00000000	00000000	00000000	00000000	00000000	00000000	00000000
(1320)	00000000	00000000	00000000	00000000	00000000	00000000	00000000	FC010000	00000000	FC010000
(1360)	00000000	02000100	0D000000	00002100	00000000	00000000	00000000	00000000	00000000	02000200
(1400)	0D000000	3F003001	21000000	00000000	00000000	00000000	00000000	03000400	0D000000	00000000
(1440)	29030000	00000000	00000000	00000000	00000000	03000300	0D000000	3E002500	00000000	00000000
(1480)	00000000	00000000	00000000	02000300	0D000000	95010200	51000000	00000000	00000000	00000000
(1520)	00000000	02000100	0D000000	49007E00	00000000	00000000	00000000	00000000	00000000	06000700
(1560)	0D000000	4F000E00	00000000	00000000	00000000	00000000	00000000	0E000F00	0D000000	30000E00
(1600)	00000000	00000000	00000000	00000000	00000000	9900ED00	0D000000	7B010E00	00000000	00000000
(1640)	00000000	00000000	00000000	F900FD00	0D000000	0E000D00	00000000	00000000	00000000	00000000
(1680)	00000000	A3010B01	0D000000	FE008100	00000000	00000000	00000000	00000000	00000000	00001C00
(1720)	0D000000	10019900	B8EA0000	00000000	00000000	00000000	00000000	1D000400	0D000000	0F01BA00
(1760)	48150000	00000000	00000000	00000000	00000000	F8001001	0D000000	09012501	1CC00000	00000000
(1800)	00000000	00000000	00000000	02010B01	0D000000	0E00BB00	E43F0000	00000000	00000000	00000000
(1840)	00000000	FA001001	0D000000	0E001C00	55000000	00000000	00000000	00000000	00000000	0E011D01
(1880)	0D000000	0E00F301	06000000	00000000	00000000	00000000	00000000	F3000B01	0D000000	0E00FF01
(1920)	14000000	00000000	00000000	00000000	00000000	02011900	0D000000	0E009900	10000000	00000000
(1960)	00000000	00000000	00000000	02011800	0D000000	DE000E00	02000000	00000000	00000000	00000000
(2000)	00000000	EB019101	0D000000	87011B00	01000000	00000000	00000000	00000000	00000000	E1011501
(2040)	0D000000	0D00CD00	00000000	00000000	00000000	00000000	00000000	0E000A01	0D000000	8501F600
(2080)	01000000	00000000	00000000	00000000	00000000	FF011801	0D000000	DC00EA01	01000000	00000000
(2120)	00000000	00000000	00000000	10000D01	0D000000	8801F201	B8EA0000	00000000	00000000	00000000
(2160)	00000000	14001601	0D000000	D100AB01	48150000	00000000	00000000	00000000	00000000	70000901

(2200)	0D000000	6F01A901	1CC00000	00000000	00000000	00000000	00000000	00000000	7C011701	0D000000	6A01AC01
(2240)	E43F0000	00000000	00000000	00000000	00000000	0A011001	0D000000	4D01A801	00000000	00000000	00000000
(2280)	00000000	00000000	00000000	00000000	E4001101	0D000000	1501AC01	00000000	00000000	00000000	00000000
(2320)	00000000	FA001401	0D000000	42012201	00000000	00000000	00000000	00000000	00000000	00000000	20010A01
(2360)	0D000000	00005100	00000000	FD010100	01000100	FD010100	01000100	02000100	0D000000	00002200	00002200
(2400)	00000000	01000100	01000100	01000100	01000100	01000100	02000200	0D000000	3F004001	22000000	01000100
(2440)	01000100	01000100	01000100	03000400	0D000000	00000000	DC000000	01000100	01000100	01000100	01000100
(2480)	01000100	03000300	0D000000	3C002400	00000000	01000100	01000100	01000100	01000100	01000100	02000300
(2520)	0D005001	93010100	52000000	01000100	01000100	01000100	01000100	02000100	0D004000	52006C00	00000000
(2560)	00000000	01000100	01000100	01000100	01000100	01000100	06000700	0D004000	4D000D00	00000000	01000100
(2600)	01000100	01000100	01000100	0F000E00	0D000000	38000E00	00000000	01000100	01000100	01000100	01000100
(2640)	01000100	9D00F100	0D000000	75010E00	00000000	01000100	01000100	01000100	01000100	01000100	09000E00
(2680)	0D000000	0E000E00	00000000	01000100	01000100	01000100	01000100	01000100	A3011301	0D000000	01018600
(2720)	00000000	01000100	01000100	01000100	01000100	00001C00	0D000000	12019900	B8EA0000	01000100	01000100
(2760)	01000100	01000100	01000100	29019501	0D000000	1001BA00	48150000	01000100	01000100	01000100	01000100
(2800)	01000100	F9000A01	0D000000	0A01ED00	1CC00000	01000100	01000100	01000100	01000100	01000100	00011401
(2840)	0F000000	0D00BA00	E43F0000	01000100	01000100	01000100	01000100	01000100	F1000A01	0F000000	0E001500
(2880)	55000000	01000100	01000100	01000100	01000100	02012A01	0F000000	0D00F601	06000000	01000100	01000100
(2920)	01000100	01000100	01000100	F7000801	0F000000	0E00FA01	14000000	01000100	01000100	01000100	01000100
(2960)	01000100	FD002500	03000000	0E009C00	10000000	01000100	01000100	01000100	01000100	01000100	F5001200
(3000)	03000000	E0000E00	02000000	01000100	01000100	01000100	01000100	ECC01A501	03000001	84011A00	01000100
(3040)	01000000	01000100	01000100	01000100	01000100	DE010E01	03001001	0E00CA00	00000000	01000100	01000100
(3080)	01000100	01000100	01000100	15000B01	03005001	7D01FB00	01000000	01000100	01000100	01000100	01000100
(3120)	01000100	FF011101	03005001	B800E801	01000000	01000100	01000100	01000100	01000100	01000100	1A000801
(3160)	03005001	7E01F001	B8EA0000	01000100	01000100	01000100	01000100	11001001	03005001	D000AB01	01000100
(3200)	48150000	01000100	01000100	01000100	01000100	20000901	03005001	6A01A901	1CC00000	01000100	01000100
(3240)	01000100	01000100	01000100	70010A01	03005001	6801AC01	E43F0000	01000100	01000100	01000100	01000100
(3280)	01000100	00000801	03005001	4E01A801	00000000	01000100	01000100	01000100	01000100	0000FA00	00000000
(3320)	03005001	0D01AC01	00000000	01000100	01000100	01000100	01000100	00000901	03005001	3D011E01	01000000
(3360)	00000000	01000100	01000100	01000100	01000100	17011201	03005001	00005200	41435155	01000000	00000000
(3400)	9695AB00	EE477103	46870000	53000000	54000000	00000000	00000000	00000000	00000000	00000000	00000000
(3440)	00000000	00000000	000068F9	1901070F	00000000	0000E801	19FCC402	00000000	00000000	00000000	00000000
(3480)	00000000	00000000	00000000	0000F001	19FCEE02	00000000	00000000	00000000	00000000	00000000	00000000
(3520)	00000000	00000000	00000000	00000000	00000000	00000000	00000000	00000000	00000000	00009904	00000000
(3560)	99049904	75040000	00000000	00000000	00000000	00000000	00000000	00000000	00000000	00000000	00000000
(3600)	00000000	00000000	00000000	00000000	00000000	00000000	00000000	00000000	00000000	00000000	00000000
(3640)	00000000	00000000	00000000	00000000	00000000	00000000	00000000	00000000	00000000	00000000	00000000
(3680)	00000000	00000000	00000000	00000000	00000000	00000000	00000000	00000000	00000000	00000000	00000000
(3720)	00000000	00000000	00000000	00000000	00000000	00000000	00000000	00000000	00000000	00000000	00000000
(3760)	00000000	00000000	00000000	00000000	00000000	00000000	00000000	00000000	00000000	00000000	00000000
(3800)	00000000	00000000	00000000	00000000	00000000	00000000	00000000	00000000	00000000	00000000	00000000
(3840)	00000000	00000000	00000000	00000000	00000000	00000000	00000000	00000000	00000000	00000000	00000000
(3880)	00000000	00000000	00000000	00000000	00000000	00000000	00000000	00000000	00000000	00000000	00000000
(3920)	00000000	00000000	00000000	00000000	00000000	00000000	00000000	00000000	00000000	00000000	00000000
(3960)	00000000	00000000	FF000000	00000000	00000000	00000000	00000000	00000000	00000000	00000000	00000000
(4000)	00000000	00000000	00000000	00000000	00000000	00000000	00000000	00000000	00000000	00000000	00000000
(4040)	00000000	00000000	00000000	00000000	00000000	00000000	00000000	00000000	00000000	00000000	00000000
(4080)	00000000	00000000	00000000	00000000	00000000	00000000	00000000	00000000	00000000	00000000	00000000
(4120)	00000000	00000000	00000000	00000000	00000000	00000000	00000000	00000000	00000000	00000000	00000000
(4160)	00000000	00000000	00000000	00000000	00000000	00000000	00000000	00000000	00000000	00000000	00000000
(4200)	00000000	00000000	00000000	00000000	00000000	00000000	00000000	00000000	00000000	00000000	00000000
(4240)	00000000	00000000	00000000	00000000	00000000	00000000	00000000	FF000000	00000000	00000000	00000000
(4280)	00000000	00000000	00000000	00000000	00000000	00000000	00000000	00000000	00000000	00000000	00000000
(4320)	00000000	00000000	00000000	00000000	00000000	00000000	00000000	00000000	00000000	00000000	00000000
(4360)	00000000	00000000	00000000	00000000	00000000	00000000	00000000	00000000	00000000	00000000	00000000
(4400)	00000000	00000000	00000000	00000000	00000000	00000000	00000000	00000000	00000000	00000000	00000000
(4440)	00000000	00000000	00000000	00000000	00000000	00000000	00000000	00000000	00000000	00000000	00000000
(4480)	FF000000	00000000	00000000	00000000	00000000	00000000	00000000	00000000	00000000	00000000	00000000
(4520)	00000000	00000000	00000000	00000000	00000000	00000000	00000000	00000000	00000000	00000000	00000000
(4560)	00000000	00000000	00000000	00000000	00000000	00000000	00000000	00000000	00000000	00000000	00000000

(Skip 3 pages)

(11800)	03004000	70010E00	00000000	00000000	00000000	00000000	00000000	00000000	0F001000	03006001	0E000D00
(11840)	00000000	00000000	00000000	00000000	00000000	A5010F01	03006001	FD009B00	00000000	00000000	00000000
(11880)	00000000	00000000	00000000	00011C00	03006000	0E019800	B8EA0000	00000000	00000000	00000000	00000000
(11920)	00000000	20012101	03006000	0E01BD00	48150000	00000000	00000000	00000000	00000000	00000000	05010F01
(11960)	03006001	0501EA00	1CC00000	00000000	00000000	00000000	00000000	FA000D01	03006001	0D00EB00	
(12000)	E43F0000	00000000	00000000	00000000	00000000	00010901	03006001	0E001100	55000000	00000000	
(12040)	00000000	00000000	00000000	FE002101	03002000	0E00FC01	06000000	00000000	00000000	00000000	
(12080)	00000000	07010501	03006000	0E00F501	14000000	00000000	00000000	00000000	00000000	00000000	FA001D00
(12120)	03006000	0E00A500	10000000	00000000	00000000	00000000	00000000	F8001300	03006001	DB000E00	
(12160)	02000000	00000000	00000000	00000000	00000000	E801DE01	03004001	84011A00	01000000	00000000	
(12200)	00000000	00000000	00000000	E4000A01	03004000	0E00CC00	00000000	00000000	00000000	00000000	
(12240)	00000000	12001101	03005000	8201F800	01000000	00000000	00000000	00000000	00000000	00000000	FF010E01
(12280)	03005000	DA00E901	01000000	00000000	00000000	00000000	00000000	18001001	03005000	8201EF01	
(12320)	B8EA0000	00000000	00000000	00000000	00000000	14000501	03005001	D000AB01	48150000	00000000	
(12360)	00000000	00000000	00000000	16001201	03005001	6A01AA01	1CC00000	00000000	00000000	00000000	
(12400)	00000000	3E010A01	03005001	5B01AC01	E43F0000	00000000	00000000	00000000	00000000	00000000	00001401
(12440)	03005001	5001A801	00000000	00000000	00000000	00000000	00000000	00000000	00000000	03005001	0F01AC01
(12480)	00000000	00000000	00000000	00000000	00000000	00001101	03005001	40011F01	00000000	00000000	
(12520)	00000000	00000000	00000000	19010601	03005001	00005700	00000000	FF010100	01000100	FF010100	
(12560)	01000100	02000100	03005001	00002400	00000000	01000100	01000100	01000100	01000100	01000100	02000200
(12600)	03005001	3D00A001	24000000	01000100	01000100	01000100	01000100	03000400	03005001	00000000	
(12640)	AB020000	01000100	01000100	01000100	01000100	03000300	03005001	38002100	00000000	01000100	
(12680)	01000100	01000100	01000100	02000300	03005001	98010100	58000000	01000100	01000100	01000100	01000100
(12720)	01000100	02000100	03005001	58002F00	00000000	01000100	01000100	01000100	01000100	01000100	06000700
(12760)	03005001	62000E00	00000000	01000100	01000100	01000100	01000100	0E000F00	03005001	49000D00	
(12800)	00000000	01000100	01000100	01000100	01000100	C1001401	03005001	5A010E00	00000000	01000100	
(12840)	01000100	01000100	01000100	0F001000	03005001	0D000E00	00000000	01000100	01000100	01000100	
(12880)	01000100	A4011101	03004001	FE009F00	00000000	01000100	01000100	01000100	01000100	01000100	C0011C00
(12920)	03004001	0F019A00	B8EA0000	01000100	01000100	01000100	01000100	2C010500	03004001	0D01BD00	
(12960)	48150000	01000100	01000100	01000100	01000100	03011201	03006001	0501EB00	1CC00000	01000100	
(13000)	01000100	01000100	01000100	01010B01	03006001	0E00BA00	E43F0000	01000100	01000100	01000100	
(13040)	01000100	03011401	03006001	0E002000	55000000	01000100	01000100	01000100	01000100	01000100	01011D01
(13080)	03006001	0E00FF01	06000000	01000100	01000100	01000100	01000100	00010F01	03006001	0E00FC01	
(13120)	14000000	01000100	01000100	01000100	01000100	00011900	03006001	0E00A700	10000000	01000100	
(13160)	01000100	01000100	01000100	08011D00	03006001	DA000E00	02000000	01000100	01000100	01000100	
(13200)	01000100	EC019B01	03004001	83011900	01000000	01000100	01000100	01000100	01000100	01000100	59001A01
(13240)	03004001	0E00C800	00000000	01000100	01000100	01000100	01000100	11000E01	03004001	7C01FB00	
(13280)	01000000	01000100	01000100	01000100	01000100	FF011501	03004001	D700EA01	01000000	01000100	
(13320)	01000100	01000100	01000100	10000801	03004000	8501F201	B8EA0000	01000100	01000100	01000100	
(13360)	01000100	1A000601	03005000	D000AB01	48150000	01000100	01000100	01000100	01000100	01000100	12000C01
(13400)	03005001	6C01A901	1CC00000	01000100	01000100	01000100	01000100	36010C01	03005001	5901AC01	
(13440)	E43F0000	01000100	01000100	01000100	01000100	00000E01	03005000	5001A801	00000000	01000100	
(13480)	01000100	01000100	01000100	00000E01	03005001	1001AC01	00000000	01000100	01000100	01000100	
(13520)	01000100	00000A01	03005001	40012001	00000000	01000100	01000100	01000100	01000100	01000100	2201FF00
(13560)	03005001	00005800									

HEX DUMP OF 16580

112 = 1/21

(0)	44455045	05000000	0403AC00	1F8D3F00	7728F501	81380100	82380100	00000000	00000000	00000000
(40)	00000000	00000000	00000000	00000000	00002C01	0F01E30E	07CAD105	C9F9E801	48712907	0000D437
(80)	44060000	00009308	2209B008	00000000	350ADE05	F2F9EE01	E972EB06	00004B39	2F060000	00003B08
(120)	B0087608	00000000	10001000	3117C916	A7074B07	C5076A07	EF06E307	48070008	59080E07	0E07C507
(160)	A7072D07	2D074B07	6A072D07	2B076A07	A707CF06	0E074B07	2D07110E	05020000	1B011801	02000800
(200)	B6003C01	08003801	38010500	0900E200	5C010E00	00000000	00000000	00000000	00000000	00000000
(240)	00000000	00000000	00000000	00000000	00000000	00000000	00000000	00000000	00000000	00000000
(280)	00000000	00000000	00000000	00000000	00000000	00000000	00000000	00000000	00000000	00000000
(320)	FE000000	00000000	00000000	00000000	00000000	00000000	00000000	00000000	00000000	00000000
(360)	00000000	00000000	00000000	00000000	00000000	00000000	00000000	00000000	00000000	00000000
(400)	00000000	00000000	00000100	00000000	00000000	00000000	00000000	00000100	00000000	00000000
(440)	00000000	00000000	00000000	00000000	00000000	00000000	00000000	00000000	00000000	00000000
(480)	00000000	00000000	00000000	00000000	00000000	00000100	00000000	00000000	00000000	00000000
(520)	00000000	00000000	00000000	00000000	00000000	00000000	00000000	00000000	00000000	00000000
(560)	00000000	00000000	00000000	00000400	FE000000	00000000	00000000	00000000	01000000	00000000
(600)	00000000	00000000	00000000	00000000	00000000	00000100	00000000	00000000	00000000	00000000
(640)	00000000	00000000	00000000	01000000	00000000	00000000	00000000	00000000	00000000	00000000
(680)	00000000	00000000	00000000	00000000	00000000	00000000	00000000	00000000	00000000	01000000
(720)	00000100	00000000	00000000	00000000	00000000	00000000	00000000	00000000	00000000	00000000
(760)	00000000	00000000	00000000	00000000	00000000	00000000	00000000	00000000	00000000	00000000
(800)	00000000	00000000	00000000	00000000	00000000	00000000	00000000	00000400	FE000000	00000000
(840)	00000000	00000000	00000000	00000000	00000000	00000000	00000000	00000000	00000000	00000000
(880)	00000000	00000000	01000000	00000000	00000000	00000000	00000000	00000000	00000000	00000000
(920)	00000000	01000000	00000000	00000000	00000000	00000000	00000000	00000000	00000000	00000000
(960)	00000000	00000000	00000000	00000000	00000000	00000000	00000000	00000000	00000000	01000000
(1000)	00000000	00000000	00000000	00000000	00000000	00000000	00000000	00000000	00000000	00000000
(1040)	00000000	00000000	00000000	00000000	00000000	00000000	00000000	00000000	00000000	00000000
(1080)	00000000	00000300	FE000000	00000000	00000000	00000100	00000000	00000000	00000000	00000000
(1120)	00000200	00000000	00000000	00000000	00000000	00000000	00000000	00000000	00000000	00000000
(1160)	00000000	01000000	00000100	00000000	00000000	00000000	00000000	00000000	00000100	00000000
(1200)	00000000	00000000	00000000	00000000	00000000	01000000	00000100	00000000	00000000	01000000
(1240)	00000000	00000000	01000000	00000100	00000000	00000000	00000000	00000000	00000000	00000000
(1280)	00000000	00000000	00000000	00000000	00000000	00000000	00000000	00000000	00000000	00000000
(1320)	00000000	01000000	00000000	01000000	00000000	00000200	09000000	FC010000	00000000	FC010000
(1360)	00000000	7601AB00	4F000400	40004B00	07000000	00000000	00000000	00000000	00000000	70009500
(1400)	4F000400	E9003000	17000000	00000000	00000000	00000000	00000000	6F013C01	4F000400	00000000
(1440)	7F030000	00000000	00000000	00000000	00000000	B1008C01	4F000400	B600AD00	01000000	02000000
(1480)	00000000	00000000	00000000	3801CA01	4F000400	87010000	81380000	00000000	00000000	00000000
(1520)	00000000	48003200	4F000400	58000F00	00000000	00000000	00000000	00000000	00000000	ED01B600
(1560)	4F000400	4A000D00	00000000	00000000	00000000	02000000	00000000	10000F00	4F000400	0D000E00
(1600)	00000000	00000000	00000000	00000000	00000000	1A016F01	4F000400	10010E00	00000000	00000000
(1640)	00000000	00000000	02000000	F900FC00	4F000400	0D00F900	00000000	00000000	00000000	00000000
(1680)	00000000	28011901	4F000400	F1003C01	00000000	00000200	00000000	00000000	02000000	00001000
(1720)	4F000400	0101BC01	B8EA0000	00000000	00000000	00000000	00000000	06000401	4F000400	F0008E01
(1760)	48150000	00000000	00000200	00000000	00000000	9C000B01	4F000400	F8002401	1CC00000	00000000
(1800)	00000000	00000000	00000000	09010E01	4F000400	0E00CA00	E43F0000	00000000	00000000	00000000
(1840)	00000000	F8000F01	4F000400	0E001B00	55000000	00000000	00000000	00000000	00000000	58010E01
(1880)	4F000400	0E000E00	06000000	00000000	00000000	00000000	00000000	70010F01	4F000400	0E001E00
(1920)	14000000	00000000	00000000	00000000	00000000	F9001100	4F000400	0E008501	10000000	00000000
(1960)	00000000	00000000	00000000	F6001900	4F000400	72010E00	02000000	00000000	00000000	00000000
(2000)	02000000	17009201	4F000400	0E001C00	01000000	00000000	00000000	00000000	00000000	00000000
(2040)	4F000400	7501BC00	00000000	00000000	00000200	00000000	00000000	1700FA00	4F000400	CC00F600
(2080)	05000000	00000000	00000000	00000000	00000000	FC011801	4F000400	CE00DA01	05000000	00000000
(2120)	00000000	00000000	00000000	12000A01	4F000400	7001DC01	B8EA0000	00000000	00000000	00000000
(2160)	00000000	19007C00	4F000400	C600D201	48150000	00000000	00000000	00000000	00000000	25010F01
(2200)	4F000400	5901CC01	1CC00000	00000200	00000000	00000000	00000000	78011301	4F000400	F001CD01
(2240)	E43F0000	00000000	00000000	00000000	00000000	0E011B01	4F000400	D401CE01	00000000	00000000
(2280)	00000000	00000000	00000000	F5000D01	4F000400	3201CD01	00000000	00000000	00000000	00000000
(2320)	00000000	DC001401	4F000400	5F014701	00000000	00000000	00000800	00000000	00000600	22010701

(Skip 3 pages)

